Journal of THERMOELECTRICITY

Editorial Board

CONTENTS

Rifert V.G., *doct. techn. Sciences* [1]
Anatychuk L.I., *acad. National Academy of Sciences of Ukraine*[2]
Barabash P.O., *cand. techn. sciences* [1]**,**
Usenko V.I., *doct. techn. sciences* [1]
Solomakha A.S., *cand. of techn. sciences* [1,2]
Petrenko V.G., *cand. of techn. sciences* [1]
Prybyla A.V., *cand. phys.- math. sciences* [2]
Sereda V.V. *cand. of techn. sciences* [1]

[1]NTUU "Ihor Sikorskyi KPI", *6 Politekhnicheskaya str,*
Kyiv, 03056, Ukraine; *e–mail: vgrifert@ukr.net;*
[2]Institute of Thermoelectricity of the NAS and MES of Ukraine,
1 Nauky str., Chernivtsi, 58029, Ukraine, *e–mail: anatych@gmail.com;*
[3]Yuriy Fedkovych Chernivtsi National University,
2 Kotsiubynskyi str., Chernivtsi,58012, Ukraine

COMPARATIVE ANALYSIS OF THERMAL DISTILLATION METHODS WITH HEAT PUMPS FOR LONG SPACE FLIGHTS

The work compares technologies currently in use for water recovery from the vital products of astronauts in the conditions of long space missions. The advantage of using centrifugal thermal distillation is demonstrated. Possible failures and disadvantages of a compression vacuum centrifugal distiller compared with a centrifugal multistage distiller with a thermoelectric heat pump are shown. Bibl. 38, Fig. 3, Tabl. 2.
Key words: thermoelectricity, heat pump, distiller.

Introduction

The thermal distillation of the wastewater of the life support system for long space flights was developed with the advent of astronautics. In [1], several distillation methods are described: an air-evaporation system (AES), a vacuum static evaporation system, and a centrifugal vacuum evaporator — an analogue of the Hickman evaporator described in [2].

In 1962, the first vacuum compression centrifugal distiller (VCD) was manufactured - a prototype of a distiller operating since 2008 at the International Space Station (ISS) [3].

In [4], a thermoelectric membrane evaporator is described in which wastewater evaporates in vacuum on porous membranes on one side of a thermoelectric module, and steam condenses on a porous plate on the other side of the module.

In 1961, the Kiev Polytechnic Institute began research on the processes of hydrodynamics and heat transfer during condensation and evaporation in liquid film on a rotating surface.

In [5], the results of studying the liquid flow on a rotating surface are presented. In [6], the research results are presented and a method for calculating the minimum irrigation density, which ensures full coverage of a rotating surface with a liquid film, is substantiated. In [7], dependences are given for calculating heat transfer during condensation, and in [8], dependences are given for calculating heat

transfer during evaporation of a laminar and turbulent liquid film on a rotating disk and conical heat transfer surfaces, as well as during evaporation in a rotating liquid ring [9].

From 1974 to 1993, on the instructions of a space company from Russia, scientists and engineers of the KPI developed and tested prototypes of centrifugal distillers made in Ukraine and designed for operation in space.

Several types of centrifugal distillers with various heat pumps were developed [10, 11]:

– thermoelectric centrifugal distiller, in which the heat exchange rotating surface was a thermoelectric heat pump;

– centrifugal steam jet distiller in which a steam jet compressor is integrated in a rotating shaft;

– centrifugal three-stage distiller.

Until 1990, publications in the USSR, which contained data on the design of spacecraft, were not permitted.

In [12-14], brief information is given on a 3-stage distiller (production, total energy consumption) without information on the degree of concentration, the hours of the distiller operation, the number of rotor revolutions, and the quality of the distillate.

Since 1999, "Thermodistillation" company (created by KPI employees) together with the Institute of Thermoelectricity (Chernivtsi) on the instructions of Honeywell Co (USA) began to develop, manufacture and test a new five-stage distiller with an improved thermoelectric heat pump (THP). In the period 2000-2007, three centrifugal distillers and two THPs were manufactured.

From 2000 to 2017, centrifugal distillation systems (distiller + THP) were tested to recover water from various wastewater of life support systems for manned spacecraft at the KPI, Honeywell Co, at the Marshall Center (NASA).

Test results have been published in numerous articles and reports at Life Support Conferences (ICES) and International Astronomical Congresses (IAC) [15-29]. The processes in a centrifugal apparatus with a thermoelectric heat pump are considered in detail in a series of articles [30–32].

These studies show in detail the effect produced on the efficiency of centrifugal distillation with THP by rotation speed, degree of water recovery, liquid flow rate in the circuits of the distillation system, quality factor of thermopile, type of solution.

Almost simultaneously with the development of VCD, a thermoelectric membrane distillation system called TIMES was manufactured in the USA [33 – 35]. In this distiller, evaporation and condensation takes place on the static surface of thermoelectric modules.

This article compares the technical and operational characteristics of three thermal distillation systems:

– static thermoelectric membrane distiller (TIMES);

– vacuum vapor compression centrifugal distiller (VCD);

– centrifugal multistage distiller with a thermoelectric heat pump (CMED + THP).

Static thermoelectric membrane distiller TIMES

This distiller was developed by Hamilton Seastrand Space Systems International in the 1970s.

The system uses a polymer membrane, from the surface of which evaporation of pure water from contaminated wastewater occurs. Ideally, solutes and solids do not pass through the membrane. The resulting steam condenses on a cooled membrane. The resulting condensate is aspirated through a cooled membrane and a high-quality distillate is obtained at the system outlet. An important feature of TIMES is total recycling of the feed stream, which is becoming more and more concentrated. Energy consumption is minimized through the use of static heat pumps (thermoelectric devices).

The evaporation of wastewater in this system occurs in vacuum. For terrestrial applications and small capacities (less than 5 liters per hour), the TIMES system is quite simple and effective, especially if

there is a slight difference in the temperature of the evaporated liquid and steam condensation in the thermoelectric module. When urine is concentrated to a salt content of 40 %, only due to physicochemical temperature depression, the temperature difference in the thermoelectric module will increase by 4 ... 5 ° C, which significantly reduces the efficiency of the system. In addition, the magnitude of this difference will depend on the pump capacity in the circulation circuit of the source fluid.

The maximum concentration of liquid in the TIMES system is limited due to salt deposits in the pores of the membrane evaporator. Similar processes are observed in reverse osmosis membranes during desalination of salt water with a concentration close to urine and a water recovery level of up to 60% [33]. The data of publications [3, 4, 34] on the TIMES system show that the maximum efficiency of this distiller, taking into account the costs of the distiller's circulation pumps, does not exceed $\eta = 2.5 ... 3$ (with $\eta THP = 3 ... 3.5$). This is close to the theoretical possibilities of such a heat pump when the temperature difference of the liquid from the heating side in the module and the steam from the cooling side is less than 4 ... 5 °C.

Centrifugal vapor compression distiller (VCD)

The vapor compression centrifugal distiller was created and manufactured in 1962 by order of NASA [34]. At the moment, the latest version of VCD is installed on the ISS. With its help, more than 13 tons of distillate have been produced at the ISS since 2008.
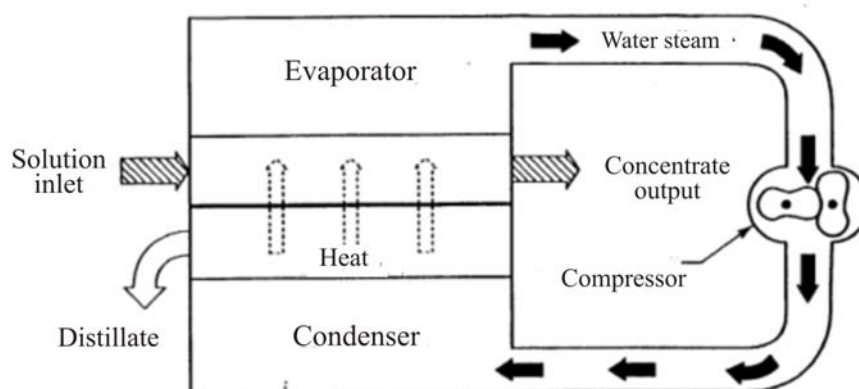
Fig.1. Circuit diagram of VCD

The vapor compression distiller utilizes the latent heat of condensation by compressing the resulting water steam in order to increase its pressure and temperature, followed by condensation on the surface in thermal contact with the evaporator.

The resulting heat flux from the condenser to the evaporator, determined by the temperature difference between saturated steam and liquid, is sufficient to evaporate an equal mass of water from water-containing waste. The need for additional energy is determined by the need to compress water vapor and replenish mechanical and heat losses.

Before delivery to the station, more than 10 prototypes were manufactured with a detailed publication of the test results of these distillers almost every year. According to the results of operation on the ISS, information is given about various damage in operation, both mechanical and problems with the quality of the distillate. Each year, reports on the ICES Life Support Conference provide information on the status of the system.

Fig. 1 shows a graph of the total production of distillate by a vapor compressor distiller in the period from 11/21/2008 to 11/21/2018 [35], from which it follows that the average VCD output was 4 ... 5 *l*/day (did not exceed 1.8 l / hour), the degree of water recovery was 75 % and only after 2016 it increased to 85 %.
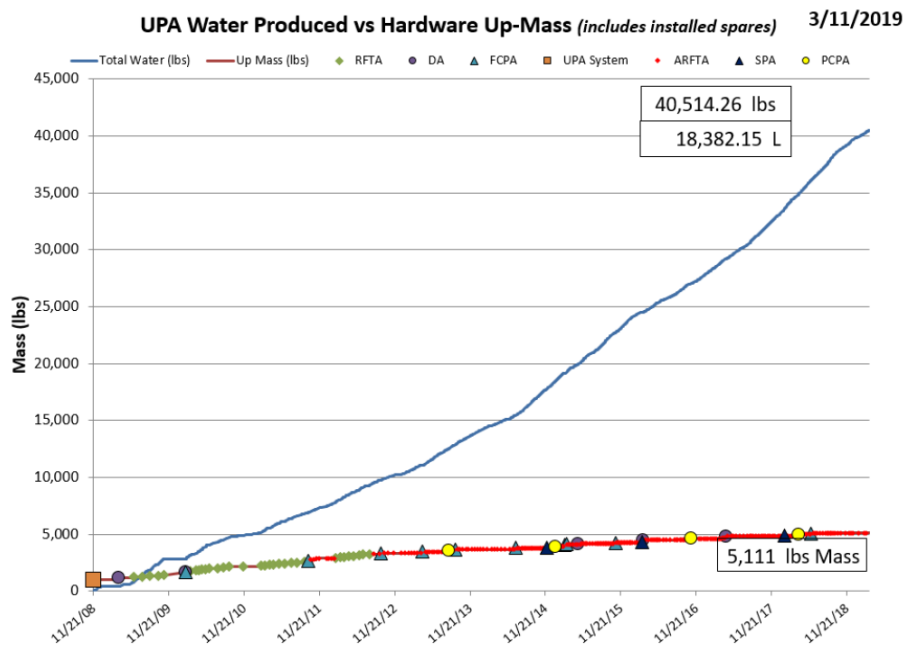
Fig. 2. Total and annual amount of distillate produced on the ISS using VCD [34, graph 7]

Back in 1989, a comparison of three technologies with a phase transition was made in [3]: TIMES, VCD, and AES (air evaporation system on a porous surface). The main characteristics of the three systems are shown in [3, table 12]. VCD has significant advantages over AES and TIMES. Already in 1990, VCD had a significantly longer test time when concentrating various wastewater compared to other systems. Therefore, in the future, VCD was installed on the ISS.

Multistage centrifugal distiller with a heat pump

In a multistage distillation system with a thermoelectric heat pump, as described in [10 – 14], two principles of reducing energy consumption are used to concentrate wastewater under zero gravity conditions: multistage evaporation and thermoelectric heat pump (CMED + THP). Figure 3 shows a centrifugal distillation scheme with a thermoelectric heat pump.
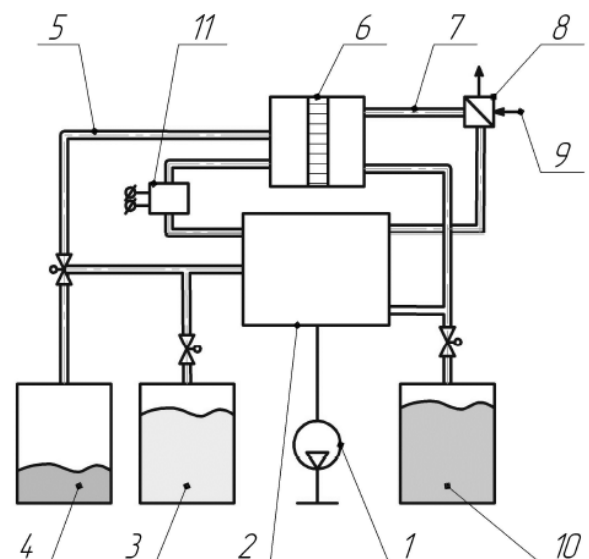
Fig. 3. Schematic of water regeneration system with a centrifugal distiller and a thermoelectric heat pump
1 – vacuum-pump; 2 – distiller; 3 – initial liquid cavity; 4 – concentrate cavity; 5 – "hot" circuit; 6 – thermoelectric heat transformer; 7 – "cold" circuit; 8 – balancing cooler; 9 – cooling liquid delivery; 10 – distillate product collector; 11 – reserve heater

The initial liquid from tank 3 enters the rotating rotor of the centrifugal distiller 2 evacuated by means of a vacuum pump 1, fills the circuit 5 and the heating cavity of the thermopile 6 to the required level of evaporation of the distiller. The cold cavity of the thermopile is connected to the condenser of the distiller using circuit 7 ("cold" circuit). The excess heat is removed from the system using a refrigerator 8. The distillate product, as a result of the evaporation-condensation process, is pumped into tank 10, and the concentrate - into tank 4.

If the thermoelectric heat pump 6 fails, the system will be able to work with reduced efficiency when heating the liquid in the hot circuit using the heater 11.

The distiller is multistage and includes 3 or 5 stages with rotating heat transfer surfaces that separate the brine and condensate. A number of built-in pumps (based on Pitot tubes) provide irrigation of heat-exchange surfaces in each stage of the distiller. Wastewater flows sequentially through each of the evaporation stages. The last evaporation stage is the instant boiling stage of an overheated solution, which is overheated on the hot side of a thermoelectric heat pump. The steam obtained in this stage is heating in the previous stage of the distiller.

The distillate from each stage and the steam of the evaporation stage with the lowest pressure enter the final condenser cooled by the distillate circulating along the circuit: the final condenser - the cold side of the thermoelectric heat pump - the final condenser.

Papers [21 – 32, 36] are concerned with numerous studies of CMED characteristics with the concentration of different types of wastewater [24], distiller simulation and system reliability issues [25 – 26].

In [30 – 32], the local characteristics of the distiller and heat pump are analyzed and the analytical model of centrifugal distillation is refined.

Analysis of the characteristics of vapor compression and multistage distiller with a thermoelectric heat pump

Technical characteristics

The main technical characteristics: production, energy consumption, degree of concentration, distillate quality, weight, volume and scalability. These data are shown in Table 1 [23].

Table 1

Comparison of centrifugal techniques

Technology	VCD	CMED + THP
Mass, kg	216	202
Volume, m^3	0.5	0.5
Production, kg/day	1.63	2…7.5
Recovery, %	Up to 85	Up to 95
Distillate quality	Meets potable water standards	Meets potable water standards
Specific energy consumption, W·h/kg	< 180	< 110

From Table 1 it follows that in CMED, depending on the power of the heat pump, it is possible to vary production over a wide range, which meets the requirements of the system according to the scalability criterion.

In VCD, it is not possible to significantly increase the production of a distiller due to a disproportionate increase in energy consumption with an increase in compressor speed. With an increase in

production of more than 1.8 l/h [34], an increase in the degree of concentration of urine leads to an almost directly proportional increase in specific energy consumption.

In CMED with THP, the effect of concentration on the production and energy consumption is significantly lower [30, 32].

System reliability

The operation of the vapor compression distillation system of liquid wastewater (urine, atmospheric moisture condensate) on the ISS for 11 years has been a significant achievement by American scientists and engineers in solving the problem of water regeneration in space flight conditions.

None of the many other technologies for concentrating liquid effluents (reverse osmosis, electrodialysis, static thermoelectric evaporator) has and cannot have such results when working in space.

At the same time, improving thermal distillation using centrifugal forces is of great importance. This is due to the fact that VCD has certain limitations on the production, the possibility of increasing the degree of concentration, as well as in some positions related to the system reliability.

During the 11 years of VCD operation, there have been a large number of failures, incidents of poor water quality and other shortcomings (see Table 2).

Table 2

The list of failures in the operation of the urine processing assembly (UPA) of the US segment on the ISS in comparison with the prototype Centrifugal Multieffect Distiller (CMED) (as of 2019)

№	VCD problem name	Source of information	CMED + THP
1	VCD Centrifuge Drive Belt Slip	[37]	There is no such drive
2	Leakage of urine into the distillate through the shaft bearing of a VCD centrifuge	[37]	In the CMED design, bearings do not come into contact with urine
3	Liquid level sensor malfunctions	[37]	There is no sensor
4	Leakage of water vapor from the condenser into the stationary housing.	[37]	CMED design eliminates steam leakage
5	Water condensation in a fixed housing	[37]	Condensation in the CMED housing is eliminated
6	Evaporation of accumulated condensate in the heater housing reduces the efficiency of the distiller	[37]	There is no such problem, since condensation in the CMED housing does not accumulate
7	Wear and breakdown of centrifuge bearing and compressor	[37]	Ceramic bearings of CMED eliminate the problem
8	Insufficient service life of the peristaltic pump	[38]	There are no peristaltic pumps
9	Worn compressor drive gears	[38]	There is no compressor
10	Failures in the transmission of the pump assembly	[38]	In CMED, fluid is pumped by a Pitot tube
11	Failures of flow control valves in the pump assembly	[38]	No pump assembly

The right column of this table contains comments regarding the possibility of a similar problem in the CMED system. Another particularly important case of damage to the heat pump and the consequences of such a case should be added to this table. In VCD, when the compressor is damaged, the system ceases to function. In CMED, when shutting down due to complete or partial damage to the heat pump, the system switches to a conventional heat exchanger-heater, in which the solution of the first stage will circulate (see pos. 11, Fig. 3). Such an accident will lead to an increase in the specific energy consumption by about a factor of 1.5 ... 2, but will not affect the performance of the entire system.

Conclusions

Comparison of different technologies for water recovery with a phase transition showed that VCD at the time of installation on the ISS had significant advantages compared to AES and TIMES. During operation, it was possible to regenerate and obtain more than 13 tons of distillate, which greatly reduced the cost of delivering fresh water to the station. At the same time, a number of significant design flaws of the system were identified during the operation, which almost completely eliminates the possibility of using VCD for long-range space missions to the Moon and Mars. In this regard, there is a need to develop a reliable and efficient water recovery system for long-range space missions. The stated requirements are most closely met by CMED with a thermoelectric heat pump.

References

1. *Space biology* (1972). Nauka [in Russian].
2. Hickman K. C. D. (1957). *Industrial and Engineering Chemistry*, 786.
3. Gorensek Max B., Baer-Peckham David. Space station water recovery trade study – Phase change technology. *SAE paper 881015.*
4. Roebelen G., Dehner G., and Winkler H. (1982). Thermoelectric integrated membrane evaporation water recovery technology. *SAE Technical Paper 820849.*
5. Muzhilko A.A., Rifert V.G., Barabash P.A. (1985). Flow of liquid film over the surface of a rotating disk. *Heat transfer. Soviet research.*
6. Butuzov A.I., Pukhovoy I.I. and Rifert V.G. (1976). Experimental determination of the minimum irrigation density in a thin-film rotating disk apparatus. *Fluid Mechanics-Soviet Research, 5(1).*
7. Butuzov A.I., Rifert V.G. (1972). An experimental study of heat transfer during condensation of steam at a rotating disk. *Heat Transfer-Soviet Research, 4(6).*
8. Butuzov A.I. and Rifert V.G. (1973). Heat transfer in evaporation of liquid from a film on a rotating disk. *Heat Transfer-Soviet Research, 5(1).*
9. Usenko V.I., Fainzilberg S.N. (1974). Effect of acceleration on the critical heat load with the boiling of freons on elements having small transverse dimensions. *High Temperature.*
10. Rifert V., Barabash P., Goliad N. (1990). Methods and processes of thermal distillation of water solutions for closed water supply systems. *The 20th Intersociety Conference on Environmental Systems. (Williamsburg, July 1990). SAE Paper 901249.*
11. Samsonov N., Bobe L., Novikov V., Rifert V. et al. (1994). Systems for water reclamation from humidity condensate and urine for space station. *The 24th International society Conference on Environmental Systems (June, 1994). SAE Paper 941536.*
12. Samsonov N.M., Bobe L.S, Novikov V., Rifert V.G., Barabash P.A et al. (1995). Development of

urine processor distillation hardware for space stations. *The 25th International Conference on Environmental Systems (San Diego, July 1995). SAE Paper 951605.*

13. Samsonov N.M., Bobe L.S, Novikov V., Rifert V.G. et al. (1997). Updated systems for water recovery from humidity condensate and urine for the International space station. *SAE Paper 972559. The 27th International Conference on Environmental Systems (Nevada, July 1997).*

14. Samsonov N.M., Bobe L.S, Novikov V., Rifert V.G. et al. (1999). Development and testing of a vacuum distillation subsystem for water reclamation from urine. *SAE Paper 1999-01-1993. The 29th International Conference on Environmental Systems.*

15. Rifert V., Usenko V., Zolotukhin I., MacKnight A., Lubman A. (1999). Comparison of secondary water processors using distillation for space applications. *SAE Paper 99-70466, 29th International Conference on Environmental Systems (Denver, July 1999).*

16. Rifert V., Stricun A., Usenko V. (2000). Study of dynamic and extreme performances of multistage centrifugal distiller with the thermoelectric heat pump. *SAE Technical Papers 2000. 30th International Conference on Environmental Systems (Toulouse, France, 10-13 July 2000).*

17. Rifert V., Usenko V., Zolotukhin I., MacKnight A. and Lubman A. (2001). Design optimization of cascade rotary distiller with the heat pump for water reclamation from urine. *SAE Paper 2001-01-2248, the 31st International Conference on Environmental Systems (Orlando, July 2001).*

18. Rifert, V. G., Usenko V.I., Zolotukhin I.V., MacKnight A. and Lubman A. (2003). Cascade distillation technology for water processing in space. *SAE Paper 2003-01-2625. 34st International Conference on Environmental Systems (Orlando, July 2003).*

19. Lubman A., MacKnight A., Rifert V., Zolotukhin I. and Pickering K. (2006). Wastewater processing cascade distillation subsystem. Design and evaluation. *SAE International, 2006-01-2273.*

20. Lubman A., MacKnight A., Rifert V., and Barabash P. (2007). Cascade distillation subsystem hardware development for verification testing. *SAE International, 2007-01-3177, July 2007.*

21. Callahan M., Lubman A., MacKnight A. et al. *Cascade distillation subsystem development testing. ICES-2008. SAE International, 2008-01-2195.*

22. Callahan M., Lubman A., Pickering K. (2009). Cascade distillation subsystem development: progress toward a distillation comparison. *39th International Conference on Environmental Systems, ICES-2009. SAE International, 2009-01-2401.*

23. McQuillan J., Pickering K., Anderson M., Carter L., Flynn M., Callahan M., Yeh J. (2010). Distillation technology down-selection for the exploration life support (ELS) water recovery systems element. *40th International Conference on Environmental Systems.*

24. Callahan M.R., Patel V., and Pickering K.D. (2010). Cascade distillation subsystem development: early results from the exploration life support distillation technology comparison test. *AIAA 2010-6149, 40th International Conference on Environmental Systems.*

25. Loeffelholz David, Baginski Ban, Patel Vipul, MacKnight Allen, Schull Sarah, Sargusingh Miriam, and Callahan Michael (2014). Unit operation performance testing of cascade distillation subsystem. *44th International Conference on Environmental Systems (13-17 July 2014, Tucson, Arizona). ICES-2014-14.*

26. Bruce A. Perry, Molly S. Anderson (2015). Improved dynamic modeling of the cascade distillation subsystem and analysis of factors affecting its performance. *45th International Conference on Environmental Systems (12-16 July 2015, Bellevue, Washington). ICES-2015-216.*

27. Rifert V.G., Anatychuk L.I., Barabash P.A., Usenko V.I., Strikun A.P., Prybyla, A.V. (2017). Improvement of the distillation methods by using centrifugal forces for water recovery in space flight applications. *J.Thermoelectricity*, 1, 71-83.

28. Rifert Vladimir G., Barabash Petr A., Usenko Vladimir, Solomakha Andrii S., Anatychuk Lukyan I.,

Prybyla Andrii V. (2017). Improvement of the cascade distillation system for long-term space flights. *68th International Astronautical Congress (IAC) (Adelaide, Australia, 25-29 September 2017).*

29. Rifert Vladimir G., Anatychuk Lukyan I., Solomakha Andrii S., Barabash Petr A., Usenko Vladimir, Prybyla A.V., Naymark Milena, Petrenko Valerii (2019). Upgrade the centrifugal multiple-effect distiller for deep space missions. *70th International Astronautical Congress (IAC) (Washington D.C., United States, 21-25 October 2019). IAC-19-A1, IP, 11x54316.*

30. Rifert V.G., Anatychuk L.I., Barabash P.O., Usenko V.I., Strikun A.P., Solomakha A. S, Petrenko V.G., Prybyla A.V. (2019). Evolution of centrifugal distillation system with a thermoelectric heat pump for space missions. Part 1. Review of publications on centrifugal distillation in the period of 1990 – 2017. *J.Thermoelectricity*, 1, 57 – 67.

31. Rifert V.G., Anatychuk L.I., Barabash P.O., Usenko V.I., Strikun A.P., Solomakha A. S, Petrenko V.G., Prybyla A.V. (2019). Evolution of centrifugal distillation system with a thermoelectric heat pump for space missions. Part 2. Study of the variable characteristics of a multi-stage distillation system with a thermoelectric heat pump (THP). *J.Thermoelectricity*, 2, 62 – 77.

32. Rifert V.G., Anatychuk L.I., Barabash P.O., Usenko V.I., Strikun A.P., Solomakha A. S, Petrenko V.G., Prybyla A.V. (2019). Evolution of centrifugal distillation system with a thermoelectric heat pump for space missions. Part 3. Analysis of local and integral characteristics of centrifugal distillation system with thermoelectric heat pump. *J.Thermoelectricity*, 3, 73 – 88.

33. Thibaud-Erkey C., Fort J., and Edeen M. (2000). A new membrane for the thermoelectric integrated membrane evaporative subsystem (TIMES). *SAE Technical Paper 2000-01-2385.*

34. Noble Larry D., Schubert Franz H., Pudoka Rick J., Miernik Janie H. (1990). Phase change water recovery for the space station freedom and future exploration missions. *20th lntersociety Conference on Environmental Systems (Williamsburg, Virginia, July 9-12, 1990). SAE Technical Paper 901294.*

35. Carter Layne, Williamson Jill, Brown Christopher A., Bazley Jesse, Gazda Daniel, Schaezler Ryan, Frank Thomas, Sunday Molina (2019). Status of ISS water management and recovery. *49th International Conference on Environmental Systems (7-11 July 2019, Boston, Massachusetts). ICES 2019-36.*

36. Rifert V.G., Barabash P.A., Solomakha A.S., Usenko V., Sereda V.V., Petrenko V.G. (2018). Hydrodynamics and heat transfer in centrifugal film evaporator. *Bulgarian Chemical Communications, 50, Special Issue K, 49-57.*

37. Williamson Jill P., Carter Layne, Hill Jimmy, Jones Davey, Morris Danielle, Graves Rex (2019). Upgrades to the international space station urine processor assembly. *49th International Conference on Environmental Systems (7-11 July 2019, Boston, Massachusetts). ICES-2019-43.*

38. Pruitt Jennifer M., Carter Layne, Bagdigian Robert M., Kayatin Matthew J. (2015). Upgrades to the ISS water recovery system. *45th International Conference on Environmental Systems (12-16 July 2015, Bellevue, Washington). ICES-2015-133.*

Риферт В.Г., *док. техн. наук[1]*
Анатичук Л.І., *акад. НАН України[2]*
Барабаш П.О., *канд. техн. наук[1]*
Усенко В.І., *док. техн. наук[1]*
Соломаха А.С., *канд. техн. наук[1]*
Петренко В.Г., *канд. техн. наук[1]*
Прибула А.В., *канд. фіз.-мат. наук [1]*
Середа В.В. *канд. техн. наук[1]*

[1]НТУ «КПИ», вул. Політехнічна, 6, Київ, 03056, Україна;
[2]Інститут термоелектрики, вул. Науки, 1,
Чернівці, 58029, Україна;
e–mail: anatych@gmail.com

ПОРІВНЯЛЬНИЙ АНАЛІЗ МЕТОДІВ ТЕРМІЧНОЇ ДИСТИЛЯЦІЇ З ТЕПЛОВИМИ НАСОСАМИ ДЛЯ ТРИВАЛИХ КОСМІЧНИХ ПОЛЬОТІВ

У роботі проведено порівняння відомих технологій для витягання води з продуктів життєдіяльності космонавтів в умовах тривалих космічних місій. Показана перевага використання відцентрової термічної дистиляції. Показані можливі відмови і недоліки компресійного вакуумного відцентрового дистилятора в порівнянні з відцентровим багатоступінчастим дистилятором з термоелектричним тепловим насосом. Библ. 38, рис. 3, табл. 2.
Ключові слова: термоелектрика, тепловий насос, дистилятор.

Риферт В.Г. *док. техн. наук [1]*
Анатычук Л.И., *акад. НАН Украины[2]*
Барабаш П.О. *канд. техн. наук[1]*
Усенко В.И. *док. техн. наук[1]*
Соломаха А. С., *канд. техн. наук[1]*
Петренко В. Г., *канд. техн. наук[1]*
Прибила А. В. *канд. физ.-мат. наук [1]*
Середа В.В. *канд. техн. наук[1]*

[1]НТУ «КПИ», вул. Политехническая, 6,
Киев, 03056, Украина;
[2]Институт термоэлектричества НАН и МОН Украины,
ул. Науки, 1, Черновцы, 58029, Украина,
e–mail: anatych@gmail.com

СРАВНИТЕЛЬНЫЙ АНАЛИЗ МЕТОДОВ ТЕРМИЧЕСКОЙ ДИСТИЛЛЯЦИИ С ТЕПЛОВЫМИ НАСОСАМИ ДЛЯ ДЛИТЕЛЬНЫХ КОСМИЧЕСКИХ ПОЛЕТОВ

В работе проведено сравнение известных технологий для извлечения воды из продуктов жизнедеятельности космонавтов в условиях длительных космических миссий. Показано преимущество использования центробежной термической дистилляции. Показаны возможные отказы и недостатки компрессионного вакуумного центробежного дистиллятора по сравнению с центробежным многоступенчатым дистиллятором с термоэлектрическим тепловым насосом. Библ. 38 , рис. 3, табл. 2.

Ключевые слова: термоэлектричество, тепловой насос, дистиллятор.

References

1. *Space biology* (1972). Nauka [in Russian].

2. Hickman K. C. D. (1957). *Industrial and Engineering Chemistry*, 786.

3. Gorensek Max B., Baer-Peckham David. Space station water recovery trade study – Phase change technology. *SAE paper 881015.*

4. Roebelen G., Dehner G., and Winkler H. (1982). Thermoelectric integrated membrane evaporation water recovery technology. *SAE Technical Paper 820849.*

5. Muzhilko A.A., Rifert V.G., Barabash P.A. (1985). Flow of liquid film over the surface of a rotating disk. *Heat transfer. Soviet research*.

6. Butuzov A.I., Pukhovoy I.I. and Rifert V.G. (1976). Experimental determination of the minimum irrigation density in a thin-film rotating disk apparatus. *Fluid Mechanics-Soviet Research, 5(1).*

7. Butuzov A.I., Rifert V.G. (1972). An experimental study of heat transfer during condensation of steam at a rotating disk. *Heat Transfer-Soviet Research, 4(6).*

8. Butuzov A.I. and Rifert V.G. (1973). Heat transfer in evaporation of liquid from a film on a rotating disk. *Heat Transfer-Soviet Research, 5(1).*

9. Usenko V.I., Fainzilberg S.N. (1974). Effect of acceleration on the critical heat load with the boiling of freons on elements having small transverse dimensions. *High Temperature*.

10. Rifert V., Barabash P., Goliad N. (1990). Methods and processes of thermal distillation of water solutions for closed water supply systems. *The 20th Intersociety Conference on Environmental Systems. (Williamsburg, July 1990). SAE Paper 901249.*

11. Samsonov N., Bobe L., Novikov V., Rifert V. et al. (1994). Systems for water reclamation from humidity condensate and urine for space station. *The 24th International society Conference on Environmental Systems (June, 1994). SAE Paper 941536.*

12. Samsonov N.M., Bobe L.S, Novikov V., Rifert V.G., Barabash P.A et al. (1995). Development of urine processor distillation hardware for space stations. *The 25th International Conference on Environmental Systems (San Diego, July 1995). SAE Paper 951605.*

13. Samsonov N.M., Bobe L.S, Novikov V., Rifert V.G. et al. (1997). Updated systems for water recovery from humidity condensate and urine for the International space station. *SAE Paper 972559. The 27th International Conference on Environmental Systems (Nevada, July 1997).*

14. Samsonov N.M., Bobe L.S, Novikov V., Rifert V.G. et al. (1999). Development and testing of a vacuum distillation subsystem for water reclamation from urine. *SAE Paper 1999-01-1993. The 29th International Conference on Environmental Systems.*

15. Rifert V., Usenko V., Zolotukhin I., MacKnight A., Lubman A. (1999). Comparison of secondary water processors using distillation for space applications. *SAE Paper 99-70466, 29th International Conference on Environmental Systems (Denver, July 1999).*

16. Rifert V., Stricun A., Usenko V. (2000). Study of dynamic and extreme performances of multistage centrifugal distiller with the thermoelectric heat pump. *SAE Technical Papers 2000. 30th International Conference on Environmental Systems (Toulouse, France, 10-13 July 2000).*

17. Rifert V., Usenko V., Zolotukhin I., MacKnight A. and Lubman A. (2001). Design optimization of cascade rotary distiller with the heat pump for water reclamation from urine. *SAE Paper 2001-01-2248, the 31st International Conference on Environmental Systems (Orlando, July 2001).*

18. Rifert, V. G., Usenko V.I., Zolotukhin I.V., MacKnight A. and Lubman A. (2003). Cascade distillation technology for water processing in space. *SAE Paper 2003-01-2625. 34st International Conference on Environmental Systems (Orlando, July 2003).*

19. Lubman A., MacKnight A., Rifert V., Zolotukhin I. and Pickering K. (2006). Wastewater processing cascade distillation subsystem. Design and evaluation. *SAE International, 2006-01-2273.*

20. Lubman A., MacKnight A., Rifert V., and Barabash P. (2007). Cascade distillation subsystem hardware development for verification testing. *SAE International, 2007-01-3177, July 2007.*

21. Callahan M., Lubman A., MacKnight A. et al. *Cascade distillation subsystem development testing. ICES-2008. SAE International, 2008-01-2195.*

22. Callahan M., Lubman A., Pickering K. (2009). Cascade distillation subsystem development: progress toward a distillation comparison. *39th International Conference on Environmental Systems, ICES-2009. SAE International, 2009-01-2401.*

23. McQuillan J., Pickering K., Anderson M., Carter L., Flynn M., Callahan M., Yeh J. (2010). Distillation technology down-selection for the exploration life support (ELS) water recovery systems element. *40th International Conference on Environmental Systems.*

24. Callahan M.R., Patel V., and Pickering K.D. (2010). Cascade distillation subsystem development: early results from the exploration life support distillation technology comparison test. *AIAA 2010-6149, 40th International Conference on Environmental Systems.*

25. Loeffelholz David, Baginski Ban, Patel Vipul, MacKnight Allen, Schull Sarah, Sargusingh Miriam, and Callahan Michael (2014). Unit operation performance testing of cascade distillation subsystem. *44th International Conference on Environmental Systems (13-17 July 2014, Tucson, Arizona). ICES-2014-14.*

26. Bruce A. Perry, Molly S. Anderson (2015). Improved dynamic modeling of the cascade distillation subsystem and analysis of factors affecting its performance. *45th International Conference on Environmental Systems (12-16 July 2015, Bellevue, Washington). ICES-2015-216.*

27. Rifert V.G., Anatychuk L.I., Barabash P.A., Usenko V.I., Strikun A.P., Prybyla, A.V. (2017). Improvement of the distillation methods by using centrifugal forces for water recovery in space flight applications. *J.Thermoelectricity*, 1, 71-83.

28. Rifert Vladimir G., Barabash Petr A., Usenko Vladimir, Solomakha Andrii S., Anatychuk Lukyan I., Prybyla Andrii V. (2017). Improvement of the cascade distillation system for long-term space flights. *68th International Astronautical Congress (IAC) (Adelaide, Australia, 25-29 September 2017).*

29. Rifert Vladimir G., Anatychuk Lukyan I., Solomakha Andrii S., Barabash Petr A., Usenko Vladimir, Prybyla A.V., Naymark Milena, Petrenko Valerii (2019). Upgrade the centrifugal multiple-effect distiller for deep space missions. *70th International Astronautical Congress (IAC) (Washington D.C., United States, 21-25 October 2019). IAC-19-A1, IP, 11x54316.*

30. Rifert V.G., Anatychuk L.I., Barabash P.O., Usenko V.I., Strikun A.P., Solomakha A. S, Petrenko V.G., Prybyla A.V. (2019). Evolution of centrifugal distillation system with a thermoelectric heat

pump for space missions. Part 1. Review of publications on centrifugal distillation in the period of 1990 – 2017. *J.Thermoelectricity*, 1, 57 – 67.

31. Rifert V.G., Anatychuk L.I., Barabash P.O., Usenko V.I., Strikun A.P., Solomakha A. S, Petrenko V.G., Prybyla A.V. (2019). Evolution of centrifugal distillation system with a thermoelectric heat pump for space missions. Part 2. Study of the variable characteristics of a multi-stage distillation system with a thermoelectric heat pump (THP). *J.Thermoelectricity*, 2, 62 – 77.

32. Rifert V.G., Anatychuk L.I., Barabash P.O., Usenko V.I., Strikun A.P., Solomakha A. S, Petrenko V.G., Prybyla A.V. (2019). Evolution of centrifugal distillation system with a thermoelectric heat pump for space missions. Part 3. Analysis of local and integral characteristics of centrifugal distillation system with thermoelectric heat pump. *J.Thermoelectricity*, 3, 73 – 88.

33. Thibaud-Erkey C., Fort J., and Edeen M. (2000). A new membrane for the thermoelectric integrated membrane evaporative subsystem (TIMES). *SAE Technical Paper 2000-01-2385.*

34. Noble Larry D., Schubert Franz H., Pudoka Rick J., Miernik Janie H. (1990). Phase change water recovery for the space station freedom and future exploration missions. *20th lntersociety Conference on Environmental Systems (Williamsburg, Virginia, July 9-12, 1990). SAE Technical Paper 901294.*

35. Carter Layne, Williamson Jill, Brown Christopher A., Bazley Jesse, Gazda Daniel, Schaezler Ryan, Frank Thomas, Sunday Molina (2019). Status of ISS water management and recovery. *49th International Conference on Environmental Systems (7-11 July 2019, Boston, Massachusetts). ICES 2019-36.*

36. Rifert V.G., Barabash P.A., Solomakha A.S., Usenko V., Sereda V.V., Petrenko V.G. (2018). Hydrodynamics and heat transfer in centrifugal film evaporator. *Bulgarian Chemical Communications, 50, Special Issue K, 49-57.*

37. Williamson Jill P., Carter Layne, Hill Jimmy, Jones Davey, Morris Danielle, Graves Rex (2019). Upgrades to the international space station urine processor assembly. *49th International Conference on Environmental Systems (7-11 July 2019, Boston, Massachusetts). ICES-2019-43.*

38. Pruitt Jennifer M., Carter Layne, Bagdigian Robert M., Kayatin Matthew J. (2015). Upgrades to the ISS water recovery system. *45th International Conference on Environmental Systems (12-16 July 2015, Bellevue, Washington). ICES-2015-133.*

Submitted 01.08.2019

Gorskyi P.V. *doc. phys.-math. science*[1,2]

[1]Institute of Thermoelectricity of the NAS and MES of Ukraine,
1, Nauky str., Chernivtsi, 58029, Ukraine;
[2]Yu.Fedkovych Chernivtsi National University,
2, Kotsiubynskyi str., Chernivtsi, 58012, Ukraine

EFFECT OF NONPARABOLICITY DESCRIBED BY THE FIVAZ MODEL ON THE ELECTRICAL RESISTANCE OF THERMOELECTRIC MATERIAL-METAL CONTACT

The temperature dependences of thermoelectric material-metal electrical contact resistance were investigated in the case when a band spectrum of free charge carriers in material is described by the Fivaz model. A transient contact layer formed by the deviation of the surface of superlattice semiconductor thermoelectric material (SL TEM) from the ideal plane and transient contact layers with and without clusters formed in the process of steady-state diffusion of metal particles in SL TEM were considered. It was established that contact resistance drastically decreases with increase in the degree of nonparabolicity of SL TEM band spectrum, which is determined as the ratio of the Fermi energy of ideal two-dimensional electron (hole) gas with a quadratic dispersion law to the miniband width describing translation motion of charge carriers in the direction perpendicular to the plane of layers. This decrease is explained by blocking of free carrier scattering in the direction perpendicular to the plane of layers. It is shown that in the range of degrees of nonparabolicity K from 0.1 to 10, transient layer thicknesses from 20 to 150 μm, dimensionless intensities of metal atoms entering the volume of transient layer A from 0 to 1 and temperatures from 200 to 400 K, the electrical contact resistance of transient layer due to the deviation of SL TEM surface from the ideal plane varies from $8\cdot10^{-9}$ to $1.9\cdot10^{-7} Ohm\cdot cm^2$, transient layer due to steady-state diffusion of metal into SL TEM without formation of clusters – from $8\cdot10^{-9}$ to $4\cdot10^{-7}$ $Ohm\cdot cm^2$, transient layer due to steady-state diffusion of metal in SL TEM with formation of clusters – from $8\cdot10^{-9}$ to $4.5\cdot10^{-7}$ $Ohm\cdot cm^2$.

Key words: Fivaz model, superlattice, Fermi energy, miniband, degree of nonparabolicity, thermoelectric material–metal contact, electrical contact resistance of transient layer, deviation of thermoelectric material surface from the ideal plane, steady-state diffusion, intensity of metal particles entering semiconductor, clusters.

Introduction

The thermoelectric material (TEM)–metal electrical contact resistance, all other conditions being equal, essentially depends on the resistivities of metal and TEM. In turn, the resistivity of TEM depends not only on the concentration and scattering mechanisms of free charge carriers in it, but also on the nature of the TEM band structure, because the mobility of free charge carriers depends not least on it.

Layered TEM, which, in particular, include bismuth telluride and alloys on its basis, are more or less prone to the formation of superlattices. In turn, thermoelectric converters from these materials are usually made so that the planes of the contact electrodes are perpendicular to the

planes of layers. Therefore, the TEM-metal electrical contact resistance in this case depends essentially on the resistivity of TEM in the plane of layers. But it is known that the formation of a superlattice, that is, a gradual transformation of a material with a three-dimensional parabolic band spectrum into a material with a quasi-two-dimensional substantially non-parabolic band spectrum, reduces the TEM resistivity in the plane of layers. The study of the influence of the degree of quasi-two-dimensional TEM with a superlattice (SL TEM) on the electrical resistance of TEM-metal electrical contact resistance under different conditions is the purpose of this article.

The resistivity of TEM described by the Fivaz model

The energy spectrum of charge carriers in SL TEM is rather often described by the Fivaz model [1]. Within this model, the motion of electrons and holes along the layers is described by the effective mass approximation, and across – by the tight-binding method. It can be presented as follows:

$$\varepsilon\left(k_x, k_y, k_z\right) = \frac{\hbar^2}{2m^*}\left(k_x^2 + k_y^2\right) + \Delta\left(1 - \cos a k_z\right), \tag{1}$$

where k_x, k_y, k_z – the quasi-momentum components of electron (hole), m^* – the effective mass of electron (hole) in the plane of layers, Δ – the half-width of the mini-band that describes the motion of electrons (holes) in the direction perpendicular to the layers, a – the distance between the translation equivalent layers.

Therefore, the electrical resistivity of "superlattice" thermoelectric material (SL TEM) in the plane of layers as determined as follows [2]:

$$\sigma_s = \sigma_{0l} \int\limits_0^\infty \int\limits_0^\pi \frac{y \exp\left\{\left[y + K^{-1}(1 - \cos x) - \gamma^*\right]/t_{2D}\right\}}{\left\{\exp\left\{\left[y + K^{-1}(1 - \cos x) - \gamma^*\right]/t_{2D}\right\} + 1\right\}^2 \sqrt{2y + 4\pi K^{-2} n_0 a^3 \sin^2 x}} \, dx \, dy, \tag{2}$$

where $\sigma_{0l} = 8\pi^{5/2} e^2 l \sqrt{n_0 a}\big/(a h t_{2D})$, l – mean free path of electrons (holes), n_0 – concentration of electrons (holes), $t_{2D} = kT/\zeta_{02D}$, $\zeta_{02D} = h^2 n_0 a/4\pi m^*$ – the Fermi energy of an ideal two-dimensional Fermi-gas with a quadratic law of dispersion at the absolute zero temperature, $K = \zeta_{02D}/\Delta$, $\gamma^* = \zeta/\zeta_{02D}$, ζ – chemical potential of electron (hole) gas in SL TEM. Parameter K characterizes the degree of quasi-dimensionality of SL TEM, or, in other words, the degree of openness of its electron (hole) Fermi surface.

Chemical potential is determined from the equation:

$$\frac{t_{2D}}{\pi} \int\limits_0^\pi \ln\left[1 + \exp\left(\frac{\gamma^* - K^{-1}(1 - \cos x)}{t_{2D}}\right)\right] dx - 1 = 0. \tag{3}$$

It is believed that scattering of charge carriers mainly occurs on the deformation potential of acoustic phonons, and, hence, the mean free path of charge carriers is inversely proportional to temperature and does not depend on the energy of charge carriers. To calculate the temperature

dependences of SL TEM resistivity at different values of the degree of nonparabolicity K, the following parameters of SL TEM were taken: $n_0 = 3 \cdot 10^{19}\, \text{cm}^{-3}$, $a = 3\,\text{nm}$, $m^* = m_0$, $T_0 = 300\,\text{K}$, $l_0 = 20\,\text{nm}$.

Based on these dependences, the temperature dependences of the SL TEM-metal electrical contact resistance were calculated for two cases: when transient contact layer is due to the deviation of the SL TEM surface from the ideal plane and when it is due to steady-state diffusion of the metal in SL TEM without the formation of intermetallic compounds.

SL TEM-metal electrical contact resistance due to a deviation of SL TEM surface from the ideal plane

The calculations were performed on the assumption that "hollows" and "humps", caused by the deviation of SL TEM surface from the ideal plane, are distributed evenly over it. Therefore, for the thickness h of the damaged layer which is recognized at the vertical distance between the deepest "hollow" and the highest "hump", the TEM-metal electrical contact resistance caused by this deviation was determined through the resistivities of semiconductor ρ_s and metal ρ_m as follows [3]:

$$r_{ce} \equiv r_c = \frac{h(\rho_s - \rho_m)}{\ln(\rho_s / \rho_m)}, \tag{4}$$

and the resistivity of metal was considered to be directly proportional to temperature. Nickel was taken as the metal whose resistivity at 300 K is $8 \cdot 10^{-6}$ Ohm·cm.

The results of calculations of the temperature dependences of thermoelectric material-metal contact resistance caused by the deviation of TEM surface from the ideal plane are shown in Figs. 1 and 2.
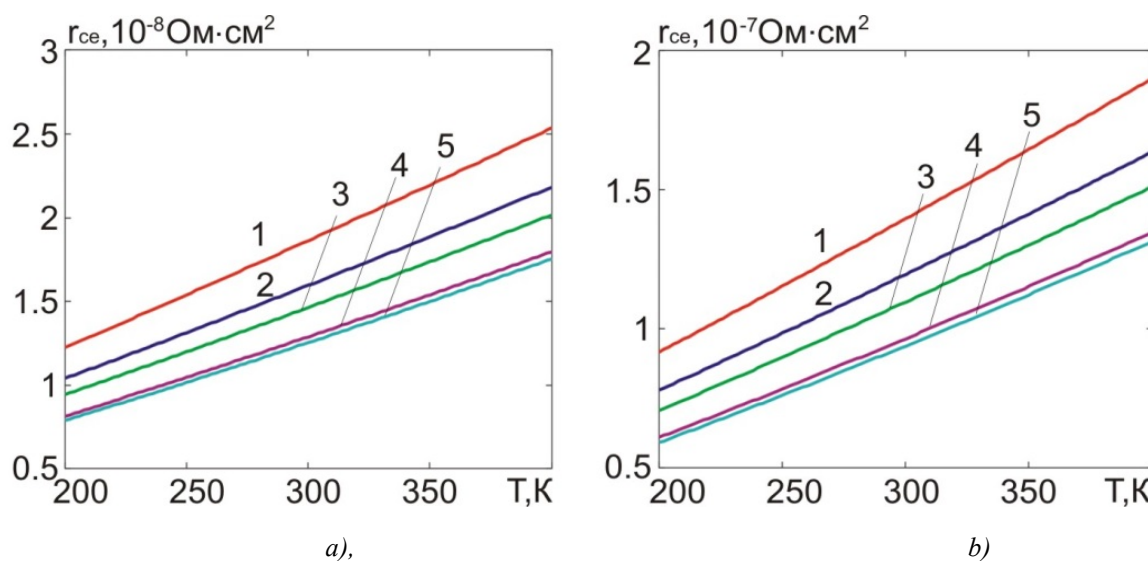

Fig.1.Temperature dependences of TEM-metal electrical contact resistance at damaged layer thickness: a) h=20 μm, n) h=150 μm. 1 – K=0.1; 2 – K=0.5; 3 – K=1; 4 – K=5; 5 – K=10.

It can be seen from the figures that with an increase in the degree of nonparabolicity of the band spectrum of free charge carriers, and, consequently, in the degree of openness of the Fermi surface (FS) of TEM, the TEM-metal electrical contact resistance, due to the deviation of TEM surface from the ideal plane, decreases significantly, and with a rise in temperature grows in conformity with the temperature dependences of the resistivities of both metal and SL TEM. In the whole temperature range of $200 - 400$ K at the degree of openness $0.1 \le K \le 10$ the specific electrical resistance of TEM – metal contact varies from $8 \cdot 10^{-9}$ to $2.5 \cdot 10^{-8}$ Ohm·cm^2 at the thickness of damaged layer 20 μm, and from $6 \cdot 10^{-8}$ to $1.9 \cdot 10^{-7}$ Ohm·cm^2 at the thickness of damaged layer 150 μm, which is not only in qualitative, but also in quantitative agreement with the experimental data. The larger contact resistances observed by the authors can be explained by the lower degree of nonparabolicity of the band spectrum of bismuth telluride-based alloys used for the manufacture of thermoelectric legs.

SL TEM-metal electrical contact resistance due to steady-state diffusion of metal in SL TEM without formation of clusters

If transient contact layer is formed in the process of steady-state diffusion of metal in SL TEM, then the distribution of metal atoms over the depth of this layer is determined as [4]:

$$n(x) = n_0 \left[1 - (1-A)x - Ax^2 \right], \tag{5}$$

where x – depth normalized to layer thickness, n_0 – concentration of metal atoms close to metal-transient layer boundary, A – dimensionless parameter which characterizes the mode of contact creation as is determined as:

$$A = Qh^2 / 2Dn_0 , \tag{6}$$

where Q – the intensity of metal entering TEM, D – coefficient of metal diffusion in TEM. From formula (5) follows the distribution of the relative volumetric fraction of metal in the transient layer:

$$v(x) = \frac{(A_m/\gamma_m)\left[1 - (1-A)x - Ax^2\right]}{(A_m/\gamma_m)\left[1 - (1-A)x - Ax^2\right] + (A_s/\gamma_s)\left[(1-A)x + Ax^2\right]}, \tag{7}$$

where A_m, A_s, γ_m, γ_s – atomic (molecular) masses and densities of metal and TEM, respectively. So, if there are no clusters in transient layer, the dependence of its electrical conductivity on the depth is determined as:

$$\sigma_l(x) = \sigma_s + (\sigma_m - \sigma_s)v(x), \tag{8}$$

and, thus, the SL TEM-metal electrical contact resistance with the uneven distribution of metal atoms in transient layer is determined as:

$$r_{ce} = h \int_0^1 \frac{dx}{\sigma_l(x)}. \tag{9}$$

If, however, the distribution of metal atoms in transient layer becomes uniform, for instance, due to annealing of contact structure, its electrical conductivity is determined as:

$$\sigma_0 = \sigma_s + (\sigma_m - \sigma_s)v_0, \tag{10}$$

where

$$v_0 = \int_0^1 \frac{(A_m/\gamma_m)\left[1-(1-A)x-Ax^2\right]}{(A_m/\gamma_m)\left[1-(1-A)x-Ax^2\right]+(A_s/\gamma_s)\left[(1-A)x+Ax^2\right]}. \tag{11}$$

Hence, in this case

$$r_{ce} = h/\sigma_0. \tag{12}$$

The results of calculation of the electrical contact resistance of transient layer without clusters are shown in Figs.2 – 5.

a)

b)

Fig.2. Temperature dependences of TEM-metal electrical contact resistance at uneven distribution of metal particles in transient layer without clusters at the value of A=0: a) h=20 μm, b) h=150 μm. 1 – K=0.1; 2 – K=0.5; 3 – K=1; 4 – K=5; 5 – K=10.

a)

b)

Fig.3. Temperature dependences of TEM-metal electrical contact resistance at uneven distribution of metal particles in transient layer without clusters at the value of A=1: a) h=20 μm, b) h=150 μm. 1 – K=0.1; 2 – K=0.5; 3 – K=1; 4 – K=5; 5 – K=10.

a)

b)

Fig.4. Temperature dependences of TEM-metal electrical contact resistance after levelling
the distribution of metal particles in transient layer without clusters at the value of
A=0: a) h=20 μm,b) h=150 μm.1 – K=0.1; 2 – K=0.5; 3 – K=1; 4 – K=5; 5 – K=10.

a)

b)

Fig. 5. Temperature dependences of TEM-metal electrical contact resistance after
levelling the distribution of metal particles in transient layer without clusters
at the value of A=1: a) h=20 μm, b) h=150 μm. 1 – K=0.1;
2 – K=0.5; 3 – K=1; 4 – K=5; 5 – K=10.

It can be seen from the figures that the electrical contact resistance decreases with an increase in the degree of nonparabolicity of SL TEM band spectrum and the intensity of metal entering transient layer during its creation, and increases with a rise in temperature. Moreover, it also decreases after levelling the distribution of metal particles in transient layer. On the whole, in the considered range of degrees of nonparabolicity (openness of SL TEM FS), the intensities of metal particles entering transient layer, the thicknesses of contact layers and temperatures, the electrical contact resistance due to steady-state diffusion of metal particles without formation of clusters varies in the range of $8 \cdot 10^{-9}$ to $4 \cdot 10^{-7}$ Ohm·cm². This interval is broader than in the case when transient contact layer is formed due to the deviations of SL TEM surface from the ideal plane.

SL TEM-metal electrical contact resistance due to steady-state diffusion of metal in SL TEM with formation of clusters

Due to the large number of defects in layered SL TEM, clusters of atoms can form in the interlayer space. In this case, the conductivity calculation should be performed using percolation theory. In accordance with this theory, taking into account the depth dependence of the concentration of metal atoms in transient layer, the electrical conductivity of transient layer is determined as [5]:

$$\sigma_l(x) = 0.25\left\{\sigma_s[2-3v(x)]+\sigma_m[3v(x)-1]+\sqrt{\{\sigma_s[2-3v(x)]+\sigma_m[3v(x)-1]\}^2+8\sigma_m\sigma_s}\right\}, \quad (13)$$

and in the case when the distribution of atoms over the depth of transient layer becomes uniform, as:

$$\sigma_0 = 0.25\left\{\sigma_s(2-3v_0)+\sigma_m(3v_0-1)+\sqrt{[\sigma_s(2-3v_0)+\sigma_m(3v_0-1)]^2+8\sigma_m\sigma_s}\right\}. \quad (14)$$

Further, the calculation of the electrical contact resistance is performed in the same order as in the case of transient layer without clusters. The results of calculating the temperature dependences of the SL TEM-metal electrical contact resistance in the case of transient contact layer with clusters are shown in Figs. 6 - 9.
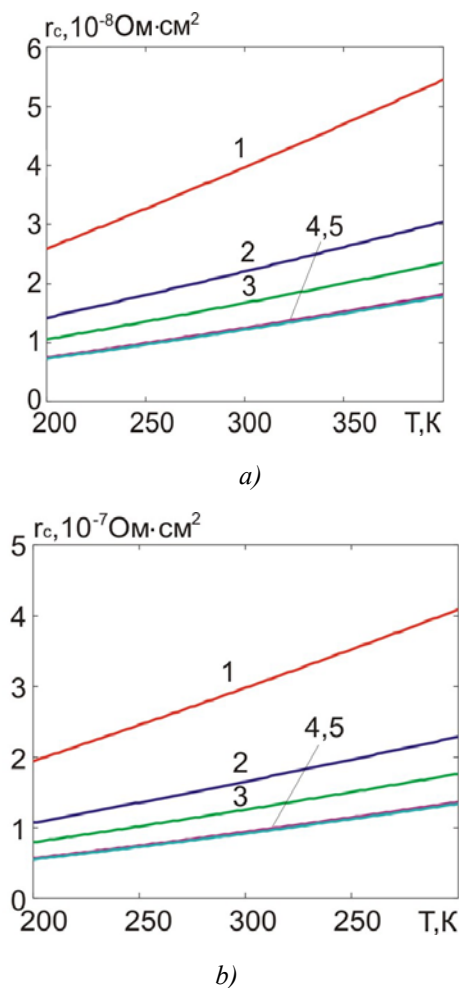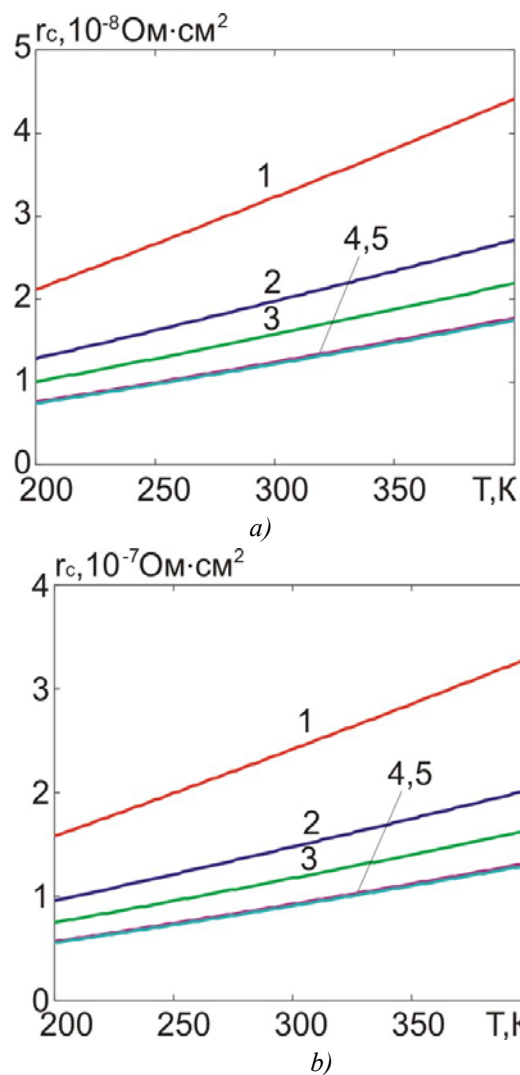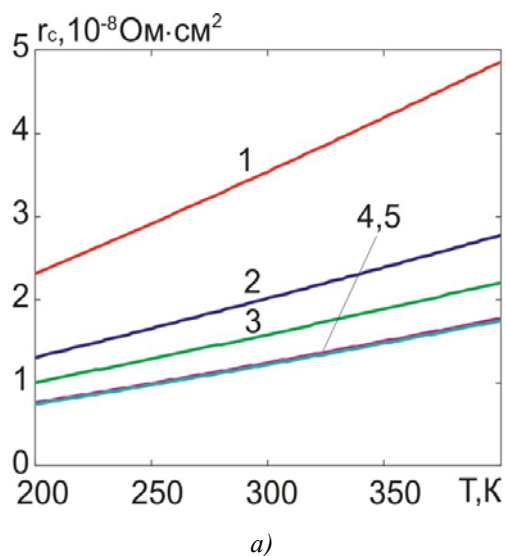

a)   *b)*
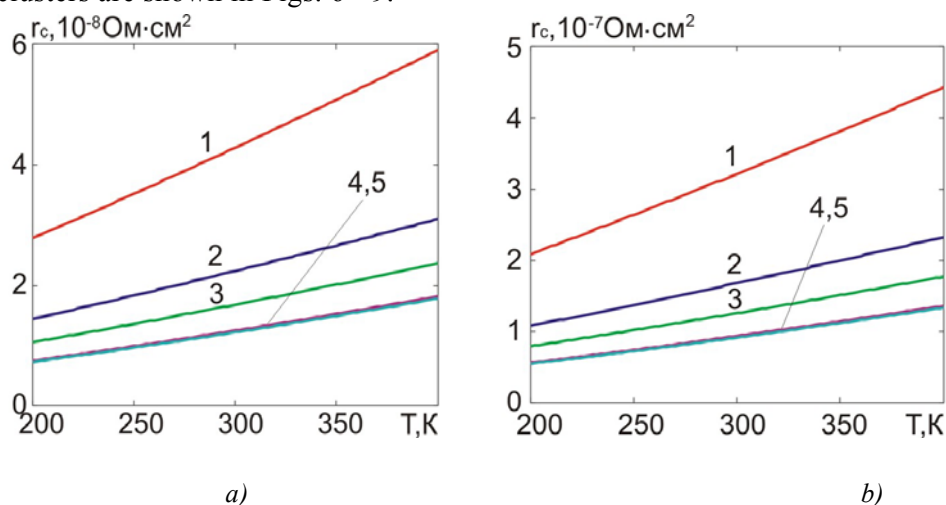
Fig.6. Temperature dependences of TEM-metal electrical contact resistance at uneven distribution of metal particles in transient layer with clusters at the value of A=0: a) h=20 μm, b) h=150 μm. 1 – K=0.1;2 – K=0.5; 3 – K=1; 4 – K=5; 5 – K=10.
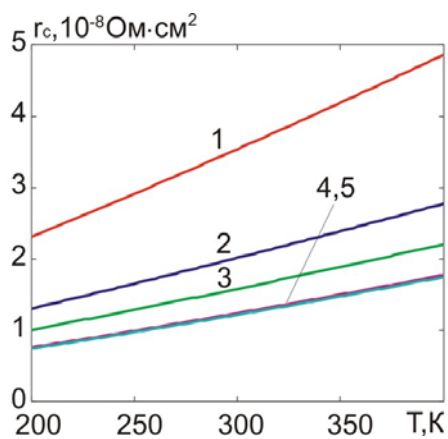
a)
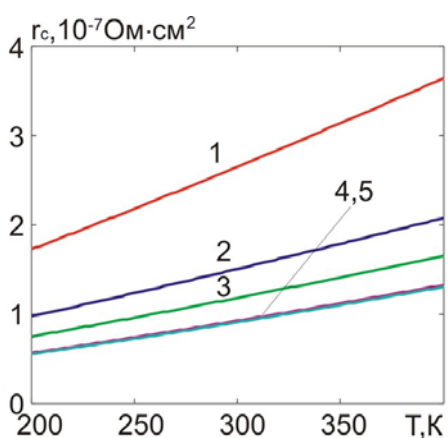
b)

Fig.7. Temperature dependences of TEM-metal electrical contact resistance at uneven distribution of metal particles in transient layer with clusters at the value of A=1: a) h=20 μm, b) h=150 μm. 1 – K=0.1;2 – K=0.5; 3 – K=1; 4 – K=5; 5 – K=10.
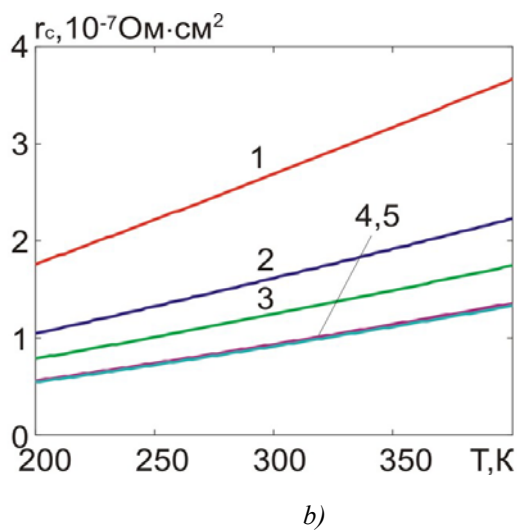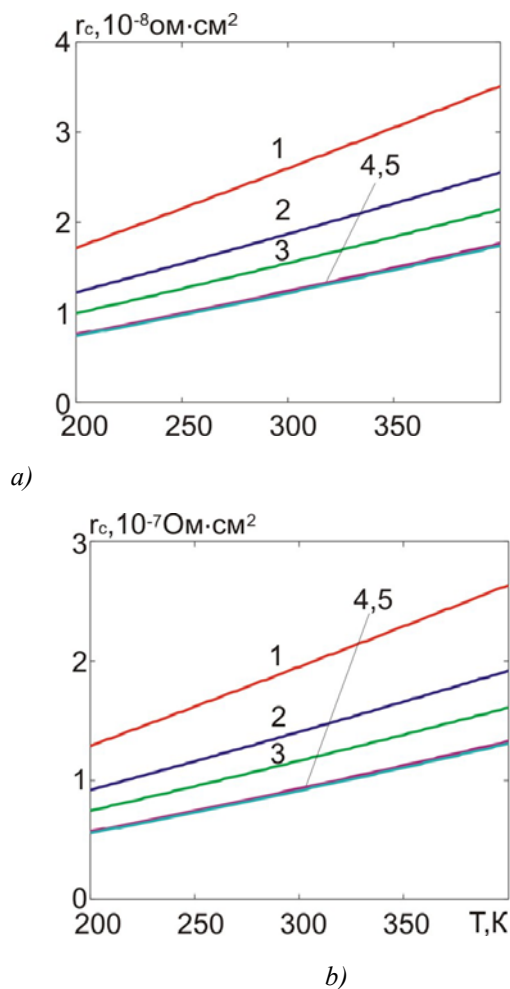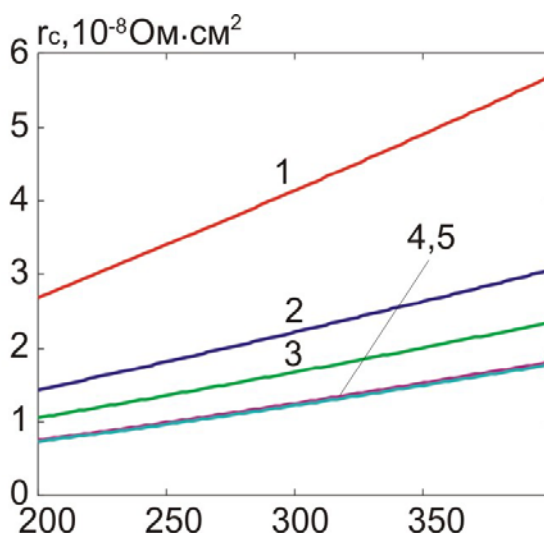

a)
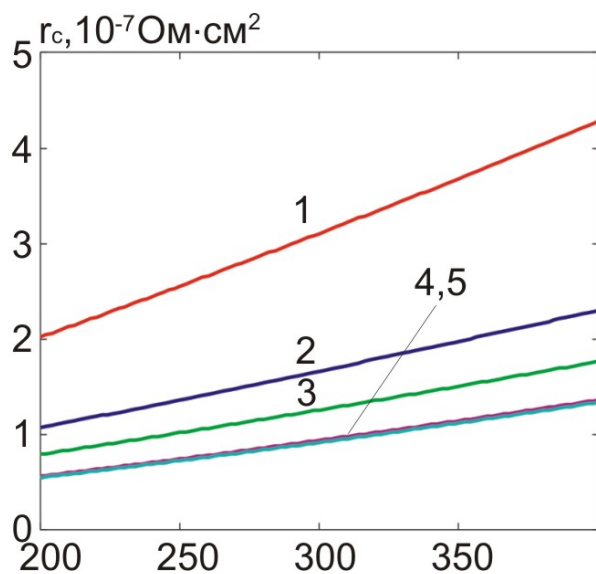
b)

*Fig.8. Temperature dependences of TEM-metal specific electrical
contact resistance after levelling the distribution of metal particles in
transient layer with clusters at the value of
A=0: a) h=20 µm, b) h=150 µm.
1 – K=0.1; 2 – K=0.5; 3 – K=1;
4 – K=5; 5 – K=10.*

a)

b)
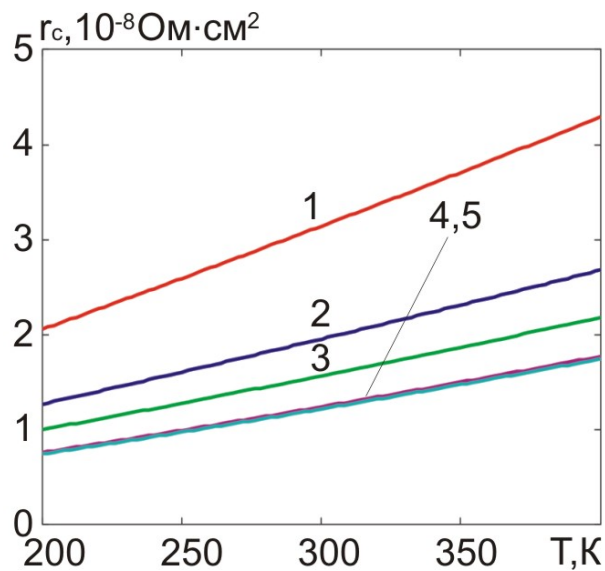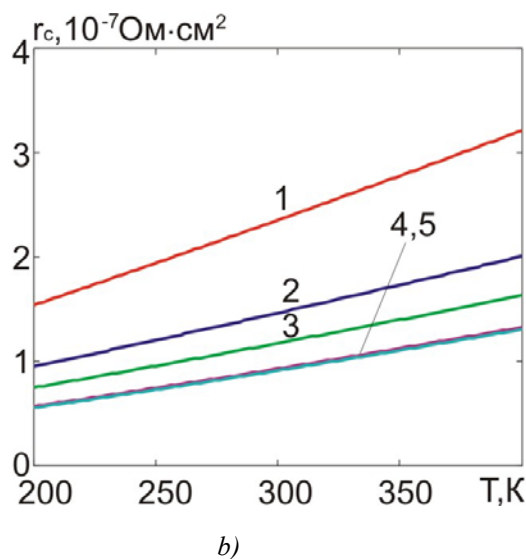
Puc.9.Temperature dependences of TEM-metal specific electrical contact resistance
after levelling the distribution of metal particles in transient layer with clusters at
the value of A=1: a) h=20 μm, b) h=150 μm. 1 – K=0.1; 2 – K=0.5;
3 – K=1; 4 – K=5; 5 – K=10.

From the figures it is seen that just as in the case of transient contact layer without clusters, the electrical contact resistance decreases with increase in the nonparabolicity degree of the band spectrum of SL TEM and the intensity of metal entering transient layer in the process of its creation, and increases with a rise in temperature. In so doing, it also decreases after levelling the distribution of metal particles in transient layer. On the whole, in the considered range of degrees of nonparabolicity (openness of SL TEM FS), the intensities of metal particles entering transient layer, the thicknesses of contact layers and temperatures, the electrical contact resistance due to steady-state diffusion of metal particles with formation of clusters varies in the range from $8 \cdot 10^{-9}$ to $4.5 \cdot 10^{-7}$ Ohm·cm^2. This range is somewhat broader than in the case when transient contact layer formed in the process of steady-state diffusion of metal atoms in SL TEM has no clusters.

Conclusions

1. It was established that, just as in the case of formation of SL TEM-metal transient contact layer due to the deviation of SL TEM surface from the ideal plane, in the cases of said transient contact layer formation due to steady-state diffusion of metal in SL TEM with or without formation of clusters, SL TEM-metal electrical contact resistance decreases essentially with increase in the degree of nonparabolicity of SL TEM band spectrum, or, which is the same, the degree of openness of SL TEM FS.

2. As in the case of TEM with a parabolic band spectrum, the TEM-metal electrical contact resistance decreases with increasing intensity of metal entering transient layer and as a result of subsequent levelling the distribution of metal atoms in transient layer, for instance, due to annealing.

3. At the thickness of transient layer 20 μm and the degree of nonparabolicity of SL TEM band spectrum $K=10$, which corresponds to strongly open SL TEM FS, the electrical contact resistance at a temperature of 200 K tends to the asymptotic value equal to $8 \cdot 10^{-9}$ Ohm·cm^2. This value can be considered as minimum for this temperature. Though the character of

temperature dependence of the electrical contact resistance even at such degree of nonparabolicity depends on contact creation conditions, at 400 K this contact resistance does not exceed $2 \cdot 10^{-8}$ Ohm·cm^2.

4. On the whole, in the range of degrees of nonparabolicity K from 0.1 to 10, the thicknesses of contact layers from 20 to 150 μm and temperatures from 200 to 400 K, the electrical contact resistance of transient contact layer due to the deviation of SL TEM surface from the ideal plane varies from $8 \cdot 10^{-9}$ to $1.9 \cdot 10^{-7}$ Ohm·cm^2, the electrical contact resistance of transient contact layer due to steady-state diffusion of metal in SL TEM without formation of clusters – from $8 \cdot 10^{-9}$ to $4 \cdot 10^{-7}$ Ohm·cm^2, the electrical contact resistance of transient contact layer due to steady-state diffusion of metal in SL TEM with formation of clusters – from $8 \cdot 10^{-9}$ to $4.5 \cdot 10^{-7}$ Ohm·cm^2. Therefore, in the case of SL TEM the formation of clusters affects the SL TEM-metal electrical contact resistance significantly less than in the case of SL TEM with a parabolic band spectrum.

References

1. Fivaz R.F. (1967). Theory of layered structures. *J. Phys. Chem. Sol.*, 28 (5), 839-845.
2. Gorskyi P.V. (2019). The effect of nonparabolicity described by Fivaz model on the "thermoelectric material - metal" electrical contact resistance. In: Physics and Technology of Thin Films and Nanosystems. *XVII Freik International Conference. Abstract book (Ivano-Frankivsk, Ukraine, May 20 – 25, 2019).*
3. Gorskyi P.V. (2018). Estimation of the electrical and thermal contact resistances and thermoEMF of "thermoelectric material-metal" transient contact layer due to semiconductor surface roughness. *J.Thermoelectricity*, 4, 5-13.
4. Vikhor L. N., Anatychuk L.I., Gorskyi P.V. (2019). Electrical resistance of metal contact to Bi_2Te_3 based thermoelectric legs. *J. Appl. Phys.*, 126, 64503-1 – 164503-8. Available at: https://doi.org /10.1063/1.5117183.
5. Zaiman G. (1982). *Models of disorder*. Moscow: Mir.
6. Snarskii A.O., Zhenirovskii M.I., Bezsudnov I.V. (2006). The law of Wiedemann-Franz in thermoelectric composites. *J.Thermoelectricity*, 3, 59-65.

Горский П.В. *док. фіз.– мат. наук*[1,2]

[1]Институт термоэлектричества НАН и МОН Украины,
ул. Науки, 1, Черновцы, 58029, Украина
[2]Черновицкий национальный университет имени Юрия Федьковича,
ул. Коцюбинского 2, Черновцы, 58012, Украина

ВЛИЯНИЕ НЕПАРАБОЛИЧНОСТИ, ОПИСЫВАЕМОЙ МОДЕЛЬЮ ФИВАЗА НА ЭЛЕКТРИЧЕСКОЕ КОНТАКТНОЕ СОПРОТИВЛЕНИЕ ТЕРМОЭЛЕКТРИЧЕСКИЙ МАТЕРИАЛ - МЕТАЛЛ

Исследованы температурные зависимости электрического контактного сопротивления термоэлектрический материал - металл в случае, когда зонный спектр свободных носителей заряда в материале описывается моделью Фиваза. Рассмотрены переходный контактный слой, образованный отклонением поверхности полупроводникового термоэлектрического материала со сверхрешеткой (СРТЭМ) от идеальной плоскости и переходные контактные слои без кластеров и с кластерами, образованные в процессе стационарной диффузии частиц металла в СРТЭМ. Установлено, что контактное сопротивление резко снижается с ростом степени непараболичности зонного спектра СРТЭМ, которая определяется как отношение энергии Ферми идеального двумерного электронного (дырочного) газа с квадратичным законом дисперсии к ширине минизоны, описывающей трансляционное движение носителей заряда в направлении, перпендикулярном плоскости слоев. Такое снижение объясняется блокированием рассеяния свободных носителей заряда в направлении, перпендикулярном плоскости слоев. Показано, что в интервале степеней непараболичности К от 0.1 до 10, толщин переходного слоя от 20 до 150 мкм, безразмерных интенсивностей поступления атомов металла в объем переходного слоя А от 0 до 1 и температур от 200 до 400 К электрическое контактное сопротивление переходного слоя, обусловленного отклонением поверхности СРТЭМ от идеальной плоскости меняется от $8 \cdot 10^{-9}$ до $1.9 \cdot 10^{-7}$ Ом·см^2, переходного слоя, обусловленного стационарной диффузией металла в СРТЭМ без образования кластеров - от $8 \cdot 10^{-9}$ до $4 \cdot 10^{-7}$ Ом·см^2, переходного слоя, обусловленного стационарной диффузией металла в СРТЭМ с образованием кластеров - от $8 \cdot 10^{-9}$ до $4.5 \cdot 10^{-7}$ Ом· см^2.

Ключевые слова: модель Фиваза, сверхрешетки, энергия Ферми, минизоны, степень непараболичности, контакт термоэлектрический материал - металл, электрическое контактное сопротивление переходного слоя, отклонения поверхности термоэлектрического материала от идеальной плоскости, стационарная диффузия, интенсивность поступления частиц металла в полупроводник, кластеры.

Горський П.В. *док. фіз.– мат. наук*[1,2]

[1]Інститут термоелектрики НАН і МОН України,
вул. Науки, 1, Чернівці, 58029, Україна
[2]Чернівецький національний університет імені Юрія Федьковича,
вул. Коцюбинського 2, Чернівці, 58012, Україна

ВПЛИВ НЕПАРАБОЛІЧНОСТІ, ОПИСУВАНОЇ МОДЕЛЛЮ ФІВАЗА НА ЕЛЕКТРИЧНИЙ КОНТАКТНИЙ ОПІР ТЕРМОЕЛЕКТРИЧНИЙ МАТЕРІАЛ – МЕТАЛ

Досліджено температурні залежності електричного контактного опору термоелектричний матеріал – метал у випадку, коли зонний спектр вільних носіїв заряду у матеріалі описується моделлю Фіваза. Розглянуто перехідний контактний шар, утворений відхиленням поверхні напівпровідникового термоелектричного матеріалу з надграткою (НГТЕМ) від ідеальної площини та перехідні контактні шари без кластерів і з кластерами, утворені у процесі стаціонарної дифузії частинок металу у НГТЕМ. Встановлено, що контактний опір різко знижується зі зростанням ступеня непараболічності зонного спектру НГТЕМ, який визначається як відношення енергії Фермі ідеального двовимірного електронного (діркового) газу з квадратичним законом дисперсії до ширини мінізони, яка описує трансляційний рух носіїв заряду у напрямку, перпендикулярному до площини шарів. Таке зниження пояснюється блокуванням розсіювання вільних носіїв заряду у напрямку, перпендикулярному до площини шарів. Показано, що в інтервалі ступенів непараболічності K від 0.1 до 10, товщин перехідного шару від 20 до 150 мкм, безрозмірних інтенсивностей надходження атомів металу в об'єм перехідного шару A від 0 до 1 та температур від 200 до 400 К електричний контактний опір перехідного шару, зумовленого відхиленням поверхні НГТЕМ від ідеальної площини змінюється від 8·10⁻⁹ до 1.9·10⁻⁷ Ом·см², перехідного шару,зумовленого стаціонарною дифузією металу у НГТЕМ без утворення кластерів – від 8·10⁻⁹ до 4·10⁻⁷ Ом·см², перехідного шару,зумовленого стаціонарною дифузією металу у НГТЕМ з утворенням кластерів – від 8·10⁻⁹ до 4.5·10⁻⁷ Ом·см².

Ключові слова: *модель Фіваза, надгратка, енергія Фермі, мінізона, ступінь непараболічності, контакт термоелектричний матеріал – метал, електричний контактний опір перехідного шару, відхилення поверхні термоелектричного матеріалу від ідеальної площини, стаціонарна дифузія, інтенсивність надходження частинок металу у напівпровідник, кластери.*

References

1. Fivaz R.F. (1967). Theory of layered structures. *J. Phys. Chem. Sol.*, 28 (5), 839-845.
2. Gorskyi P.V. (2019). The effect of nonparabolicity described by Fivaz model on the "thermoelectric material - metal" electrical contact resistance. In: Physics and Technology of Thin Films and Nanosystems. *XVII Freik International Conference. Abstract book (Ivano-Frankivsk, Ukraine, May 20 – 25, 2019).*
3. Gorskyi P.V. (2018). Estimation of the electrical and thermal contact resistances and thermoEMF of "thermoelectric material-metal" transient contact layer due to semiconductor surface roughness. *J.Thermoelectricity*, 4, 5-13.
4. Vikhor L. N., Anatychuk L.I., Gorskyi P.V. (2019). Electrical resistance of metal contact to Bi_2Te_3 based thermoelectric legs. *J. Appl. Phys.*, 126, 64503-1 – 164503-8. Available at: https://doi.org /10.1063/1.5117183.
5. Zaiman G. (1982). *Models of disorder*. Moscow: Mir.
6. Snarskii A.O., Zhenirovskii M.I., Bezsudnov I.V. (2006). The law of Wiedemann-Franz in thermoelectric composites. *J.Thermoelectricity*, 3, 59-65.

Cherkez R.G., *doc. phys. - math. sciences*, *acting Professor*[1,2]

[1]Institute of Thermoelectricity of the NAS and MES of Ukraine,
1, Nauky str., Chernivtsi, 58029, Ukraine
[2]Yuriy Fedkovych Chernivtsi National University,
2, Kotsiubynsky str., Chernivtsi, 58012, Ukraine

Cherkez R.G.

INFLUENCE OF PLATE THICKNESS ON THE EFICIENCY OF A PERMEABLE PLANAR COOLING THERMOELEMENT

This paper presents the theory of calculation and computer methods of search for optimal parameters (electric current density, heat carrier flow rate) of a permeable planar cooling thermoelement whereby the energy conversion efficiency will be maximum. The thickness of leg plates of a permeable thermoelement based on Bi-Te at which the coefficient of performance will be maximum is calculated. It is shown that the rational use of such energy converters allows increasing the coefficient of performance by 20-40 %. Bibl. 9, Fig. 2, table 1.
Key words: *thermoelectric materials, coefficient of performance, cooling capacity, design of a permeable planar thermoelement.*

Introduction

There are thermoelements in which heat exchange with the heat source and sink occurs not only on the thermoelement junctions, but also in the bulk of the leg material [1 – 3]. Variants of implementation of such models are permeable thermoelements where in the leg material along the direction of electric current flow there are channels (pores) for pumping of the heat carrier. By controlling the heat transfer conditions (heat carrier velocity, heat transfer intensity, etc.) in combination with the distribution of physical effects in the leg material, it is possible to influence the energy conversion efficiency.

The study of permeable thermoelements [3 – 5] showed a good outlook for their use, since it allows increasing the coefficient of performance by a factor of 1.3-1.6.

However, their practical implementation is related to certain material research and technological difficulties, which encourages the search and study of simpler variants of physical models of converters with internal heat transfer.

A variant of implementation of internal heat exchange are permeable planar thermoelements where each leg consists of a certain number of plates spaced apart. The gaps between the plates form channels through which the heat carrier (liquid or gas) is pumped.

Research on such thermoelements with a view to determine the optimal thickness of plates and maximum characteristics of energy conversion is a relevant task, which is the purpose of this paper.

Physical model and its mathematical description

A physical model of a planar permeable thermoelement working in the mode of thermoelectric cooling is shown in Fig. 1. It comprises *n*- and *p*-type legs, each leg consisting of N_p segments (planes) that are h_k apart. The width of the segment is h, and its thickness – h_p. The gaps between the segments

form channels through which the heat carrier (air or liquid) is pumped to cool it. The hot and cold junctions of the thermoelement are maintained at constant values of T_h and T_c, respectively. The coolant is pumped in the direction from the hot to cold junctions. The temperature of the heat carrier at the inlet of the thermoelement is T_a. The heat transfer coefficient of the heat carrier inside the channels of a permeable planar thermoelement is α_T.
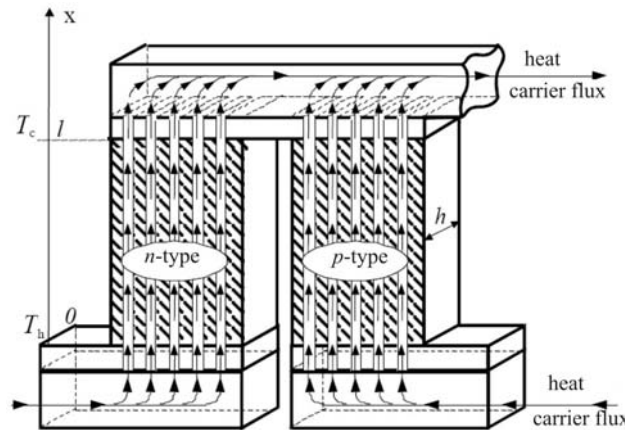
Fig. 1. Model of a permeable planar thermoelement.

To find the distribution of temperatures in thermoelement material, it is necessary to solve a differential equation

$$\frac{d}{dx}\left(\kappa(T)\frac{dT}{dx}\right) + i^2\rho(T) - Ti\frac{d\alpha(T)}{dx} - \frac{2}{h_p}\alpha_T(T-t) = 0, \qquad (1)$$

Where t is heat carrier temperature at point x; T is leg temperature at point x; α_T is heat transfer coefficient; i is electric current density ($i = I/S$ - S_K) $\alpha(T)$, $\kappa(T)$, $\rho(T)$ – the Seebeck coefficient, thermal conductivity and resistivity of material are functions of temperature T. Note that thermoelectric medium parameters α, κ, ρ are interdependent. The system of these relations sets certain area G_ξ of change in the inhomogeneity ξ. Specifying material of the leg, one must assign these relations, for instance, in the form of theoretical or experimental dependences of α, κ, ρ on T and determine G_ξ.

On the area of leg segment dx, a change in heat carrier temperature dt is determined by the law of conservation of energy. A differential equation for the distribution of heat carrier temperature t is of the form

$$\frac{dt}{dx} = \frac{2}{Vc_Ph_p}\alpha_T(T-t). \qquad (2)$$

where V is specific mass velocity of heat carrier in the channel ($V = v\rho_T$; v is velocity, ρ_T is heat carrier density); c_P is specific heat of heat carrier.

Eqs. (1) and (2), written for n- and p-type thermoelement legs, form a system of differential equations to determine the distribution of temperatures.

$$\left. \begin{cases} \dfrac{d}{dx}\left(\kappa(T,\xi)\dfrac{dT}{dx}\right)+i^2\rho(T,\xi)- \\ \qquad\qquad -Ti\dfrac{d\alpha(T,\xi)}{dx}-\dfrac{2\alpha_T}{h_p}(T-t)=0, \\ \dfrac{dt}{dx}=\dfrac{2\alpha_T}{Vc_p h_P}(T-t). \end{cases} \right\}_{n,p} \qquad (3)$$

Consider the problem of the maximum energy efficiency of thermoelectric cooling at fixed temperatures of heat sources T_h and T_c.

The problem reduces to finding coefficient of performance maximum

$$\varepsilon = \frac{Q_c}{Q_h - Q_c}, \qquad (4)$$

at differential relations (3) and boundary conditions:

$$T_{n,p}(0)=T_h, \quad T_{n,p}(1)=T_c, \quad t_{n,p}(0)=T_s. \qquad (5)$$

where T_h is the hot side temperature of junctions, T_c is the cold side temperature of junctions, T_s is the initial temperature of heat carrier; Q_h, Q_c, are thermal fluxes which the thermoelement exchanges with the external heat sources

$$Q_h = Q_n(0)+Q_p(0),$$

$$Q_c = Q_n(1)+Q_p(1)+Q_L,$$

where Q_L is the heat supplied due to internal heat exchange

$$Q_L = \sum_{n,p} Vc_P S_R \left(t(0)-t(1)\right).$$

Hereinafter, instead of maximum ε it is convenient to consider minimum of functional I:
$$I = \ln q(0) - \ln q(1), \qquad (6)$$
where

$$q(0)=\frac{Q_h}{I}=q_n(0)+q_p(0),$$

$$q(1)=\frac{Q_c}{I}=q_n(1)+q_p(1)+\frac{Q_L}{j(S\text{-}S_K)}l,$$

where $q_n(1), q_p(1), q_n(0), q_n(0)$ are the values of specific heat fluxes on the cold and hot thermoelement junctions for n and p–type legs that are determined from solving the system of differential equations (3).

The optimization problem is to *choose* from the control area $\xi \in G_\xi$ such concentration functions $\xi^{n,p}(x)$ and simultaneously *assign* such a specific mass velocity of heat carrier in the channels $V=V_O$ which under *restrictions* (3),(4) and *the condition* for electric current density

$$q_n(1)+q_p(1)=0, \qquad (7)$$

impart to *functional* I *the lowest value*, in which case the coefficient of performance ε will be maximum [7].

Problem solving method and calculation results

To solve the problem, we use the mathematical optimal control theory, developed under the guidance of L.S. Pontryagin, as applied to permeable thermoelements [8]. We specify the formalism of the mathematical optimal control theory in relation to our problem.

Functions $\psi(x)$ (pulses) must satisfy a system of equations that is canonically conjugate to system (3) and is given by:

$$
\left.
\begin{cases}
\dfrac{d\psi_1}{dx} = \dfrac{\alpha\, j}{\kappa} R_1 \psi_1 - \left(\dfrac{\alpha\, j}{\kappa} R_2 - \dfrac{\alpha_T \Pi_K N_K l^2}{(S-S_K)j} \right)\psi_2 \\
\qquad\qquad - \dfrac{\alpha_T \Pi_K N_K l}{V c_P S_R}\psi_3, \\[2mm]
\dfrac{d\psi_2}{dx} = \dfrac{j}{\kappa}\psi_1 - \dfrac{\alpha\, j}{\kappa}\psi_2, \\[2mm]
\dfrac{dt}{dx} = -\dfrac{\alpha_T \Pi_K N_K l^2}{(S-S_K)j}\psi_2 + \dfrac{\alpha_T \Pi_K N_K l}{V c_P S_R}\psi_3.
\end{cases}
\right\}_{n,p}
$$

where

$$
\left.
\begin{cases}
R_1 = 1 + \dfrac{d\ln\alpha}{dT}T - \dfrac{d\ln\kappa}{dT}\left(T+\dfrac{q}{\alpha}\right), \\[2mm]
R_2 = R_1 + \dfrac{1}{Z_K}\dfrac{d\ln\sigma}{dT} + \dfrac{d\ln\kappa}{dT}\left(T+\dfrac{q}{\alpha}\right).
\end{cases}
\right\}_{n,p}
$$

The boundary (transversality) conditions for this system are as follows:

$$\psi(0) = \left.\frac{\partial \overline{J}}{\partial y}\right|_{x=0}, \qquad \psi(1) = -\left.\frac{\partial \overline{J}}{\partial y}\right|_{x=1}$$

where $\overline{J} = J + \sum(v,g)$ is an expanded functional; v, g are vectors of undetermined Lagrange multipliers and the boundary conditions (5).

Then the boundary conditions for the conjugate system will take on the form

$$\psi_2^{n,p}(0) = \frac{1}{q_n(0) + q_p(0)},$$

$$\psi_2^{n,p}(1) = -\frac{(S - S_K)j}{lVc_P S_R\left(2t(0) - t_n(1) - t_p(1)\right)},$$

$$\psi_3^{n,p}(1) = -\frac{1}{2t(0) - t_n(1) - t_p(1)}.$$

Using the above system of equations with regard to relations (3),(5) and the numerical methods, we created a program of computer design of optimal functions of thermoelectric material inhomogeneity $\xi(x)$ and optimal heat carrier velocity V with a view to achieve maximum energy efficiency of a permeable planar cooling thermoelement.

Results of studying a permeable planar thermoelement for Bi-Te based materials

We present the results of computer design of the optimal inhomogeneity of semiconductor thermoelectric material in combination with the optimal distribution function of heat sources (sinks) for permeable planar cooling thermoelements. The heat transfer coefficient of the heat carrier inside the channels was 0.01 W / cm^{2}K.

As the initial data for such optimization, the experimental temperature dependences of characteristics of *n*- and *p*-type *Bi-Te* based semiconductor materials α, σ, κ for various impurity concentrations were used [9].

Dependences of maximum coefficient of performance (COP), thermoelement cooling capacity (Qcc), power consumption (W), voltage (U), heat carrier temperature at the outlet from thermoelement (Tc_v), optimal heat carrier flow rate (V_O) on plate thickness (h_p) for the height of legs *l*= 1.0 cm are presented in the table

Таблица

Залежності характеристик термоелемента від ширини пластини

h_p, cm	0.5	0.1	0.05	0.01	0.005
COP	0.524	0.566	0.574	0.581	0.58
Q_c, Вт	2.660	0.5654	0.2869	0.0582	0.029
W, W	5.06	0.999	0.500	0.100	0.050
U, V	0.071	0.071	0.071	0.071	0.071
T_{cv}, K	280.3	255.1	252.5	250.5	250.25
V_{opt}, kg/(cm^2 s)	0.135	0.0126	0.006	0.0012	0.0006

It is seen that there is an optimal plate thickness (0.1 cm) whereby the characteristics of the thermoelement have the most favorable values.

The results of calculation of the influence of channel width on the characteristics of a permeable thermoelement with the number of channels 10 pcs, the height of legs 1 cm are presented in Fig. 2. The plots of characteristics of a permeable planar cooling thermoelement (coefficient of performance ε, heat flux Q, heat carrier velocity V) on channel width $H_к$ are constructed here.
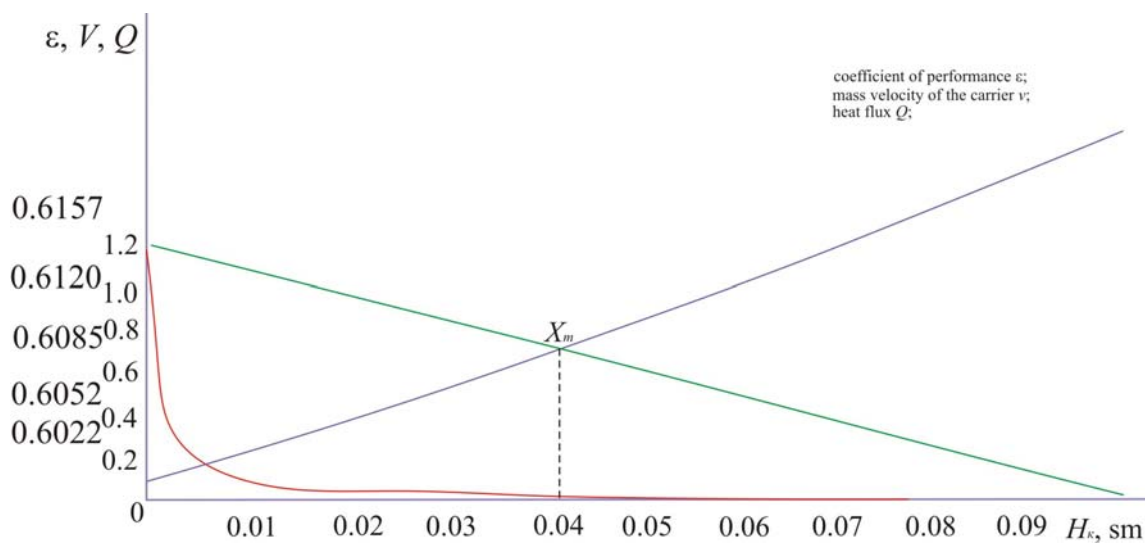
Fig. 2. Dependence of coefficient of performance ε, heat carrier velocity V
and heat flux Q on channel width.

The intersection of the two lines will show us the rational value of channel width whereby the cooling capacity and coefficient of performance will have the most favorable values. In this case, channel width is approximately 0.04 cm

Efficiency comparison with classical thermoelements indicates the possibility of improving the coefficient of performance by a factor of 1.2-1.4.

Conclusions

1. The optimal thickness of leg plate whereby the thermoelement characteristics have the most favourable values for *Bi-Te* based material is 0.1 cm.

2. The use of permeable thermoelectric coolers of such power converters allows increasing the coefficient of performance by 20-40%.

3. The results demonstrate the prospects of research and creation of permeable planar thermoelectric coolers.

References

1. Kozliuk V.N., Shchegolev G.M. (1973). Termodinamicheskii analiz pronitsaiemykh termoelektricheskikh kholodilnikov [Thermodynamic analysis of permeable thermoelectric coolers]. *Teplofizika i teplotekhnika – Thermophysics and Heat Engineering*, issue 25, 96-100 [in Russian].

2. Kotyrlo G.K., Kozliuk V.N., Lobunets Yu.N. (1975). Termoelektricheskii generator s razvitoi poverkhnostiu teploobmena [Thermoelectric generator with a developed heat exchange surface].

Teplotekhnicheskiie problemy priamogo preobrazovaniia energii – Thermotechnical Problems of Direct Power Conversion, issue 7, 85-95 [in Russian].

3. Lobunets Yu.N. (1989). *Metody rascheta i proektirovaniia termoelektricheskiikh preobrazovatelei energii [Methods for calculation and design of thermoelectric power converters]*. Kyiv: Naukova Dumka [in Russian].

4. Anatychuk L.I., Cherkez R.G. (2003). On the properties of permeable thermoelements. *Proc. of XXII Intern. Conf. on Thermoelectrics* (France), 480-483.

5. Cherkez R.G. (2003). Thermoelements with internal and lateral heat exchange. *J.Thermoelectricity*, 1, 70-77.

6. Anatychuk L.I., Vikhor L.N., Cherkez R.G. (2000). Optimal control of the inhomogeneity of semiconductor material for permeable cooling thermoelements. *J.Thermoelectricity*, 3, 46-57.

7. *Pontriagin L.S., Boltianskii V.G., Gamkrelidze R.V., Mishchenko E.F. (1976). Matematicheskaia teoriia optimalnykh processov [Mathermatical theory of optimal processes]*. Moscow: Nauka [in Russian].

8. Cherkez R.G. (2016). On the simulation of permeable thermoelements. *J.Thermoelectricity*, 1.

9. Anatychuk L.I., Vikhor L.N. (2012). *Thermoelectricity. Vol. 4. Functionally graded thermoelectric materials*. Chernivtsi: Bukrek.

Черкез Р.Г. *док. фіз.-мат. наук, в.о. професора*[1,2]

[1]Інститут термоелектрики НАН і МОН України, вул. Науки, 1,
Чернівці, 58029, Україна, *e-mail: anatych@gmail.com*;
[2]Чернівецький національний університет ім. Юрія Федьковича,
вул. Коцюбинського 2, Чернівці, 58000, Україна

ВПЛИВ ТОВЩИНИ ПЛАСТИН НА ЕФЕКТИВНІСТЬ РОНИКНОГО ПЛОЩИННОГО ТЕРМОЕЛЕМЕНТА ОХОЛОДЖЕННЯ

Представлено теорію розрахунку та комп'ютерні методи пошуку оптимальних параметрів (густина електричного струму, витрати теплоносія) проникного площинного термоелемента охолодження, при яких ефективність перетворення енергії буде максимальною. Розрахована товщина пластин вітки проникного термоелемента на основі матеріалу Bi-Te, при якій холодильний коефіцієнт буде максимальним. Показано, що раціональне використання таких перетворювачів енергії дозволяє підвищити холодильний коефіцієнт на 20-40 %. Бібл. 9, рис. 2, таблиця 1.

Ключові слова: термоелектричні матеріали, холодильний коефіцієнт, холодопродуктивність, проектування проникного площинного термоелемента.

Черкез Р,Г. [1,2], *док. физ.-мат. наук, в.о. профессора*[1,2]

[1]Институт термоэлектричества НАН и МОН Украины ул. Науки, 1,
Черновцы, 58029, Украина; *e - mail: anatych@gmail.com;*
[2]Черновицкий национальный университет имени Юрия Федьковича,

ул. Коцюбинського 2 Черновцы, 58012, Украина

ВЛИЯНИЕ ТОЛЩИНЫ ПЛАСТИН НА ЭФФЕКТИВНОСТЬ ПРОНИЦАЕМОГО ПЛОСКОСТНОГО ТЕРМОЭЛЕМЕНТА ОХЛАЖДЕНИЯ

Представлены теория расчета и компьютерные методы определения оптимальных параметров (плотность электрического тока, расхода теплоносителя) проницаемого плоскостного термоэлемента охлаждения, при которых эффективность преобразования энергии максимальна. Рассчитана толщина пластин ветви проницаемого термоэлемента на основе материала Bi-Te, при которой холодильный коэффициент максимален. Показано, что рациональное использование таких преобразователей энергии позволяет повысить холодильный коэффициент на 20-40 %. Библ. 9, рис. 2 таблица 1.

Ключевые слова: термоэлектрические материалы, холодильный коэффициент, холодопроизводительность, проектирование проницаемого плоскостного термоэлемента

References

10. Kozliuk V.N., Shchegolev G.M. (1973). Termodinamicheskii analiz pronitsaiemykh termoelektricheskikh kholodilnikov [Thermodynamic analysis of permeable thermoelectric coolers]. *Teplofizika i teplotekhnika – Thermophysics and Heat Engineering*, issue 25, 96-100 [in Russian].

11. Kotyrlo G.K., Kozliuk V.N., Lobunets Yu.N. (1975). Termoelektricheskii generator s razvitoi poverkhnostiu teploobmena [Thermoelectric generator with a developed heat exchange surface]. *Teplotekhnicheskiie problemy priamogo preobrazovaniia energii – Thermotechnical Problems of Direct Power Conversion*, issue 7, 85-95 [in Russian].

12. Lobunets Yu.N. (1989). *Metody rascheta i proektirovaniia termoelektricheskiikh preobrazovatelei energii [Methods for calculation and design of thermoelectric power converters]*. Kyiv: Naukova Dumka [in Russian].

13. Anatychuk L.I., Cherkez R.G. (2003). On the properties of permeable thermoelements. *Proc. of XXII Intern. Conf. on Thermoelectrics* (France), 480-483.

14. Cherkez R.G. (2003). Thermoelements with internal and lateral heat exchange. *J.Thermoelectricity*, 1, 70-77.

15. Anatychuk L.I., Vikhor L.N., Cherkez R.G. (2000). Optimal control of the inhomogeneity of semiconductor material for permeable cooling thermoelements. *J.Thermoelectricity*, 3, 46-57.

16. *Pontriagin L.S., Boltianskii V.G., Gamkrelidze R.V., Mishchenko E.F. (1976). Matematicheskaia teoriia optimalnykh processov [Mathermatical theory of optimal processes]*. Moscow: Nauka [in Russian].

17. Cherkez R.G. (2016). On the simulation of permeable thermoelements. *J.Thermoelectricity*, 1.

18. Anatychuk L.I., Vikhor L.N. (2012). *Thermoelectricity. Vol. 4. Functionally graded thermoelectric materials*. Chernivtsi: Bukrek.

Kshevetsky O.S., *cand. Phys. - math. Sciences,*
assistant professor
Orletskyi O.V.

Chernivtsi Institute of Trade and Economics
of Kyiv National University of Trade and Economics**,**
7, Tsentralna Square, Chernivtsi, 58002, Ukraine

Kshevetsky O.S

Orletskyi O.V.

ESTIMATION OF THE EFFICIENCY OF PARTIAL CASE OF HEAT AND MASS TRANSFER PROCESSES BETWEEN HEAT PUMPS AND MOVING SUBSTANCE PART 3

A theoretical model for evaluating the efficiency of the partial case of heat and mass transfer processes between a moving substance and thermoelectric heat pumps with their heat exchange parts, in which the moving substance (or at least part of this moving substance) is brought into thermal contact with heat absorbing and heat dissipating heat exchangers , which can operate in modes that may differ from the mode of maximum energy efficiency, in particular, taking into account the amounts of materials required for the manufacture of these thermoelectric heat pumps. The results of the corresponding theoretical estimation are given. Bibl. 9, Tabl. 1, Fig. 2.
Key words: heat pump, moving substance, heat and mass transfer, efficiency, energy efficiency, thermoelectric heat pump, thermoelements, thermoelectric material.

Introduction

This paper (part 3) is a continuation of the previous works [1, 2] (part 1 and part 2). In this part 3 we will use abbreviations that were introduced in [1, 2], in the same sense as in [1, 2]. We will also use the word combination the investigated process in order to indicate the process which corresponds to the investigated method of heat and mass transfer [1 - 5]. In [1, 2], mathematical expressions were obtained for estimating the efficiency of the investigated method of heat and mass transfer and examples of appropriate calculations were given, in particular, for the case of using thermoelectric heat pumps (THPs) that operate in the modes if maximum energy efficiency. According to the data of these calculations, there exists a possibility to increase the energy efficiency of the investigated method of heat and mass transfer owing to increased number of heat pumps (HPs) that are used in this case. At the same time, in [1, 2], the details of how the amount of materials from which the HPs are made changes with a change in the number of HPs.

The purpose of this work is to create theoretical prerequisites for an approximate quantitative estimation of the efficiency (primarily energy efficiency) of the investigated method of heat and mass transfer using THPs that can operate in the modes that may differ from the maximum energy efficiency, in particular, with regard to the amount of materials of which these THPs are made. To achieve this purpose, the objectives of this work are to create an appropriate estimation model, obtain mathematical expressions for estimation calculations and obtain examples of relevant calculations.

Description of estimation model

Consider the following example of *the investigated processes*. Consider the processes involving moving substance (MS) and at least one THP (all HPs used in these processes are THPs based on thermocouples), in which according to Fig. 2 [1] MS in its input flow is cooled by all individual THPs.

Let the useful effect of these processes be to maintain the temperature difference of the MS in its input flow between the positions 1.0 and 1.n according to Fig. 2 [1] (for some MS the inlet temperature in position 1.0). This useful effect is carried out due to the total power consumption of all THPs W^{TTH} (and more directly due to the total cooling capacity of all THPs Q_{cool}^{TTH}). In this work (part 3) we will not take into account the energy consumption to create a MS flow [6].

Consider an individual *i*-th THP.

We use a well-known ratio to determine the coefficient of performance of the *i*-th THP ε_i^{TE} [7, 8]:

$$\varepsilon_i^{TE} = \frac{Q_{cool,i}^{TE}}{W_i^{TE}}, \tag{3.1}$$

where

$$Q_{cool,i}^{TE} = \alpha_i I_i T_{cool,i}^{TE} - \frac{1}{2} I_i^2 r_i - k_i \left(T_{hot,i}^{TE} - T_{cool,i}^{TE} \right); \tag{3.2}$$

$$W_i^{TE} = I_i^2 r_i + \alpha_i \left(T_{hot,i}^{TE} - T_{cool,i}^{TE} \right) I_i; \tag{3.3}$$

$Q_{cool,i}^{TE}$ – is total cooling capacity of thermoelements of the *i*-th THP; W_i^{TE} is total electrical power consumed by thermoelements of the *i*-th THP; α_i is total differential Seebeck coefficient of material of thermoelements of the *i*-th THP; I_i is strength of current flowing through thermoelements of the *i*-th THP; r_i is total electrical resistance of thermoelements of the *i*-th THP; k_i is total thermal conductivity of thermoelements of the *i*-th THP; $T_{hot,i}^{TE}$ is temperature of heat-releasing junctions of thermoelements of the *i*-th THP; $T_{cool,i}^{TE}$ is temperature of heat-absorbing junctions of the *i*-th THP.

The coefficient of performance of the *i*-th THP that works in the investigated process according to Fig. 2 [1] and with regard to assumption 6 [1] ($d = const$) ε_i^{TTH}:

$$\varepsilon_i^{TTH} = \frac{Q_{cool,i}^{TTH}}{W_i^{TTH}} = \frac{T_{cool,(i-1)}^{PP} - T_{cool,i}^{PP}}{\left(T_{hot,(i-1)}^{PP} - T_{hot,i}^{PP} \right) - \left(T_{cool,(i-1)}^{PP} - T_{cool,i}^{PP} \right)}, \tag{3.4}$$

where $Q_{cool,i}^{TTH}$ is cooling capacity of the *i*-th THP; W_i^{TTH} is power consumed by the *i*-th THP; $T_{hot,i}^{MS}$ is temperature of MS immediately before its thermal contact with heat-releasing heat-exchange part (HE) of the *i*-th THP; $T_{hot,(i-1)}^{MS}$ is temperature of MS immediately after its thermal contact with heat-releasing HE of

the *i*-th THP; $T_{cool,i}^{MS}$ is temperature of MS immediately after its thermal contact with heat-absorbing HE of the *i*-th THP; $T_{cool,(i-1)}^{MS}$ is temperature of MS immediately before its thermal contact with heat-absorbing HE of the *i*-th THP.

Let $Q_{cool,i}^{TTH} = Q_{cool,i}^{TE}$ and $W_i^{TTH} = W_i^{TE}$. Then, on the basis of expressions (1) and (4) one can write:

$$\varepsilon_i^{TE} = \varepsilon_i^{TTH}, \tag{3.5}$$

$$\frac{T_{cool,(i-1)}^{MS} - T_{cool,i}^{MS}}{\left(T_{hot,(i-1)}^{MS} - T_{hot,i}^{MS}\right) - \left(T_{cool,(i-1)}^{MS} - T_{cool,i}^{MS}\right)} = \frac{\alpha_i I_i T_{cool,i}^{TE} - \frac{1}{2} I_i^2 r_i - k_i \left(T_{hot,i}^{TE} - T_{cool,i}^{TE}\right)}{I_i^2 r_i + \alpha_i \left(T_{hot,i}^{TE} - T_{cool,i}^{TE}\right) I_i}. \tag{3.6}$$

We will assume that heat transfer from MS to heat-absorbing junctions of thermoelements of the *i*-th THP is carried out through the medium characterized by the corresponding resistance of heat transfer (thermal resistance) $R_{cool,i}$, and heat transfer from heat-releasing junctions of thermoelements of the *i*-th THP to MS is carried out through the medium heat transfer resistance (thermal resistance). We will also assume that there are no other additional factors that could affect the heat transfer between the MS and the *i*-th THP. Then we can write the following equations, which, in particular, reflect the relationship between the junction temperatures of thermoelements of the *i*-th THP and MS (in the corresponding positions of its motion):

$$T_{cool,i}^{MS} - T_{cool,i}^{TE} = Q_{cool,i}^{TE} R_{cool,i}, \tag{3.7}$$

$$T_{cool,i}^{MS} - T_{cool,i}^{TE} = \left(\alpha_i I_i T_{cool,i}^{TE} - \frac{1}{2} I_i^2 r_i - k_i \left(T_{hot,i}^{TE} - T_{cool,i}^{TE}\right)\right) R_{cool,i} \tag{3.8}$$

(expression (3.8) was obtained with the use of expression (2));

$$T_{hot,i}^{TE} - T_{hot,(i-1)}^{MS} = Q_{hot,i}^{TE} R_{hot,i}, \tag{3.9}$$

$$T_{hot,i}^{TE} - T_{hot,(i-1)}^{MS} = \left(\alpha_i I_i T_{hot,i}^{TE} + \frac{1}{2} I_i^2 r_i - k_i \left(T_{hot,i}^{TE} - T_{cool,i}^{TE}\right)\right) R_{hot,i}, \tag{3.10}$$

where $Q_{hot,i}^{TE}$ is total calorific power of thermoelements of the *i*-th THP

$$Q_{hot,i}^{TE} = \alpha_i I_i T_{hot,i}^{TE} + \frac{1}{2} I_i^2 r_i - k_i \left(T_{hot,i}^{TE} - T_{cool,i}^{TE}\right) [7, 8]).$$

As a characteristic of MS flow we will use heat capacity losses of MS (the rate of losing MS, if the amount of MS is expressed in the units of its heat capacity) V_C^{MS}, (J/K)/s or W/K:

$$V_C^{MS} = \frac{C^{MS}}{\Delta \tau},$$

(3.11)

where C^{MS} is heat capacity of MS that takes part in the corresponding process during time interval $\Delta \tau$ (in some position of MS motion, for instance, according to Fig. 2 [1] – in position 1.1; in the context of this work we will consider that V_C^{MS} is the same in all positions of MS motion).

For instance, if we know the specific mass heat capacity of MS c_m^{MS} and mass losses of MS M^{MS}, then the heat capacity losses of MS can be determined by the formula:

$$V_C^{MS} = c_m^{MS} M^{MS}.$$

(3.12)

With regard to assumption 6 [1] and the information given above, we write the equation, which, in particular, reflects the relationship between the total cooling capacity of thermocouples of the *i*-th THP, the change in MS temperature as a result of its thermal contact with heat-absorbing HE of the *i*-th THP and the heat capacity losses of MS:

$$V_C^{MS} \left(T_{cool,(i-1)}^{MS} - T_{cool,i}^{MS} \right) = \alpha_i I_i T_{cool,i}^{TE} - \frac{1}{2} I_i^2 r_i - k_i \left(T_{hot,i}^{TE} - T_{cool,i}^{TE} \right).$$

(3.13)

With regard to assumption 6 [1] and the information given above, we write the equation which, in particular, reflects the relationship between total calorific power of thermoelements of the *i*-th THP, change in MS temperature as a result of its thermal contact with heat-releasing HE of the *i*-th THP and heat capacity losses of MS:

$$V_C^{MS} \left(T_{hot,(i-1)}^{MS} - T_{hot,i}^{MS} \right) = \alpha_i I_i T_{hot,i}^{TE} + \frac{1}{2} I_i^2 r_i - k_i \left(T_{hot,i}^{TE} - T_{cool,i}^{TE} \right).$$

(3.14)

With regard to assumption 6 [1] and the information given above, we write the equation which, in particular, reflects the relationship between the total power consumption of thermoelements of the *i*-th THP, total change in MS temperature as a result of its thermal contact with heat-absorbing and heat-releasing HEs of the *i*-th THP and heat capacity losses of MS:

$$V_C^{MS} \left(\left(T_{hot,(i-1)}^{MS} - T_{hot,i}^{MS} \right) - \left(T_{cool,(i-1)}^{MS} - T_{cool,i}^{MS} \right) \right) = I_i^2 r_i + \alpha_i \left(T_{hot,i}^{TE} - T_{cool,i}^{TE} \right) I_i.$$

(3.15)

In this work (part 3) we will assume that the values $R_{hot,i}$, $R_{cool,i}$, α_i, r_i, k_i are constant (their possible temperature and other dependences will be disregarded) for an individual case.

Equations (3.6), (3.8), (3.10), (3.13), (3.14), (3.15) can be used for estimation calculations of the operating modes of individual THPs and the investigated processes in general.

For the above described example we will use an indicator of the energy efficiency of the investigated process ω_{cool}:

$$\omega_{cool} = \frac{Q_{cool}^{\text{TTH}}}{W^{TTH}} = \frac{\Delta T_{cool}^{PP}}{\Delta T_{hot}^{PP} - \Delta T_{cool}^{PP}} \qquad (3.16)$$

(the right-hand side of this expression was obtained with the use of expressions (1), (23) and (24) [1]), where ΔT_{cool}^{MS} in conformity with the diagram in Fig. 2 [1] is the temperature difference of MS which is formed as a result of cooling MS in its input flow by all individual THPs; ΔT_{hot}^{MS} in conformity with the diagram in Fig. 2 [1] is the temperature difference of MS which is formed as a result of heating MS in its output flow by all individual THPs.

Note that when in the investigated process only one THP is used, then ω_{cool} is equal to the coefficient of performance of this single THP ε_1^{TTH}.

On the change in the amount of materials

The technical implementation of the investigated method of heat and mass transfer can be carried out using a suitable device. The cost, weight, size and other characteristics of such a device may depend on the quantities (e.g. masses) of the materials of which THPs are made, for example, in particular, on the amount of thermoelectric material of which the thermocouple legs are made (e.g. bismuth telluride material) and on the amount of material of which HEs are made (for example, in the first place, the aluminum-based material of which the heat exchangers are made). With a change in the number of THPs n, which are used to implement the investigated method of heat and mass transfer, the above amounts of this or other material can remain unchanged, decrease or increase. As characteristics of this, you can use the coefficient of change in the amount of thermoelectric material (with a corresponding change in the implementation of the investigated method of heat and mass transfer) and the coefficient of change in the amount of material of which the heat exchangers $\varphi_{l_0}^{l_x}$ are made (with a corresponding change in the implementation of the investigated method of heat and mass transfer):

$$\gamma_{l_0}^{l_x} = \frac{m_{l_x}^{TM}}{m_{l_0}^{TM}} ; \qquad (3.17)$$

$$\varphi_{l_0}^{l_x} = \frac{m_{l_x}^{MHE}}{m_{l_0}^{MHE}} , \qquad (3.18)$$

where $m_{l_0}^{TM}$ is the amount of thermoelectric material, expressed in appropriate units (for example, mass, expressed in kilograms) in the case (variant) of the implementation of the investigated method of heat and mass transfer, with which the comparison is carried out (in the initial case); l_0 is designation of this initial case (as a variant – its number in Table 3.1); $m_{l_x}^{TM}$ is the corresponding amount of thermoelectric material (expressed in the same units) in the case (variant) of implementation of the investigated method of heat and mass transfer which is considered (compared); l_x is designation of this compared case (as a variant – its number in Table 1); $m_{l_0}^{MHE}$ is the amount of material of which the heat exchangers are made, expressed in

appropriate units (for instance, mass, expressed in kilograms) in the case (variant) of implementation of the дinvestigated method of heat and mass transfer, with which the comparison is carried out (in the initial case); l_0 is designation of this initial case (as a variant – its number in Table); $m_{n_{ch}}^{MHE}$ is the corresponding amount of material of which the heat exchangers are made (expressed in the same units) in the case (variant) of implementation of the investigated method of heat and mass transfer, which is considered (compared); l_x is the designation of this compared case (as a variant – its number in Table).

Let us make the following assumptions.

10. Suppose that with a change in the implementation of the investigated method of heat and mass transfer, which may be accompanied by a change in the number of THPs, the following relations are fulfilled, which are related to the amount of thermoelectric material (provided that all thermoelements of the *i*-th THP are electrically connected in series, and in terms of heat flows - in parallel):

$$\alpha_{i;x} = \frac{n_0}{n_x} \gamma_{l_0}^{l_x} \alpha_{i;0} ; \qquad (3.19)$$

$$r_{i;x} = \frac{n_0}{n_x} \gamma_{l_0}^{l_x} r_{i;0} ; \qquad (3.20)$$

$$k_{i;x} = \frac{n_0}{n_x} \gamma_{l_0}^{l_x} k_{i;0} , \qquad (3.21)$$

where n_0 is the number of THPs in the case (variant) of implementation of the investigated method of heat and mass exchange, with which the comparison is carried out (in the initial case); n_x is the number of THPs in the case (variant) of implementation of the investigated method of heat and mass transfer which is considered (compared); $\alpha_{i;x}$ is total differential Seebeck coefficient of the material (legs) of thermoelements of the *i*-th THP in the case (variant) of implementation of the investigated method of heat and mass transfer, which is considered (compared); $\alpha_{i;0}$ is total differential Seebeck coefficient of the material (legs) of thermoelements of the *i*-th THP in the case (variant) of implementation of the investigated method of heat and mass exchange, with which a comparison is carried out (in the initial case); $r_{i;x}$ is total electrical resistance of thermoelements of the *i*-th THP in the case (variant) of implementation of the investigated method of heat and mass transfer, which is considered (compared); $r_{i;0}$ is total electrical resistance of thermoelements of the *i*-th THP in the case (variant) of implementation of the investigated method of heat and mass transfer, with which a comparison is carried out (in the initial case); $k_{i;x}$ is thermal conductivity of thermoelements of the *i-th* THP in the case (variant) of implementation of the investigated method of heat and mass transfer, which is considered (compared); $k_{i;0}$ is thermal conductivity of thermoelements of the *i*-th THP in the case (variant) of implementation of the investigated

method of heat and mass transfer, with which a comparison is carried out (in the initial case).

11. Suppose that with a change in the implementation of the investigated method of heat and mass transfer the following relations are fulfilled, which are related to the amount of material of which the heat exchangers are made (provided that all thermoelements of the *i*-th THP are connected in parallel in terms of heat flows):

$$R_{hot,i;l_x} = \frac{n_x}{n_0 \varphi_{l_0}^{l_x}} R_{hot,i;l_0} \; ; \tag{3.22}$$

$$R_{cool,i;l_x} = \frac{n_x}{n_0 \varphi_{l_0}^{l_x}} R_{cool,i;l_0} \; , \tag{3.23}$$

where $R_{hot,i;l_x}$ is total resistance of heat transfer from heat-releasing thermoelement junctions of the *i*-th THP to MS in the case (variant) of implementation of the investigated method of heat and mass exchange which is considered (compared); $R_{hot,i;l_0}$ is total resistance of heat transfer from heat-releasing thermoelement junctions of the *i*-th THP to MS in the case (variant) of implementation of the investigated method of heat and mass exchange, with which a comparison is carried out (in the initial case); $R_{cool,i;l_x}$ is total resistance of heat transfer from MS to heat-absorbing thermoelement junctions of the *i*-th THP in the case (variant) of implementation of the investigated method of heat and mass exchange, which is considered (compared); $R_{cool,i;l_0}$ is total resistance of heat transfer from MS to heat-absorbing thermoelement junctions of the *i*-th THP in the case (variant) of implementation of the investigated method of heat and mass exchange, with which a comparison is carried out (in the initial case).

Hereinafter, in this work (part 3) we will use assumptions 10 and 11.

Results of estimation calculations and their peculiarities

The initial data and the results of the corresponding calculations related to example under study are presented (in abbreviated form) in Table. Column headings of Table contain, sequentially, from top to bottom, a textual description of the corresponding quantities, their symbolic designation (if any) and dimension (if any), which are separated by dotted lines. In Table 1, the initial data and calculated results are designated by different colours (the initial data – in this colour, and calculated results – in this, different colour). Case numbers of example under study for which the value V_C^{MS} is identical are designated by the same colours.

For all the cases of example under study the total temperature difference of MS in its input flow according to expression (23) [1] and diagram in Fig. 2 [1] is identical and equal to 5 K :

$$\Delta T_1^{MS} = 5 \; K \; . \tag{3.24}$$

<u>*Table*</u>

Initial data and some results of corresponding estimation calculations of the efficiency of the investigated method of heat and mass exchange with the use of THP for the case of cooling MS in its input flow by all individual THPs (according to Fig. 2 [1]; according to assumptions 1, 2, 4-8 [1]; $T_{1.n}^{PP} = T_{2.n}^{PP} = 298.15\ K$)

Case № of example under study	Total number of THPs	Coefficient of change in the amount of thermoelectric material	Coefficient of change in the amount of material of heat echnagers	Total differential Seebeck coefficient of material (legs) of thermoelements of each individual *i*-th THP	Total electrical resistance of thermoelements of each individual *i*-th THP	Strength of current flowing through each thermoelement of each individual *i*-th THP	Total thermal conductivity of thermoelement legs of each individual *i*th THP	Total resistance of heat transfer from heat-releasing thermoelement junctions of each individual *i*-th THP to MS	Total resistance of heat transfer from MS to heat-absorbing thermoelement junctions of each individual *i*-th THP	Heat capacity losses of MS (heat capacity rate of \ms)	Total temperature difference of MS in its input flow	Temperature difference at $R_{cool,n}$, K	Temperature difference on thermoelements of *n*-th THP	Coefficient of performance of thermoelemnts of *n*-th THP	Indicator of energy efficiency of the *investigated process*
l	*n*	$\gamma_{l_0}^{l_x}$	$\varphi_{l_0}^{l_x}$	α_i	r_i	I_i	k_i	$R_{hot,i}$	$R_{cool,i}$	V_C^{MS}	ΔT_1^{MS}	$\Delta T_{cool,n}^R$	ΔT_n^{TE}	ε_n^{TE}	ω_{cool}
				V	Ohm	A	W/K	K/W	K/W	W/K	K	K	K		
1[(1)]	1	1	1	0.048	2.6	1.617	0.34	0.1	0.1	3.152	5	1.5762	11.36	2.051	2.051
2	1	2	1	0.096	5.2	0.863	0.68	0.1	0.1	3.152	5	1.5762	10.12	3.343	3.343
3	1	16	1	0.768	41.6	0.364	5.44	0.1	0.1	3.152	5	1.5762	11.829	1.789	1.789
4	2	1	1	0.024	1.3	1.49	0.17	0.2	0.2	3.152	5	1.5835	7.306	2.517	2.492
5	2	2	1	0.048	2.6	0.768	0.34	0.2	0.2	3.152	5	1.5844	6.601	4.458	4.411
6	2	2	2	0.048	2.6	0.713	0.34	0.1	0.1	3.152	5	0.791	4.712	5.337	5.288
7	2	0.87	0.87	0.021	1.128	1.765	0.148	0.23	0.23	3.152	5	1.825	8.255	2.074	2.051
8	2	0.9	0.9	0.022	1.17	1.689	0.153	0.222	0.222	3.152	5	1.760	7.989	2.183	2.160
9	8	1	1	0.006	0.325	1.403	0.042	0.8	0.8	3.152	5	1.586	4.560	2.923	2.878
10	16	1	1	0.003	0.162	1.3895	0.021	1.6	1.6	3.152	5	1.565	5.677	2.997	2.948
11	16	4	4	0.012	0.65	0.313	0.085	0.4	0.4	3.152	5	0.396	1.155	14.51	14.32
12	16	16	16	0.048	2.6	0.082	0.34	0.1	0.1	3.152	5	0.0991	0.521	50.44	49.71
13	16	32	16	0.096	5.2	0.047	0.68	0.1	0.1	3.152	5	0.0994	0.520	71.02	69.72
14	16	32	32	0.096	5.2	0.045	0.68	0.05	0.05	3.152	5	0.050	0.419	81.05	79.69
15	16	0.78	0.78	0.002	0.127	1.882	0.017	2.042	2.042	3.152	5	2.028	5.492	2.089	2.051
16	16	0.9	0.9	0.003	0.146	1.579	0.019	1.778	1.778	3.152	5	1.764	4.648	2.582	2.538
17	48	48	48	0.048	2.6	0.0272	0.34	0.1	0.1	3.152	5	0.033	0.172	153.5	151.2

l	n	$\gamma_{l_0}^{l_x}$	$\varphi_{l_0}^{l_x}$	α_i	r_i	I_i	k_i	$R_{hot,i}$	$R_{cool,i}$	V_C^{MS}	ΔT_1^{MS}	$\Delta T_{cool,n}^R$	ΔT_n^{TE}	ε_n^{TE}	ω_{cool}
				V	Ohm	A	W/K	K/W	K/W	W/K	K	K	K		
18	1	1	1	0.048	2.6	0.314 (2)	0.34	0.1	0.1	0.445	5	0.223	6.267	6.360	6.360
19	1	1	1	0.048	2.6	0.350 (3)	0.34	0.1	0.1	0.536	5	0.268	6.374	6.293	6.293
20	2	1	1	0.024	1.3	0.274	0.17	0.2	0.2	0.536	5	0.270	3.300	11.31	11.18
21	16	1	1	0.003	0.1625	0.214	0.02125	1.6	1.6	0.536	5	0.269	0.881	21.12	20.839
22	16	0.314	0.314	0.00094	0.051	0.699	0.0067	5.098	5.098	0.536	5	0.859	2.216	6.383	6.293
23	64	1	1	0.00075	0.041	0.207	0.0053	6.4	6.4	0.536	5	0.269	0.632	22.816	22.516
24	64	8	8	0.006	0.325	0.027	0.0425	0.8	0.8	0.536	5	0.034	0.147	160.4	158.1
25	1	1	1	0.048	2.6	4.502 (4)	0.34	0.1	0.1	5.669	5	2.834	26.841	0.484	0.484
26	1	1	1	0.048	2.6	5.455 (5)	0.34	0.1	0.1	5.343	5	2.671	35.21	0.309	0.309
27	2	1	1	0.024	1.3	3.086	0.17	0.2	0.2	5.343	5	2.694	13.08	1.009	0.994
28	16	1	1	0.003	0.1625	2.846	0.02125	1.6	1.6	5.343	5	2.704	8.201	1.219	1.191
29	16	0.828	0.828	0.002483	0.1345	4.838	0.01759	1.93	1.93	5.343	5	3.327	14.008	0.519	0.495
30	16	0.801	1	0.002404	0.1302	4.928	0.01703	1.6	1.6	5.343	5	2.751	11.724	0.521	0.497

[1] coefficients of change in the amount of materials for all other cases were calculated with respect to the amount of materials in this case (the amount of materials in this case is initial); [2] in the mode of maximum energy efficiency of THP working in the investigated process; [3] corresponds to the mode of maximum energy efficiency of THP thermoelements working at the temperature values of their heat-absorbing and heat-releasing junctions that correspond to this case [4] in the mode of maximum cooling capacity of THP working in the investigated process; [5] corresponds to the mode of maximum cooling capacity of THP thermoelements working at the temperature values of their heat-absorbing and heat-releasing junctions that correspond to this case.

In the 1st case of example under study only one THP is used, the thermoelements of which work in the intermediate mode between the modes of maximum energy efficiency and the mode of maximum cooling capacity. The parameters of this process were calculated with the use of a system of 4 equations (3.8), (3.10), (3.13), (3.14) (it is also possible to use a system of 4 equations (3.8), (3.10), (3.13), (3.15), or a system of 4 equations (3.8), (3.10), (3.14), (3.15) or a system of 4 equations (3.6), (3.8), (3.10), (3.13), or a system of 4 equations (3.6), (3.8), (3.10), (3.14), or a system of 4 equations (3.6), (3.8), (3.10), (3.15)). In so doing, the values of $T_{hot,(i-1)}^{PP}$, $T_{cool,i}^{TE}$, $T_{hot,i}^{TE}$, V_C^{PP} are unknown, and other values are known. The initial data and the results of calculations for this case are given in the row of table 3.1, which corresponds to this case.

In the following cases of the considered example in which several THPs are used, these several THPs are identical (the values of α_i, r_i, k_i, $R_{hot,i}$ anda $R_{cool,i}$ for all these THPs are identical) and also for all these THPs the strength of current flowing through them, I_i is the same.

Fig. 3.1 shows some peculiarities of cases 18 and 19 of example under study. Plot *a* in Fig. 3.1 was built on the basis of a function that reflects a dependence of the coefficient of performance of respective *i*-th THP on the strength of current flowing through thermoelements of this *i*-th THP $\varepsilon_i^{TTH}(I_i)$, which, in turn, was obtained on the basis of equations, such as (3.6), (3.8), (3.10), (3.13) and expression (3.4), provided that $\Delta T_1^{MS} = const = 5\,K$. Coordinates of point **18** in Fig. 3.1 (which corresponds to case 18 of example under study) were obtained, in particular, with the use of condition $\left(\varepsilon_i^{TTH}(I_i)\right)' = 0$. Plots *b* and *c* in Fig. 3.1 were built on the basis of expression (3.1) (with the use of expressions (2) and (3)).

The results of calculations for case 19 were obtained using a system of 5 equations, for instance, (6), (8), (10), (13) and a commonly known expression to determine the strength of current flowing through thermoelements that work in the mode of maximum energy efficiency $I_i^{\varepsilon_{i,\max}^{TE}}$ [9]:

$$I_i^{\varepsilon_{i,\max}^{TE}} = \frac{\alpha_i(T_{hot,i}^{TE} - T_{cool,i}^{TE})}{r_i\left(\sqrt{1+0.5\dfrac{\alpha_i^2}{k_i r_i}(T_{hot,i}^{TE} + T_{cool,i}^{TE})} - 1\right)}. \tag{3.25}$$

In this case 19 $I_i = I_i^{\varepsilon_{i,\max}^{TE}}$.

Fig. 3.1. Figure showing some peculiarities of cases 18 and 19 of example under study:
a – plot $\varepsilon_i^{TTH}(I_i)$ ($\Delta T_1^{MS} = const = 5\,K$, $V_C^{MS} \neq const$); b – plot of ε_i^{TE} versus I_i for fixed temperature values of heat-absorbing and heat-releasing thermoelement junctions of the i-th THP that correspond to case 19 of example under study; c – plot of ε_i^{TE} versus I_i for fixed temperature values of heat-absorbing and heat-releasing thermoelement junctions of the i-th THP that correspond to case 18 of example under study; point **18** corresponds to case 18 of example under study; point **19** corresponds to case 19 of example under study.

Fig. 3.2 shows some peculiarities of cases 25 and 26 of example under study. Plot *a* in Fig. 3.2 was built on the basis of a function showing a dependence of cooling capacity of corresponding *i*-th THP on the strength of current flowing through thermoelements of this *i*-th THP $Q_{cool,i}^{TTH}(I_i)$, which, in turn, was obtained on the basis of equations, such as (3.6), (3.8), (3.10), (3.13) and the expression to determine cooling capacity of the *i*-th THP by its effect on MS:

$$Q_{cool,i}^{TTH} = V_C^{PP}\left(T_{cool,(i-1)}^{PP} - T_{cool,i}^{PP}\right)$$

(3.26)

(with regard to the respective assumptions) provided that $\Delta T_1^{MS} = const = 5\,K$.

Coordinates of point **25** in Fig. 3.2 (which corresponds to case 25 of example under study) were obtained, in particular, with the use of condition $\left(Q_{cool,i}^{TTH}(I_i)\right)' = 0$. Plots *b* and *c* in Fig. 3.2 were built on the basis of Eq.(2).
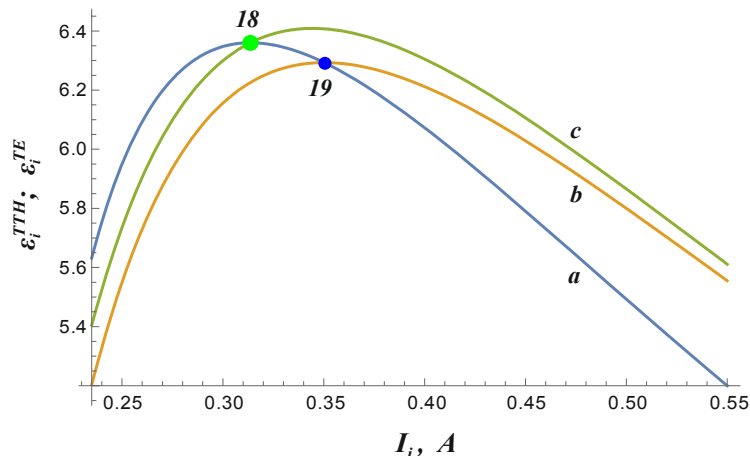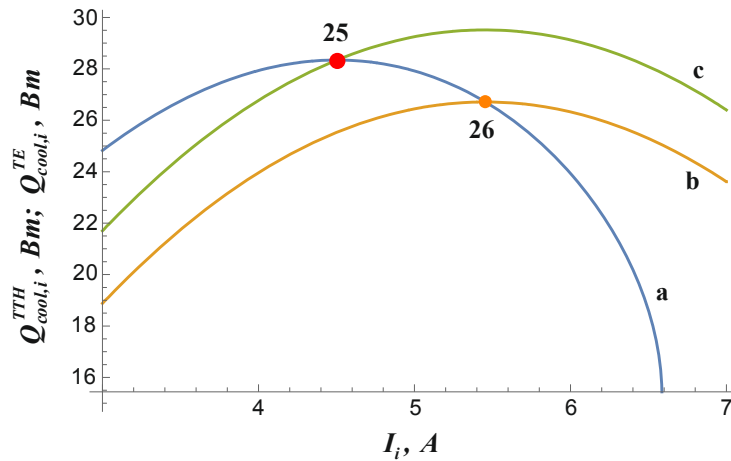

Fig. 3.2. Figure showing some peculiarities of cases 25 and 26 of example under study:
a –plot $Q_{cool,i}^{TTH}(I_i)$ ($\Delta T_1^{MS} = const = 5\,K$, $V_C^{MS} \neq const$); b – plot of $Q_{cool,i}^{TE}$ versus I_i for fixed
temperature values of heat-absorbing and heat-releasing thermoelement junctions of the i-th THP
that correspond to case 26 of example under study; c – plot of $Q_{cool,i}^{TE}$ versus I_i for fixed temperature
values of heat-absorbing and heat-releasing thermoelement junctions of the i-th THP that correspond
*to case 25 of example under study; point **25** corresponds to case 25 of example under study;*
*point **26** corresponds to case 26 of example under study.*

The results of calculations for case 26 of example under study were obtained using a system of 5 equations, such as (3.6), (3.8), (3.10), (3.13) and a commonly known expression to determine the strength of current flowing through thermoelements that work in the mode of maximum cooling capacity $I_i^{Q_{cool,i,max}^{TE}}$ [8]:

$$I_i^{Q_{cool,i,max}^{TE}} = \frac{\alpha_i T_{cool,i}^{TE}}{r_i} .$$

(3.27)

In this case 26 $I_i = I_i^{Q_{cool,i,max}^{TE}}$.

Conclusions

From the calculations described in this paper it can be concluded that increase in the quantity of THPs used in the above described processes, in particular, can:

1) create the possibility of reducing the amount of thermoelectric material and/or the amount of material of heat exchangers of which all THPs are made, with constant energy efficiency of the respective process;

2) create the possibility of increasing the energy efficiency of the respective process with constant amount of thermoelectric material and/or material of heat exchangers of which all THPs are made;

3) create the possibility of increasing the energy efficiency of the respective process with a change (in particular, increase) in the amount of thermoelectric material and/or material of heat exchangers of which all THPs are made.

References

1. Kshevetsky O.S. (2017). Estimation of the efficiency of partial case of heat and mass transfer processes between heat pumps and moving substance, part 1. *J.Thermoelectricity, 6,* 39–55.

2. Kshevetsky O.S. (2018). Estimation of the efficiency of partial case of heat and mass transfer processes between heat pumps and moving substance, part 2. *J.Thermoelectricity, 2,* 56–68.

3. Kshevetsky, O. (2019). About some of the possibilities of using heat pumps in processes that involve the movement of substance. *Thermophysics and Thermal Power Engineering*, *41*(3), 70-76. https://doi.org/https://doi.org/10.31472/ttpe.3.2019.10

4. Kshevetsky O.S. (2017). *On the possibility of increasing the energy efficiency of heat and mass transfer processes that provide for heating and cooling of moving substance*. Khimichna Tekhnologiia ta Ingeneriia: zbirnyk tez dopovidei Mizhnarodnoi naukovo-praktychnoi konferentsii - Chemical Technology and Engineering: Abstracts of International scientific and practical conference (Lviv, June 26–30, 2017) (pp.96-97).

5. *Patent of Ukraine №118972* (2019). Kshevetsky O.S. Process of heat and mass transfer between moving substance and heat pumps. Bul. №7 [in Ukrainian].

6. Anatychuk L.I., Prybyla A.V. (2017). On the coefficient of performance of thermoelectric liquid-liquid heat pumps with regard to energy loss for heat carrier transfer. *J.Thermoelectricity, 6,* 34 – 40.

7. Anatychuk L.I., Prybyla A.V. (2016). Comparative analysis of thermoelectric and compression heat pumps for individual air-conditioners. *J.Thermoelectricity,* 2, 33 – 42.

8. Ioffe A.F. (1960). Poluprovodnikovyie termoelementy [Semiconductor thermoelements]. Moscow-Leningrad: AN SSSR Publ. [in Russian].

9. Anatychuk L.I. (2005). *Thermoelectricity. Vol. 2. Thermoelectric Power Converters*. Kyiv, Chernivtsi, Institute of Thermoelectricity.

Submitted 28.08.2019

Кшевецький О.С., *канд. физ.-мат. наук*[1]
Орлецький О. В.

Чернівецький національний університет імені Юрія Федьковича,
вул. Коцюбинського 2, Чернівці, 58012, Україна

ОЦІНКА ЕФЕКТИВНОСТІ ЧАСТИННОГО ВИПАДКУ ПРОЦЕСІВ ТЕПЛОМАСООБМІНУ МІЖ ТЕПЛОВИМИ НАСОСАМИ І РУХОМОЮ РЕЧОВИНОЮ
Частина 3

Представлена теоретична модель для оцінки ефективності роботи частинного випадку процесів тепломасообміну між рухомою речовиною і термоелектричними тепловими насосами з їх теплообмінними частинами, при якому рухому речовину (або принаймні частину цієї рухомої речовини) приводять у тепловий контакт з теплопоглинальною і тепловиділяючою теплообмінними частинами принаймні двох термоелектричних теплових насосів, які можуть працювати в режимах, які можуть відрізнятися від режиму максимальної енергоефективності, зокрема, з врахуванням кількостей матеріалів, що необхідні для виготовлення цих термоелектричних теплових насосів. Наведені результати відповідної теоретичної оцінки. . Бібл. 9, табл. 1, рис. 2.
Ключові слова: тепловий насос, рухома речовина, тепломасообмін, ефективність, енергоефективність, термоелектричний тепловий насос, термоелементи, термоелектричний матеріал.

Кшавецкий .А. С., *канд. физ. мат наук*[1]
Орлецкий А.В.

[1]Черновицкий национальный университет
им. Юрия Федьковича, ул. Коцюбинского, 2,
Черновцы, 58012, Украина

ОЦЕНКА ЭФФЕКТИВНОСТИ ЧАСТНОМ СЛУЧАЕ ПРОЦЕССОВ ТЕПЛОМАССООБМЕНУ МЕЖДУ ТЕПЛОВЫХ НАСОСОВ И ДВИЖЕНИЕМ ВЕЩЕСТВОМ
Часть 3

Представлена теоретическая модель для оценки эффективности работы в частном случае процессов тепломассообмена между движущимся веществом и термоэлектрическими тепловыми насосами с их теплообменными частями, при котором движущееся вещество (или хотя бы часть этого движущегося вещества) приводят в тепловой контакт с теплопоглощающей и тепловыделяющей теплообменными частями по крайней мере двух термоэлектрических тепловых насосов, могущих работать в режимах, отличающихся от режима максимальной энергоэффективности, в частности, с учетом количеств материалов, необходимых для изготовления этих термоэлектрических тепловых насосов. Приведены

результаты соответствующей теоретической оценки.Библ. 9, табл. 1, рис. 2.

Ключевые слова: тепловый насос, подвижне вещество, тепломассообмен, КПД, энергоэффективность, термоэлектрический тепловой насос, термоэлементы, термоэлектрический материал.

References

1. Kshevetsky O.S. (2017). Estimation of the efficiency of partial case of heat and mass transfer processes between heat pumps and moving substance, part 1. *J.Thermoelectricity, 6,* 39–55.

2. Kshevetsky O.S. (2018). Estimation of the efficiency of partial case of heat and mass transfer processes between heat pumps and moving substance, part 2. *J.Thermoelectricity, 2,* 56–68.

3. Kshevetsky, O. (2019). About some of the possibilities of using heat pumps in processes that involve the movement of substance. *Thermophysics and Thermal Power Engineering*, *41*(3), 70-76. https://doi.org/https://doi.org/10.31472/ttpe.3.2019.10

4. Kshevetsky O.S. (2017). *On the possibility of increasing the energy efficiency of heat and mass transfer processes that provide for heating and cooling of moving substance*. Khimichna Tekhnologiia ta Ingeneriia: zbirnyk tez dopovidei Mizhnarodnoi naukovo-praktychnoi konferentsii - Chemical Technology and Engineering: Abstracts of International scientific and practical conference (Lviv, June 26–30, 2017) (pp.96-97).

5. *Patent of Ukraine №118972* (2019). Kshevetsky O.S. Process of heat and mass transfer between moving substance and heat pumps. Bul. №7 [in Ukrainian].

6. Anatychuk L.I., Prybyla A.V. (2017). On the coefficient of performance of thermoelectric liquid-liquid heat pumps with regard to energy loss for heat carrier transfer. *J.Thermoelectricity, 6,* 34 – 40.

7. Anatychuk L.I., Prybyla A.V. (2016). Comparative analysis of thermoelectric and compression heat pumps for individual air-conditioners. *J.Thermoelectricity,* 2, 33 – 42.

8. Ioffe A.F. (1960). Poluprovodnikovyie termoelementy [Semiconductor thermoelements]. Moscow-Leningrad: AN SSSR Publ. [in Russian].

9. Anatychuk L.I. (2005). *Thermoelectricity. Vol. 2. Thermoelectric Power Converters*. Kyiv, Chernivtsi, Institute of Thermoelectricity.

L.I. Anatychuk, *academician of the NAS of Ukraine,* [1,2]

O.V. Nitsovich, *cand. of phys. and math. sciences* [1,2]

[1]Institute of Thermoelectricity of the NAS and MES of Ukraine, 1, Nauky str., Chernivtsi, 58029, Ukraine

[2]Yuriy Fedkovych Chernivtsi National University, 2, Kotsiubynsky str., Chernivtsi, 58012, Ukraine

L.I. Anatychuk

O.V. Nitsovich

SIMULATION OF THE EFFECT OF THERMAL UNIT VELOCITY ON THE PROCESS OF GROWING Bi_2Te_3 BASED MATERIALS BY VERTICAL ZONE MELTING METHOD

The paper presents the results of computer simulation of the process of growing Bi_2Te_3 based thermoelectric materials by vertical zone melting method. It was found that, depending on the velocity of the heater and coolers, not only the curvature of the crystallization front changes, but also its shape. At temperatures of the heater and coolers $T_h = 1058K$, $T_h = 303K$ for velocities greater than 1.25 cm/h, the crystallization front along the entire crystal becomes convex into the solid phase, but at lower velocities it changes its shape from convex to concave along the grown sample. Bibl. 5, Fig. 6.

Key words: simulation, vertical zone melting, thermoelectric material, bismuth telluride.

Introduction

Zone melting is one of the most commonly used methods for the production of semiconductor materials, in particular thermoelectric. However, obtaining thermoelectric materials (TEM) with the required properties is possible only under the conditions of a controlled crystallization process, since the curvature of the crystallization front, the temperature gradient at the interface between the solid and liquid phases, the geometry of the melt zone, and the velocity of zone motion have a great influence on the stability of growth and uniformity of a single crystal, etc [1, 2].

Computer simulation of TEM growing processes makes it possible to determine the growth conditions and explain possible difficulties that may arise as a result of changes in these conditions. It cannot replace, but presupposes and complements the experiment, providing information that can be experimentally obtained only indirectly. Therefore, the improvement and development of the technology for growing thermoelectric materials by means of multiparameter computer optimization of the controlled process parameters is urgent.

This study is a continuation of [3], in which the shape of the crystallization front depending on the temperature and size of the heater was studied by computer simulation.

The purpose of this work is a computer study of the effect of thermal unit velocity on the process of growing Bi_2Te_3 based materials by vertical zone melting method. In particular, the analysis of the influence of TEM growth conditions on the formation of a flat crystallization front.

Physical model of vertical zone melting

The circuit diagram of the process of growing thermoelectric materials by vertical zone melting is represented in Fig.2.
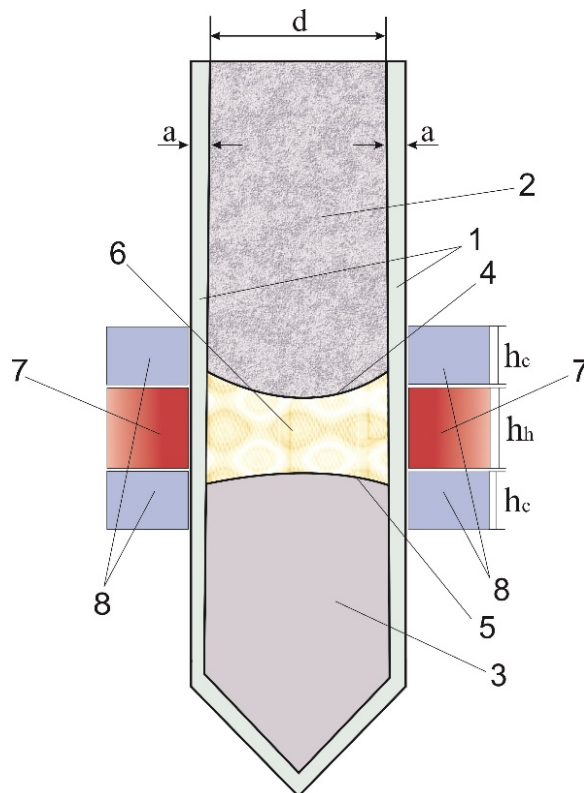

Fig.1. Physical model of installation for growing TEM by vertical zone melting method: 1 – container, 2 – material in solid phase (polycrystal), 3 – material in solid phase (single crystal), 4 – melt front, 5 – crystallization front, 6 – material in liquid phase (melt zone), 7 – heater, 8 – coolers.

The figure depicts a fragment of an ingot comprising polycrystalline material 2, a molten zone 6, and a single crystal 3. The ingot is placed in a container 1. Using a heater 7 and a system of coolers 8, a molten zone 6 is formed that moves together with the heater along the sample to provide melting of the polycrystal and crystallization of the melt below the boundary 5, which is called the crystallization front. The system which is composed of a heater 7 and coolers 8 is commonly referred to as a thermal unit.

Mathematical model of zone melting process

COMSOL Multiphysics software package was used for computer simulation of the process of growing the Bi₂Te₃ thermoelectric material, which allows simulating almost all physical processes described by algebraic and differential equations in partial derivatives. To do this, it is sufficient to use ready-made modules of the corresponding physical phenomenon. If necessary, the researcher can change the equation built into the COMSOL module, or specify his own. Numerical calculation is performed by the finite element method [5].

Simulation of the motion of the heater and coolers in the COMSOL Multiphysics system was carried out by using the Moving Mesh module, which allows changing the mesh during the calculations of unsteady processes (Fig. 2).
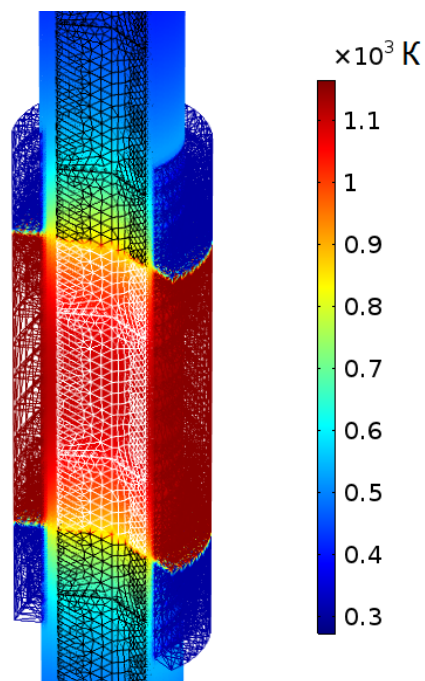

Fig.2. Image of computer model mesh of the plant for growing
TEM by vertical zone melting method.

The temperature distribution in the test sample was found from solving the differential equation of thermal conductivity, supplemented by the dependences of the physical properties of the test material as a function of the phase state at a given point at a given temperature:

$$\rho \, C_p \frac{\partial T}{\partial t} + \rho \, C_p u \, \nabla T + \nabla q = Q \tag{1}$$

$$q = -\kappa \nabla T, \tag{2}$$

$$\rho = \theta \rho_{phase1} + (1 - \theta)\rho_{phase2}, \tag{3}$$

$$C_p = \frac{1}{2}\left(\theta \rho_{phase1} C_{p_{phase1}} + (1 - \theta)\rho_{phase2} C_{p_{phase2}}\right) + L \frac{d\alpha_m}{dT}, \tag{4}$$

$$\alpha_m = \frac{1}{2} \cdot \frac{(1-\theta)\rho_{phase2} - \theta \rho_{phase1}}{\theta \rho_{phase1} + (1-\theta)\rho_{phase2}}, \tag{5}$$

$$\kappa = \theta \kappa_{phase1} + (1 - \theta)\kappa_{phase2}. \tag{6}$$

where ρ is the density; C_p is the heat capacity of material; κ is thermal conductivity; u is the velocity of the medium which in the problem under study is equal to zero; *T* is

temperature; θ is phase ratio at a given temperature; α_m is mass ratio between phases; L is latent heat of phase transition; Q is external heat flux. The indices $phase1$ and $phase2$ indicate to which phase, solid or liquid, respectively, the properties are related.

To account for heat transfer due to radiation to the physical interface Heat Transfer in Solids in the COMSOL Multiphysics system, the boundary condition Surface-to-Surface Radiation is added, selecting the outer boundaries of the container and the thermal unit (Fig. 3). :
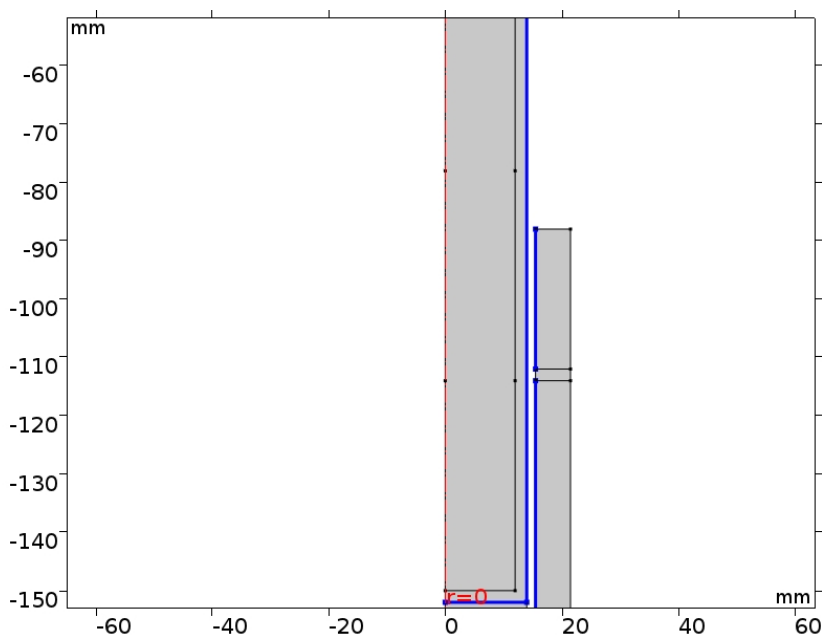

Fig.3. Radiation boundaries between the surfaces.

$$-n(-\kappa\nabla T) = \varepsilon\sigma_b(T_{ext}^4 - T^4), \tag{7}$$

where T_{ext} is temperature of thermal unit wall; T is temperature of container wall, n is vector directed along the normal to the surface of cylinder (container); $\varepsilon = \left(\dfrac{1}{\varepsilon_1} + \dfrac{1}{\varepsilon_2} - 1\right)^{-1}$ is reduced radiation coefficient of the system; ε_1 is radiation coefficient of thermal unit, ε_2 is radiation coefficient of container; σ_b is the Stephan-Boltzmann constant.

To calculate the computer model, the geometric dimensions of the system elements, the initial temperatures of the heater and coolers, the liquidus and solidus temperatures of Bi₂Te₃ as well as the temperature dependences of the properties of the grown material are set [4]. Convection and mass transfer of molten Bi₂Te₃ are not taken into account.

Computer simulation results

With regard to the results obtained in [3], the study of the effect of thermal unit velocity on the process of growing Bi₂Te₃ was carried out with the following input parameters of the system: wall thickness of the quartz container 3 mm; the diameter d of the grown crystal was assumed to be 24 mm, its length l = 30 cm; height and temperature of the heater $h_h = 3d$, $T_h = 1058K$; height

and temperature of coolers $h_c = 1d$, $T_c = 303K$. The thermal unit velocity varied from 0.5 to 4 cm/h. The temperature of the heater was selected based on the initial simulation results such that even at high velocities, the heater had time to completely melt the crystal under study.

The change of the temperature gradient at the crystallization front depending on the velocity of the heater and coolers was studied. The simulation results are shown in Fig.4.
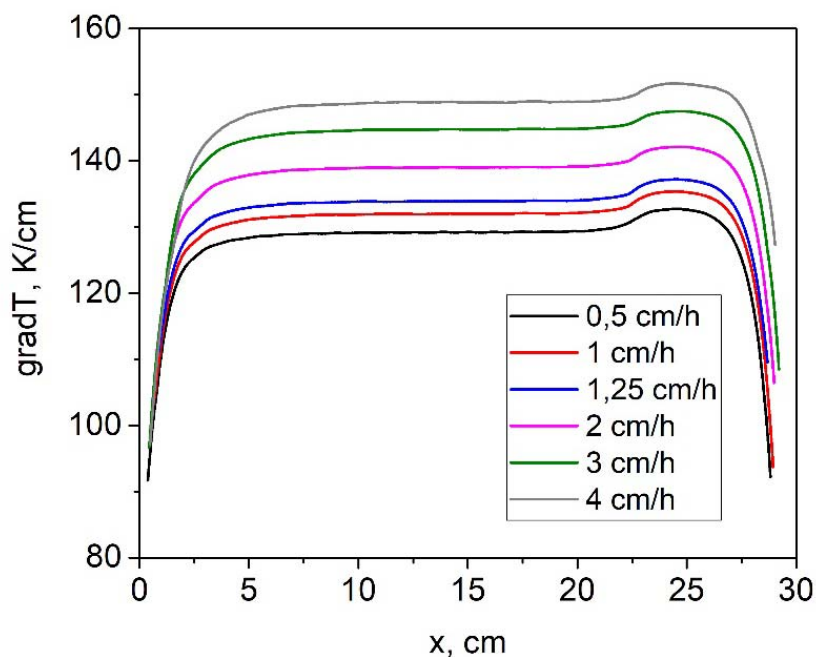

Fig.4. Change in the temperature gradient at the crystallization front along the grown crystal at thermal unit velocities v=0.5 – 4cm/h.

As can be seen from the figure, the temperature gradient at the crystallization front increases with increasing growth rate. In addition, you can see that regardless of the rate, there is a clear change in the magnitude of the gradient near the coordinate of 21 cm, which is due to the exit of the upper cooler outside the grown ingot and the violation of the thermal balance of the system.

As is known, when TEM is obtained by vertical zone melting, the curvature of the crystallization front has a great influence on the stability of the growth of a single crystal and its homogeneity [2, 3]. With directional crystallization, the cleavage planes are oriented along the normal to the crystallization front. If the front is flat, then the polycrystalline ingot consists of grains, the cleavage planes of which are oriented parallel to its axis, i.e., a directional structure is formed. Therefore, it is important to study the effect of thermal unit velocity on the nature of change in the shape of crystallization front along the crystal during its growth.

Fig. 5 shows how the shape of the crystallization front changes during the motion of the melt zone along the crystal at growth rates $v = 1$ cm/h and $v = 4$ cm/h.

It can be seen from the figure that in the lower part of the grown ingot the crystallization front is substantially convex into the solid phase for thermal unit velocity of 4 cm / h and slightly convex for a velocity of 1 cm/h. As the molten zone moves, the curvature of the front decreases in both cases, but at the end the front is again curved.
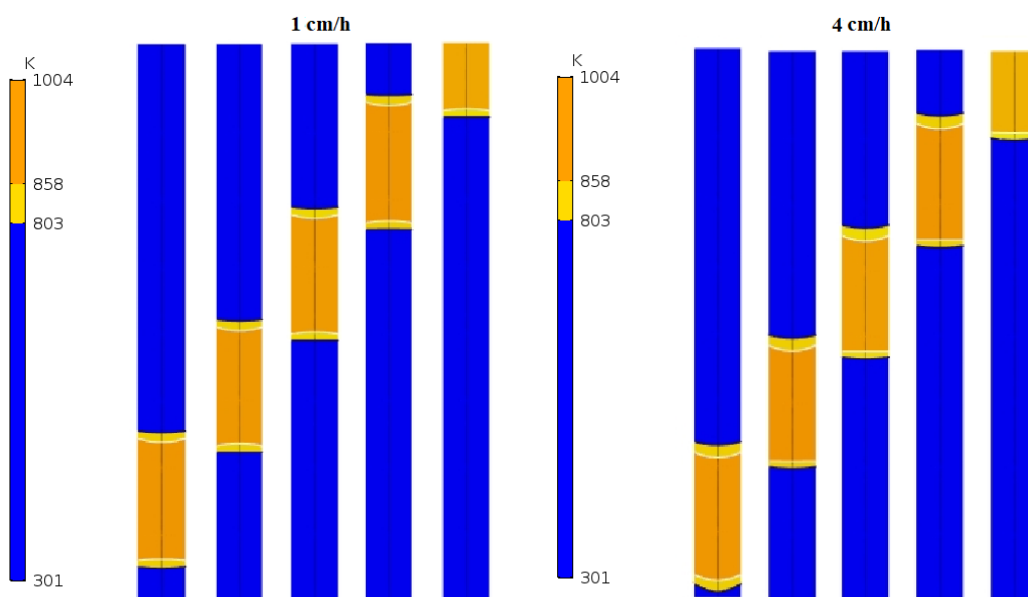
Fig.5. Image of melt zone motion along the crystal at growth
rates $v = 1 cm/h$ and $v = 4\ cm/h$.

Fig.6 shows a dependence of the value of crystallization front curvature along the crystal at various thermal unit velocities. The curvature was calculated as a difference between the maximum and minimum points $\Delta z = z_{max} - z_{min}$ of the front.
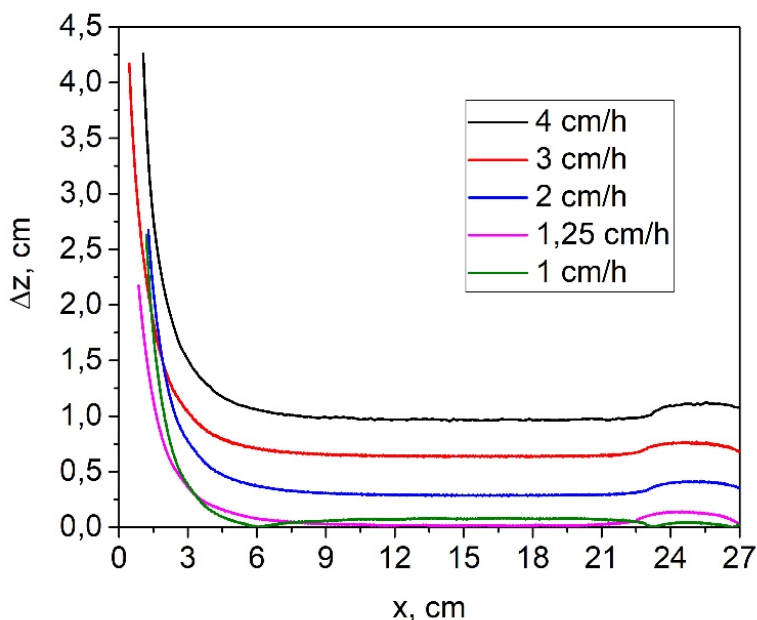
Fig.6. Dependence of the value of crystallization front curvature
along the crystal on thermal unit velocity.

As can be seen from the figure, maximum flat crystallization front was achieved at a growth rate of v=1.25 cm/h. A detailed analysis of the simulation results showed that at the given temperatures of the heater and coolers (T_h = 1058 K, T_c = 303 K) for velocities greater than 1.25

cm/h the crystallization front along the whole crystal was convex into a solid phase. For velocities lower than the specified value, the front changed its shape and at the initial section of the grown crystal it was convex, then it became concave into the melt and at the end of the crystal it again became convex.

Conclusions

1. A procedure has been developed for computer simulation of the effect of the growth rate of thermoelectric materials on the crystallization process of Bi_2Te_3 based TEM by vertical zone melting method.

2. It is shown that with increasing the growth rate the temperature gradient at the crystallization front increases slightly.

3. It was established that depending on the velocity of the heater and coolers, not only the curvature of the crystallization front changes, but also its shape. At the temperatures of the heater and coolers $T_h = 1058K$, $T_c = 303K$ for velocities greater than 1.25 cm/h, the crystallization front along the entire crystal was convex into the solid phase, but at lower velocities it changed its shape from convex to concave along the grown sample.

References

1. Goltsman B.M., Kudinov V.A., Smirnov I.A. (1972). *Poluprovodnikovyie termoelektricheskiie materialy na osnove Bi₂Te₃ [Semiconductor thermoelectric materials based on Bi₂Te₃]*. Moscow: Nauka [in Russian].

2. U.G. Pfan. (1970). Zonnaya plavka [Zone melting]. V.N.Vigdorovich (Ed.) [in Russian].

3. Nitsovich O.V. (2018). Research on the conditions of forming a flat crystallization front when growing Bi_2Te_3 based thermoelectric material by vertical zone melting method. J.Thermoelectricity, 3, 76-82.

4. Nitsovich O.V. (2018). Computer simulation of Bi_2Te_3 crystallization process in the presence of electrical current. J.Thermoelectricity, 5, 12-21.

5. COMSOL Multiphysics Modeling Software. COMSOL INC. – Retrieved from: https://www.comsol.com/.

Анатичук Л.І. , *ак. НАН України,* [1,2]
Ніцович О.В. , *канд. фіз.-мат. наук* [1,2]

[1] Інститут термоелектрики НАН і МОН України,
вул. Науки, 1, Чернівці, 58029, Україна,
[2] Чернівецький національний університет ім. Юрія Федьковича,
вул. Коцюбинського 2, Чернівці, 58000, Україна,
e-mail: anatych@gmail.com

МОДЕЛЮВАННЯ ВПЛИВУ ШВИДКОСТІ РУХУ ТЕПЛОВОГО ВУЗЛА НА ПРОЦЕС ВИРОЩУВАННЯ МАТЕРІАЛІВ НА ОСНОВІ *Bi₂Te₃* МЕТОДОМ

ВЕРТИКАЛЬНОЇ ЗОННОЇ ПЛАВКИ

У статті наведено результати комп'ютерного моделювання процесу вирощування термоелектричних матеріалів на основі Bi₂Te₃ методом вертикальної зонної плавки. Встановлено, що в залежності від швидкості руху нагрівника та охолоджувачів змінюється не лише кривизна фронту кристалізації, але й його форма. При температурах пічки та холодильників T_h=1058К, T_c=303К для швидкостей більших 1.25 см/год фронт кристалізації вздовж всього кристалу стає опуклим в тверду фазу, але при менших швидкостях він змінює свою форму від опуклого до увігнутого вздовж вирощуваного зразка. Бібл. 5, рис. 6.

Ключові слова: моделювання, вертикальна зонна плавка, термоелектричний матеріал, телурид вісмуту.

Анатычук Л.И. , ак. НАН Украины, [1,2]
Ницович О.В., *канд. физ.-мат. наук*[1,2]

[1]Институт термоэлектричества НАН и МОН Украины,
ул. Науки, 1, Черновцы, 58029, Украина,
[2]Черновицкий национальный университет им. Юрия Федьковича,
ул. Коцюбинского 2, Черновцы, 58000, Украина,
e-mail:anatych @ gmail. com

МОДЕЛИРОВАНИЕ ВЛИЯНИЯ СКОРОСТИ ДВИЖЕНИЯ ТЕПЛОВЫХ УЗЛОВ НА ПРОЦЕСС ВЫРАЩИВАНИЯ МАТЕРИАЛОВ НА ОСНОВЕ Bi₂Te₃ МЕТОДОМ ВЕРТИКАЛЬНОЙ ЗОННОЙ ПЛАВКИ

В статье приведены результаты компьютерного моделирования процесса выращивания термоэлектрических материалов на основе Bи2Te3 методом вертикальной зонной плавки. Установлено, что в зависимости от скорости движения нагревателя и охладителей изменяется не только кривизна фронта кристаллизации, но и его форма. При температурах печи и холодильников T_h = 1058К, T_c = 303К для скоростей больших 1.25 см/ч фронт кристаллизации вдоль всего кристалла становится выпуклым в твердую фазу, но при меньших скоростях он меняет свою форму от выпуклого к вогнутого вдоль выращиваемого образца. Библ. 5, рис. 6.

Ключевые слова: моделирование, вертикальная зонная плавка, термоэлектрический материал, теллурид висмута.

References

1. Goltsman B.M., Kudinov V.A., Smirnov I.A. (1972). *Poluprovodnikovyie termoelektricheskiie materialy na osnove Bi₂Te₃ [Semiconductor thermoelectric materials based on Bi₂Te₃].* Moscow: Nauka [in Russian].
2. U.G. Pfan. (1970). Zonnaya plavka [Zone melting]. V.N.Vigdorovich (Ed.) [in Russian].
3. Nitsovich O.V. (2018). Research on the conditions of forming a flat crystallization front when growing Bi₂Te₃ based thermoelectric material by vertical zone melting method. J.Thermoelectricity, 3, 76-82.
4. Nitsovich O.V. (2018). Computer simulation of Bi₂Te₃ crystallization process in the presence of electrical current. J.Thermoelectricity, 5, 12-21.
5. COMSOL Multiphysics Modeling Software. COMSOL INC. – Retrieved from: https://www.comsol.com/.

Subminited 02.09.2019

Anatychuk L.I., *acad. National Academy of Sciences of Ukraine*[1,2]
Denysenko O.I., *doc.med. sciences., professor*[3]
Kobylianskyi R.R. . *cand. phys.– math. sciences*[1,2],
Stepanenko V.I., *doc.med. sciences., professor*[4],
Svyryd S.G., *doc.med. sciences., professor*[4],
Stepanenko R.L. *doc.med. sciences., dochent*[4]
Perepichka M.P.,*cand. Med. Sciences., docent*[3]

[1]Institute of Thermoelectricity of the NAS and MES of Ukraine,
1 Nauky str., Chernivtsi, 58029, Ukraine, *e-mail: anatych@gmail.com*
[2]Yu.Fedkovych Chernivtsi National University, Chernivtsi, Ukraine
[3]Higher State Educational Institution of Ukraine
"Bukovinian State Medical University" Ministry of Health
of Ukraine, 2, Theatre Square, Chernivtsi, 58002, Ukraine,
[4]National Medical University named after O.O. Bohomolets,
Taras Shevchenko Boulevard, 13, Kyiv, 01601, Ukraine

THERMOELECTRIC DEVICE FOR TREATMENT OF SKIN DISEASES

The paper presents the results of development of a thermoelectric device for treatment of skin diseases. The developed device has an extended range of operating temperatures (-50 ÷ 0) °C and visual control of the temperature of cooling work tools during therapeutic procedures. The design features of the device, its technical characteristics and the results of testing in clinical practice are given. Bibl. 44, Fig. 6, Tabl. 1.
Key words: thermoelectric device, thermoelectric cooling, treatment of skin diseases, dermatology, cosmetology.

Introduction

According to experimental and clinical studies, the influence of temperature factors is one of the effective methods for treatment of many human diseases, including skin [1-5]. However, the majority of technical devices that are currently used for temperature exposure in medical practice are cumbersome, without the proper ability to control the temperature and reproduce thermal conditions. To achieve low temperatures, in most cases, chloroethyl or liquid nitrogen systems are used, which have a number of drawbacks that significantly limit the possibilities of their use in dermatology and cosmetology practice [1 – 9].

To solve this problem, it is possible to use thermoelectric cooling [10 – 15], which has several advantages over the traditional methods of temperature exposure. Existing thermoelectric devices are used in various fields of science and technology, in particular in medicine. Structural plasticity, reliability, ease of operation and the ability to accurately adjust the temperature create favorable conditions for their wide practical application in medical practice. In particular, in dermatology and cosmetology, thermoelectric devices are promising for cryomassage in order to accelerate the regression of skin rash elements and stimulate the metabolic processes in the skin in various dermatoses, as well as for conducting cryodestruction of skin neoplasms, freezing of warts, papillomas, etc [3, 5]. Thermoelectric devices for treatment of skin diseases, created by this time, usually have a range of operating temperatures (-30 ÷ +5) ° C [11 – 15]. In most cases, such temperatures are sufficient for complex treatment of various skin diseases [16 – 21], but not

enough for the cryodestruction of pathological changes and skin neoplasms.

Therefore, *the purpose of this work* is design development and manufacture of a thermoelectric device for treatment of skin diseases with an extended range of operating temperatures (50 ÷ 0) ° C and testing the device in clinical practice.

Design and technical characteristics of device

At the Institute of Thermoelectricity of the NAS and MES of Ukraine, in the framework of an agreement on cooperation with the Higher State Educational Establishment of Ukraine "Bukovinsky State Medical University", a thermoelectric device was developed for treatment of skin diseases (Fig.1) [22]. The technical characteristics of the device are listed in Table 1.

Fig.1. Thermoelectric device for treatment of skin diseases:
1 – thermoelectric cooling unit, 2 – work tool

Table 1

Technical characteristics of the device

№	Technical characteristics of the device	Parameter values, measurement units
1.	Operating temperature range	(-50 ÷ 0) °C
2.	Temperature accuracy	± 1 ℃
3.	Time required for the device to reach temperature mode	10 min
4.	Device AC supply voltage	(220 ± 10) V
5.	Device power consumption	200 W
6.	Overall dimensions of thermoelectric cooling unit	(135×120×110) mm
7.	Overall dimensions of work tool	(215×23×18.5) mm
8.	Thermoelectric cooling unit weight	1.5 kg
9.	Work tool weight	0.08 kg
10.	Continuous work time of the device	8 h

The device consists of two main functional units (Fig. 1): thermoelectric cooling unit 1 and a set of work tools 2 with variable tips of different configuration. Moreover, the work tools of the device are not connected and functionally independent of the thermoelectric cooling unit. In turn, the thermoelectric cooling unit consists of the following elements: housing, high-efficiency two-stage thermoelectric modules "Altec-2", cooling chamber for work tools, liquid heat exchangers, thermal insulation and a set of pressure plates. The heat is removed from the hot sides of thermoelectric modules by two liquid heat exchangers. The electric power of the thermoelectric cooling unit is supplied from the power supply unit.

The work tools of the device (Fig. 1) contain built-in electronic thermometers with a stand-alone power supply unit for visual control of temperature during therapeutic procedures. Cylindrical copper nozzles of various configurations are attached to the lower part of the work tools, the internal volume of which is filled with a high heat capacity fluid. This enables sessions of the necessary therapeutic manipulations to be carried out alternately for 2-5 minutes, after which the work tool is replaced with the next cooled one. It should be noted that the work tools of the appliance are sterilizable and safe for future reuse. The availability of a replaceable set of work tools ensures continuous operation of a thermoelectric device for a long time. At the same time, it is essential that the work tool is much lighter and more compact in comparison with analogs and does not contain electrical connections to control and power units. Such a device allows with high accuracy to control the temperature of cryothermic effect on the corresponding areas of the patient's skin during therapeutic manipulations.

A block diagram of a thermoelectric device for treatment of skin diseases is shown in Fig. 2, where 1 is a cooling chamber, 2 is a two-stage thermoelectric Peltier module, 3 is a liquid heat exchanger, 4 is a housing, 5 is a power supply unit, 6 is an electrical terminal connection, 7 - union fluid connection, 8 - water supply network. The use of thermoelectric Peltier modules in the design of a system for liquid cooling of the hot sides of the thermoelectric modules makes it possible to extend the operating temperature range of the device to $(-50 \div 0)\,°C$.
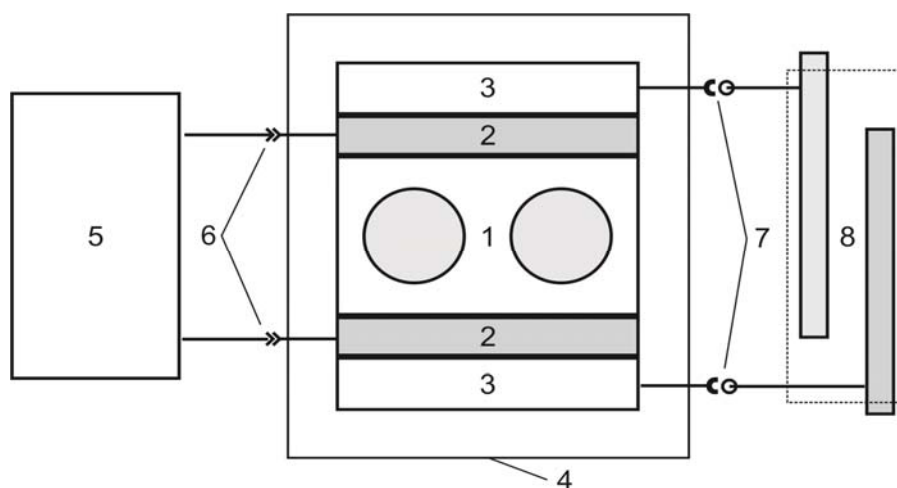

Fig.2. Block-diagram of thermoelectric device for treatment of skin diseases:
1 – cooling chamber, 2 –two-stage thermoelectric Peltier modules, 3 –liquid heat-exchangers,
4 – housing, 5 – power supply unit, 6 – electrical terminal connection, 7 –union fluid connection,
8 –water supply network

The operating principle of the device

The operating principle of the device is to cool work tools with the help of thermoelectric Peltier modules. The cooled work tool has a temperature effect on the corresponding areas of human skin. The advantages of such a device include: the presence of electronic thermometers of work tools, the lack of connection of work tools with the cooling unit and the small overall dimensions of work tools.

Cooling of work tools takes place in a thermoelectric cooling unit based on thermoelectric Peltier modules, the heat from the hot sides of which is removed using a coolant flowing through liquid heat exchangers. For this, the proposed device is connected to a central water supply. The device makes it possible to maintain the temperature of work tools in the range (50 ÷ 0) ° C, which makes it possible to carry out cryodestruction of skin defects and complex treatment of various skin diseases.

The specified device is simple, compact and reliable in operation, which allows a doctor or medical professional to use it without special training, having previously read the instructions. Therefore, the use of such a device is possible both in state medical institutions and in private practice. The introduction of such a device into medical practice will provide physicians with an effective method for the comprehensive treatment of dermatological diseases and cosmetological defects. Such a device can be recommended for practical use in dermatology and cosmetology both in Ukraine and abroad.

In order to determine the effectiveness of the created thermoelectric device and to develop methods for its application, its clinical trial was conducted in the complex treatment of skin diseases with the involvement of employees of the Department of Dermatovenerology, the HSEE of Ukraine "Bukovinsky State Medical University" in the framework of agreement on cooperation. Preliminary results of clinical trials of the device testify to its high prospects in medical practice.

Cryotherapy

A total of 43 patients (31 women, 12 men) aged 19 to 58 years were monitored, of which 22 were diagnosed with acne vulgaris (acne), and 21 were diagnosed with rosacea. During treatment, patients were divided into 2 similar groups by gender, age and diagnosis: the first (comparative) amounted to 21 people who were prescribed standardized therapy for dermatoses, and the second (main) - 22 patients who used cryomassage method in complex therapy with the aid of the developed thermoelectric device for treatment of skin diseases. Statistical processing of the research results was carried out on a personal computer using the licensed software packages Microsoft Excel and Statistica 6.0 StatSoft Inc. Student's t-test was used to assess the probability of differences in the indicators, the difference in indicators was considered probable at p <0.05. To evaluate the nature of the relationships between the indicators, Friedman nonparametric analysis of variance with the definition of χ-square (χ^2),) was used, the dependence between the indicators was considered probable if the χ-square value exceeded the critical value. Examples of clinical applications of a thermoelectric device are given below.

Acne vulgaris (acne). Among the examined patients, common acne was diagnosed in 22 people, of which 18 - clinical manifestations of moderate acne, 4 - severe acne. All patients were prescribed standard therapy for dermatosis, which included means of systemic and external exposure. After regression of pustular acne (purulent rash) in order to accelerate the resolution of inflammatory infiltrative manifestations of acne elements and prevent the development of post-acne, 11 patients (the main group), of which 9 people were previously diagnosed with moderate acne, 2 - with severe acne, additionally used the method of cryomassage with the aid of a thermoelectric device. Cryomassage sessions for patients with acne vulgaris were prescribed for 20-30 seconds 3-4 times in each field (with a total exposure of up to 7-8 minutes) daily for 5-7 days and every other day for the next 10-12 days (total for the course - 10 -12 treatments). According to the analysis of the regression dynamics of the rash elements, which were evaluated 3 months after completion of the course of treatment,

significantly better treatment results were observed in patients with acne of the main group who additionally used the method of cryomassage with the aid of a thermoelectric device (Fig. 3).

Fig.3. Patient M, 23 years. Diagnosis: Common acne, moderate severity
(before and 3 months after treatment).

So, among 11 patients with acne from the main group, the state of clinical recovery or mild manifestations of acne was noted in 9 people, moderate in 2 patients (in the comparison group, respectively, 4 and 7). When conducting Friedman's nonparametric analysis of variance, it was found that a statistically significant relationship is found between the number of patients with a clinical recovery or mild acne and the number of patients with moderate acne 3 months after standard treatment and complex therapy using cryomassage sessions (calculated value $\square 2 = 4.0$ at a critical value of 3.84).

Rosacea (acne pink). Among the examined persons, 21 patients were diagnosed with rosacea (acne pink), 12 of them had papulo-pustular and 9 had erythematous-telangiectatic form of dermatosis. All patients were assigned standard rosacea therapy, which included systemic and external exposure, and in complex therapy, 11 patients (the main group) additionally used the method of cryomassage with the aid of the developed thermoelectric device. The cryomassage method was prescribed to 5 patients with an erythematous-telangiectatic form of dermatosis from the first days of treatment, and to 6 patients with a papular-pustular form - after regression of pustular elements of the rash (7-10 days after the start of treatment). Cryomassage sessions using a thermoelectric device for patients with rosacea of the main group were performed for 20-30 seconds 3-4 times in each field (with a total exposure of up to 10 minutes) daily for 5 days, and the next 10-12 days - every other day (total for the course - 10-12 procedures).

To assess the dermatological status in patients with rosacea before and after their treatment, the rosacea diagnostic assessment scale (SDOR) was used, which includes the sum of the severity of the clinical manifestations of dermatosis: erythema (0 - no erythema; 1 - mild erythema; 2 - moderate; 3 - expressive erythema); determination of the number of papules and pustules (0 - up to 10 elements; 1 - from 11 to 20; 2 - from 21 to 30; 3 - more than 30 elements); presence of telangiectasia (0 - absence; 1 - telangiectasia occupy less than 10% of the face; 2 - from 11% to 30%; 3 - more than 30%); skin dryness and flaking (0 - dryness absent; 1 - weak; 2 - moderate dryness with slight peeling; 3 - strong with pronounced peeling); burning and tingling sensation (0 - absence; 1 - mild; 2 - moderate; 3 - severe); presence of facial edema (0 - no edema; 1 - weak; 2 - moderate; 3 - pronounced). According to clinical observations, within 3 months from the start of treatment, significantly better treatment results were observed in patients with rosacea of the main group, who additionally used the cryomassage method with the aid of the developed thermoelectric device (Fig. 4).

Fig.4. Patient B., 53 years. Diagnosis: Rosaceaa, erythematous-telangiectatic form
(before and 3 months after the start of treatment).

As the results of clinical observation showed, a positive dynamics of the clinical manifestations of rosacea after treatment was noted in patients of both groups, however, a more significant decrease in the SDOR was observed in patients of the main group as compared to its initial values before treatment (2.64 times, $p < 0.001$), and relative to the values of the SDOR after treatment in patients of the comparative group (respectively: 1.57 times, $p = 0.007$).

Cryodestruction

Clinical testing of the use of the developed thermoelectric device for cryodestruction of viral warts using special nozzles, the working surface of which corresponds to the area of the affected skin areas, was also conducted. The results of using the created thermoelectric device with an extended range of operating temperatures with maximum cooling to $-50\,°C$ are presented in Fig. 5 and Fig. 6.

Fig.5. Patient M., 26 years. Diagnosis: common wart (vulgar)
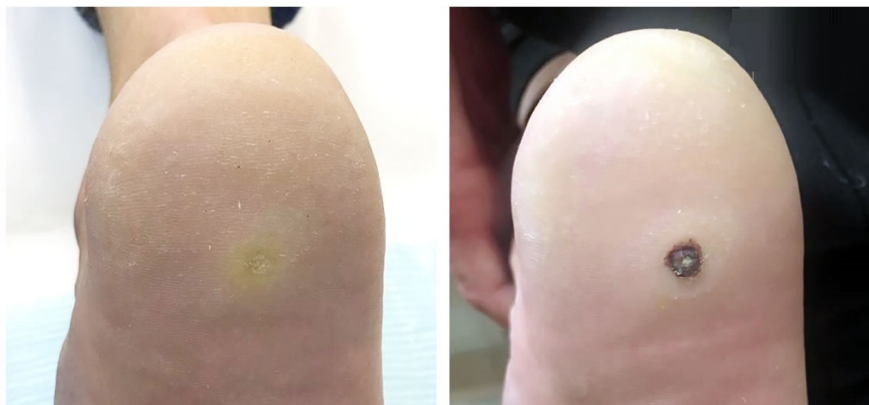*(before and after cryodestruction).*

Fig.6.Patient C., 19years. Diagnosis: plantar wart
(before and after cryodestruction).

It should be noted that all patients underwent the use of cryomassage or cryodestruction sessions with the aid of the developed thermoelectric device for treatment of skin diseases well, without adverse reactions or complications.

So, according to the results of our studies, the created thermoelectric device with an extended range of operating temperatures (50 ÷ 0) °C is effective for cryodestruction of skin defects, in particular, common and plantar warts, as well as for cryomassage in the complex treatment of chronic skin diseases (common acne, rosacea), which indicates its promise and expediency for a widespread use in both cosmetology and dermatology practice to increase the effectiveness of treatment of chronic dermatoses.

Conclusions

1. A thermoelectric device has been designed and manufactured for treatment of skin diseases that has an extended range of operating temperatures (-50 ÷ 0) °C and a visual temperature control of cooling work tools during therapeutic procedures.
2. Clinical testing was carried out and therapeutic efficiency and safety of using the elaborated thermoelectric device with an extended range of operating temperatures (-50 ÷ 0) °C for treatment of skin diseases in dermatology (acne vulgaris, rosacea) and cosmetology (ordinary warts, plantar) was established, which makes it possible to increase significantly the effectiveness of treatment of such patients.
3. The results of the studies indicate the prospects and the expediency of application of the developed thermoelectric device for treatment of skin diseases in dermatology and cosmetology practice.

References

1. Anatychuk L.I. (1979). *Termoelementy i termoelektricheskiie ustroistva. Spravochnik. [Thermoelements and thermoelectric devices. Handbook]*.Kyiv: Naukova dumka [in Russian].
2. Anatychuk L.I. (2003). *Termoelektrichesvo. T.2. Termoelektricheskiie preobrazovateli energii. [Thermoelectricity. Vol.2. Thermoelectric power converters]*. Kyiv, Chernivtsi: Institute of Thermoelectricity [in Russian].
3. Bilovol A.M., Tkachenko S.G. (2012). *Medychna kosmetologiia [Medical cosmetology]*. Vinnytsia: Nova knyha [in Ukrainian].
4. Hryshchenko V.I., Sandomyrskyi B.P., Kolontai Yu.Yu. (1987). *Prakticheskaia kriomeditsina [Practical cryomedicine]*. Kyiv: Zdorovie [in Russian].

5. *Dermatology, venerology. Textbook.* (2013). Prof. V.I.Stepanenko (Ed.). Kyiv: KIM.

6. Zadorozhnyi B.A. (1985). *Krioterapiia v dermatologii (Biblioteka practicheskogo vracha). [Cryotherapy in dermatology (Library of practicing physician)]*. Kyiv: Zdorovie [in Russian].

7. Mashkilleison A.L. (2000). *Lecheniie kozhnykh boleznei [Treatment of skin diseases]*. Moscow: Kron-Press [in Russian].

8. Zemskov V.S., Gasanov L.I. (1988). *Nizkiie temperatury v meditsine [Low temperatures in medicine]*. Kyiv: Naukova dumka [in Russian].

9. Papii N.A. (2002). *Meditsinskaia kosmetika. Spravochnik [Medical cosmetics. Handbook]*. (3d revised edition). Minsk: Belarus [in Russian].

10. *Patent of Ukraine 8462* (2005). Anatychuk L.I., Kushneryk L.Ya. Device for treatment of skin [in Ukrainian].

11. Anatychuk L.I., Kobylianskyi R.R., Mocherniuk Yu.M. (2009). Thermoelectric device for tratment of skin. *J.Thermoelectricity*, 4, 90-96.

12. Anatychuk L.I., Denisenko O.I., Kobylianskyi R.R., Kadeniuk T.Ya. (2015). On the use of thermoelectric cooling in dermatology and cosmetology. *J.Thermoelectricity*, 3, 57-71.

13. Kobylianskyi R.R., Kadeniuk T.Ya. (2016 Pro perspektyvy vykorystannia termoelektryky dlia likuvannia zakhvoriuvan shkiry kholodom [On the prospects of using thermoelectricity for treatment of skin diseases with cold]. *Naukovy visnyk Chernivetskogo universitetu: zbirnyk naukovykh ptrats. Fizyka. Elektronika - Scientific Bulletin of Chernivtsi University: Collection of Scientific Papers. Physics. Electronics,* 5, 1, 67 – 72 [in Ukrainian].

14. Anatychuk L.I., Denisenko O.I., Kobylianskyi R.R., Kadenyuk T.Ya., Perepichka M.P. (2017). Modern methods of cryotherapy in dermatological practice. *Klinichna ta etsperymentalna patologiia-Clinical and Experimental Pathology,* XVI, 1 (59), 150-156 [in Ukrainian].

15. *Patent of UA 104682* (2016). Anatychuk L.I., Kobylianskyi R.R., Kadenyuk T.Ya. Thermoelectric device for treatment of skin diseases [in Ukrainian].

16. *Patent of UA 107918* (2016). Anatychuk L.I., Denisenko O.I., Kobylianskyi R.R., Kadenyuk T.Ya. Method for complex treatment of psoriasis in the stationary and regressing stages [in Ukrainian].

17. *Patent of UA 107922* (2016). Anatychuk L.I., Denisenko O.I., Kobylianskyi R.R., Kadenyuk T.Ya. Method for complex treatment of rosacea [in Ukrainian].

18. *Patent of UA 108563* (2016). Anatychuk L.I., Denisenko O.I., Kobylianskyi R.R., Kadenyuk T.Ya. Method for complex treatment of acne [in Ukrainian].

19. *Patent of UA 108580* (2016). Anatychuk L.I., Denisenko O.I., Kobylianskyi R.R., Kadenyuk T.Ya. Method for complex treatment of limited forms of neurodermatitis [in Ukrainian].

20. *Patent of UA 108581* (2016). Anatychuk L.I., Denisenko O.I., Kobylianskyi R.R., Kadenyuk T.Ya. Method for complex treatment of prurigo [in Ukrainian].

21. *Patent of UA 108582* (2016). Anatychuk L.I., Denisenko O.I., Kobylianskyi R.R., Kadenyuk T.Ya. Method for complex treatment of verrucous flat red lichen [in Ukrainian].

22. *Patent of UA 133595* (2019). Anatychuk L.I., Kobylianskyi R.R. Thermoelectric device for treatment of skin diseases [in Ukrainian].

Submitted 16.08.2019

Анатичук Л.І., *акад. НАН України*[1,2]
Денисенко О.І., *докт. мед. наук., професор*[3]
Кобилянський Р.Р. *канд. фіз.-мат. наук*[1,2]**,**
Степаненко В.І., *докт. мед. наук., професор*[4]**,**
Свирид С.Г., *докт. мед. наук., професор*[4]**,**
Степаненко Р.Л., *док мед. наук, доцент*[4]**,**
Перепічка М.П. *канд. мед. наук, доцент*[3]

[1]Інститут термоелектрики НАН і МОН України,
вул. Науки, 1, Чернівці, 58029, Україна;
e–mail: anatych@gmail.com
[2]Чернівецький національний університет
ім. Юрія Федьковича, вул. Коцюбинського 2,
Чернівці, 58000, Україна,
[3]Вищий державний навчальний заклад України
«Буковинський державний медичний університет»,
МОЗ України, Театральна площа, 2, Чернівці, 58002, Україна
[4]Національний медичний університет імені О.О. Богомольця,
бульвар Тараса Шевченка, 13, Київ, 01601, Україна

ТЕРМОЕЛЕКТРИЧНИЙ ПРИЛАД
ДЛЯ ЛІКУВАННЯ ЗАХВОРЮВАНЬ ШКІРИ

У роботі наведено результати розробки термоелектричного приладу для лікування захворювань шкіри. Розроблений прилад має розширений діапазон робочих температур (-50 ÷ 0) °С та візуальний контроль температури охолоджуючих робочих інструментів під час проведення терапевтичних процедур. Наведено особливості конструкції приладу, його технічні характеристики та результати апробації у клінічній практиці. Бібл. 44, рис. 6, табл. 1.
Ключові слова: термоелектричний прилад, термоелектричне охолодження, лікування захворювань шкіри, дерматологія, косметологія.

Анатычук Л.И., *акад. НАН Украины*[1,2]
Денисенко О.И., *докт. мед. наук., профессор*[3]
Кобылянский Р.Р., *канд. физ.-мат. наук*[1,2]
Степаненко В.И., *докт. мед. наук., профессор*[4]**,**
Свирид С.Г., *докт. мед. наук., профессор*[4]**,**
Степаненко Р.Л., *док мед. наук, доцент*[4],
Перепичка М.П., *канд. мед. наук, доцент*[3]

[1]Институт термоэлектричества НАН и МОН Украины,
ул. Науки, 1, Черновцы, 58029, Украина,
e–mail: anatych@gmail.com;

[2]Черновицкий национальный университет
им. Юрия Федьковича, ул. Коцюбинского, 2,
Черновцы, 58012, Украина,
[3]Высшее государственное учебное заведение Украины
«Буковинский государственный медицинский университет»,
МЗО Украины, Театральная площадь, 2, Черновцы, 58002, Украина
[4]Национальный медицинский университет имени О.О. Богомольца,
бульвар Тараса Шевченко, 13, Киев, 01601, Украина

ТЕРМОЭЛЕКТРИЧЕСКИЙ ПРИБОР
ДЛЯ ЛЕЧЕНИЯ ЗАБОЛЕВАНИЙ КОЖИ

В работе приведены результаты разработки термоэлектрического прибора для лечения заболеваний кожи. Разработанный прибор имеет расширенный диапазон рабочих температур (-50 ÷ 0) °С и допускает визуальный контроль температуры охлаждающих рабочих инструментов во время проведения терапевтических процедур. Описаны особенности конструкции прибора, его технические характеристики и результаты апробации в клинической практике. Библ. 44, рис. 6, табл. 1.

Ключевые слова: термоэлектрический прибор, термоэлектрическое охлаждение, лечение заболеваний кожи, дерматология, косметология.

References

23. Anatychuk L.I. (1979). *Termoelementy i termoelektricheskiie ustroistva. Spravochnik. [Thermoelements and thermoelectric devices. Handbook]*.Kyiv: Naukova dumka [in Russian].

24. Anatychuk L.I. (2003). *Termoelektrichesvo. T.2. Termoelektricheskiie preobrazovateli energii. [Thermoelectricity. Vol.2. Thermoelectric power converters]*. Kyiv, Chernivtsi: Institute of Thermoelectricity [in Russian].

25. Bilovol A.M., Tkachenko S.G. (2012). *Medychna kosmetologiia [Medical cosmetology]*. Vinnytsia: Nova knyha [in Ukrainian].

26. Hryshchenko V.I., Sandomyrskyi B.P., Kolontai Yu.Yu. (1987). *Prakticheskaia kriomeditsina [Practical cryomedicine]*. Kyiv: Zdorovie [in Russian].

27. *Dermatology, venerology. Textbook.* (2013). Prof. V.I.Stepanenko (Ed.). Kyiv: KIM.

28. Zadorozhnyi B.A. (1985). *Krioterapiia v dermatologii (Biblioteka practicheskogo vracha). [Cryotherapy in dermatology (Library of practicing physician)]*. Kyiv: Zdorovie [in Russian].

29. Mashkilleison A.L. (2000). *Lecheniie kozhnykh boleznei [Treatment of skin diseases]*. Moscow: Kron-Press [in Russian].

30. Zemskov V.S., Gasanov L.I. (1988). *Nizkiie temperatury v meditsine [Low temperatures in medicine]*. Kyiv: Naukova dumka [in Russian].

31. Papii N.A. (2002). *Meditsinskaia kosmetika. Spravochnik [Medical cosmetics. Handbook]*. (3d revised edition). Minsk: Belarus [in Russian].

32. *Patent of Ukraine 8462* (2005). Anatychuk L.I., Kushneryk L.Ya. Device for treatment of skin [in Ukrainian].

33. Anatychuk L.I., Kobylianskyi R.R., Mocherniuk Yu.M. (2009). Thermoelectric device for tratment of skin. *J.Thermoelectricity*, 4, 90-96.

34. Anatychuk L.I., Denisenko O.I., Kobylianskyi R.R., Kadeniuk T.Ya. (2015). On the use of thermoelectric cooling in dermatology and cosmetology. *J.Thermoelectricity*, 3, 57-71.

35. Kobylianskyi R.R., Kadeniuk T.Ya. (2016 Pro perspektyvy vykorystannia termoelektryky dlia likuvannia zakhvoriuvan shkiry kholodom [On the prospects of using thermoelectricity for treatment of skin diseases with cold]. *Naukovy visnyk Chernivetskogo universitetu: zbirnyk naukovykh ptrats. Fizyka. Elektronika - Scientific Bulletin of Chernivtsi University: Collection of Scientific Papers. Physics. Electronics,* 5, 1, 67 – 72 [in Ukrainian].

36. Anatychuk L.I., Denisenko O.I., Kobylianskyi R.R., Kadenyuk T.Ya., Perepichka M.P. (2017). Modern methods of cryotherapy in dermatological practice. *Klinichna ta etsperymentalna patologiia-Clinical and Experimental Pathology,* XVI, 1 (59), 150-156 [in Ukrainian].

37. *Patent of UA 104682* (2016). Anatychuk L.I., Kobylianskyi R.R., Kadenyuk T.Ya. Thermoelectric device for treatment of skin diseases [in Ukrainian].

38. *Patent of UA 107918* (2016). Anatychuk L.I., Denisenko O.I., Kobylianskyi R.R., Kadenyuk T.Ya. Method for complex treatment of psoriasis in the stationary and regressing stages [in Ukrainian].

39. *Patent of UA 107922* (2016). Anatychuk L.I., Denisenko O.I., Kobylianskyi R.R., Kadenyuk T.Ya. Method for complex treatment of rosacea [in Ukrainian].

40. *Patent of UA 108563* (2016). Anatychuk L.I., Denisenko O.I., Kobylianskyi R.R., Kadenyuk T.Ya. Method for complex treatment of acne [in Ukrainian].

41. *Patent of UA 108580* (2016). Anatychuk L.I., Denisenko O.I., Kobylianskyi R.R., Kadenyuk T.Ya. Method for complex treatment of limited forms of neurodermatitis [in Ukrainian].

42. *Patent of UA 108581* (2016). Anatychuk L.I., Denisenko O.I., Kobylianskyi R.R., Kadenyuk T.Ya. Method for complex treatment of prurigo [in Ukrainian].

43. *Patent of UA 108582* (2016). Anatychuk L.I., Denisenko O.I., Kobylianskyi R.R., Kadenyuk T.Ya. Method for complex treatment of verrucous flat red lichen [in Ukrainian].

44. *Patent of UA 133595* (2019). Anatychuk L.I., Kobylianskyi R.R. Thermoelectric device for treatment of skin diseases [in Ukrainian].

Submitted 16.08.2019

Anatychuk L.I., *acad. National Academy of Sciences of Ukraine*[1,2]
Vikhor L.M., *doc. phys.-math. science*[1,2]
Mitskaniuk N.V.[1,2]

[1]Institute of Thermoelectricity of the NAS and MES of Ukraine,
1, Nauky str., Chernivtsi, 58029, Ukraine;
e-mail: anatych@gmail.com
[2]Yu.Fedkovych Chernivtsi National University,
2, Kotsiubynskyi str., Chernivtsi, 58012, Ukraine

CONTACT RESISTANCE DUE TO POTENTIAL BARRIER AT THERMOELECTRIC MATERIAL–METAL BOUNDARY

The theoretical aspects of estimating the resistance due to carriers passing through a potential barrier at the boundary between thermoelectric material and metal are considered. The temperature dependences of boundary resistivity were calculated for thermoelectric legs of Bi_2Te_3 based materials with the deposited anti-diffusion nickel layers. It was established that the value of boundary resistance in such legs varies with temperature from $0.5 \cdot 10^{-7}$ to $2.5 \cdot 10^{-7}$ $Ohm \cdot cm^2$. It was shown that boundary resistance can be reduced by increasing carrier concentration in the ultra-thin nickel contact layer of thermoelectric material due to doping. It was established that increasing the concentration of doping impurities in the near-contact zone by one order of magnitude with respect to its optimal value results in decreasing electrical boundary resistance by two orders. Under these conditions, the resistance value approaches minimum possible value and is 10^{-9} $Ohm \cdot cm^2$. Bibl. 35, Fig. 6, Tabl. 1.

Key words: thermoelectric material-metal contact, potential barrier, electrical boundary resistance.

Introduction

The efficiency of thermoelectric modules is mainly determined by the figure of merit of semiconductor materials of which the thermoelement legs are made. However, the efficiency of a real thermoelement essentially depends on the electrical resistance of a contact between semiconductor material and metal interconnect layers [1 – 3] connecting the thermoelectric legs of module. The Joule heat released in the contact zone reduces the energy efficiency of thermoelectric converters and leads to its dependence on the height of the thermoelement legs [4]. The negative influence of contact resistance on the characteristics of thermoelectric devices is especially perceptible in the conditions of miniaturization of the thermoelement legs, when the thickness of the transient contact layer between thermoelectric material (TEM) and metal becomes commensurate with the height of the thermoelement leg, and the contact resistance commensurate with the resistance of the leg itself [5,6].

The miniaturization of thermoelectric energy converters is a modern direction of their improvement, aimed primarily at reducing the cost of thermoelectric materials and cheapening due to this of thermoelectric modules [6-12]. Therefore, reducing the value of contact resistance to increase the energy efficiency of thermoelectric converters in miniaturization is an urgent task.

In [13], a model of TEM-metal contact structure was considered. It was shown that the contact resistance is formed by its two main components. This is, first, the electrical resistance of the transient layer at the boundary between semiconductor material and metal. This resistance depends on such factors as mutual diffusion of atoms or molecules of contacting materials, their chemical interaction, which results in the formation of new phase [14,15] and even multilayer [16,17] microstructures. Also, some action is exerted by the non-ideality of TEM-metal boundary which is due to roughness, chemical contamination of leg surface prior to deposition of metal thereupon, and other factors [18-20]. Modern technologies of manufacturing TEM-metal contacts, in particular in micromodules, by spraying, chemical deposition of anti-diffusion metal layers on the cleaned, polished and specially treated ends of thermoelectric legs allow minimizing the height of the transient layer and, therefore, its electrical resistance, and to obtain actually "ideal" (without transient layer) TEM-metal boundary. However, the sharp difference between the energy band structures of the semiconductor and the metal leads to the formation of a potential barrier at the TEM-metal boundary [21]. A potential barrier impedes the movement of current carriers across the boundary and is the cause of the second component of contact resistance, commonly called the electrical boundary resistance [22,23].

The purpose of this work is to consider theoretical methods for estimating the TEM-metal boundary resistance and the factors affecting this resistance, to calculate the potential barrier resistance for thermocouples from traditional Bi_2Te_3-based materials and to identify ways to reduce the boundary resistance to a minimum possible value.

Methods for calculating the electrical resistance of TEM-metal boundary

Methods for calculating the electrical resistance due to carriers passing through semiconductor-metal boundary are described in [21-27]. We consider the main results of these works and apply them to calculate the specific, that is, related to unit area, resistance of TEM-metal boundary.

For example, consider the contact of a metal with an *n*-type semiconductor for the case of such current polarity when electrons move from metal to semiconductor. When a metal collides with a semiconductor, due to the difference between their Fermi levels, a contact potential difference arises that distorts the energy bands of the semiconductor [26]. If the difference between the Fermi levels is such that part of the electrons from metal pass to semiconductor, then the so-called anti-locking layer is created in semiconductor near the boundary and the bands are bent down (Fig.1a). It is obvious that such contact will not interfere with the movement of electrons. If, however, the difference between the Fermi levels is such that part of the electrons at the boundary will pass from semiconductor to metal, a locking layer is formed, the bands bend upwards (Fig. 1b) and a potential barrier [27] is created for electrons moving from metal to semiconductor. As noted, this barrier is the cause of the electrical boundary resistance.

The diagram of TEM-metal energy bands in the presence of a potential barrier is shown in Fig. 2. In this figure, $E_b = \varphi_m - \chi_n - \Delta\varphi_b$ is the height of potential barrier, φ_m is electronic work function, χ_n is affinity of semiconductor electrons, $\Delta\varphi_b$ is the energy of barrier reduction due to the non-ideal metal-semiconductor contact.

The electrical boundary resistance depends on the mechanism of carriers passing through the potential barrier. Carriers can overcome the potential barrier by thermionic emission over the barrier (TIE) or tunneling through the barrier. There are two types of tunneling: tunneling of carriers with energies close to the Fermi energy in a semiconductor, the so-called field emission (FE) and tunneling of carriers with higher energies, the so-called thermionic field emission (TFE) (Fig.2). [27].
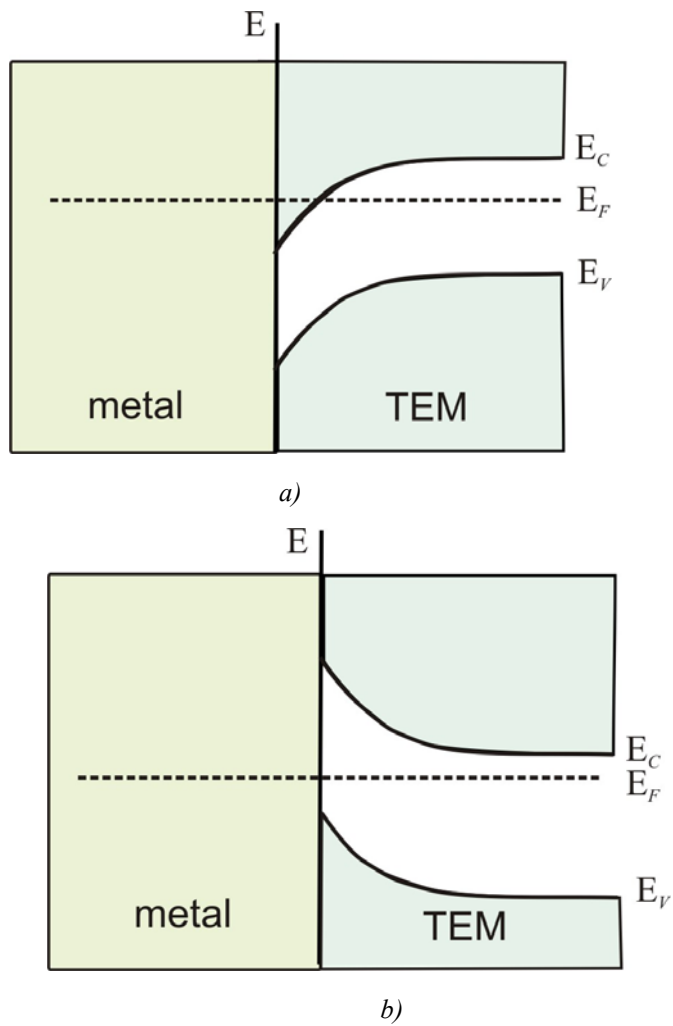
a)

b)

Fig.1. Bending of semiconductor energy bands in the zone of contact with metal.
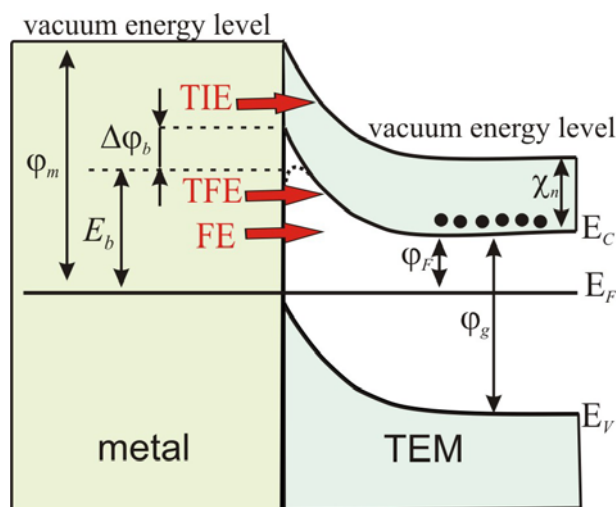*a) anti-locking layer, b) locking layer.*

Fig.2. Diagram of energy bands of metal contact with thermoelectric n-type material.
Mechanisms of electrons passing through potential barrier:
FE – field emission, TFE – thermionic field emission,
TIE –thermionic emission.

The criterion of the mechanism for carriers passing is the ratio of thermal energy kT to parameter E_{00}, which was proposed by Padovani and Stratton [28] and is defined as

$$E_{00} = \frac{e\hbar}{2}\sqrt{\frac{N_d}{m^*\varepsilon_s\varepsilon_0}} \tag{1}$$

where e is electron charge, N_d is impurity concentration in semiconductor, m^* is the effective mass of charge carriers, ε_0 is the dielectric constant, ε_s is the relative permeability of semiconductor. Under high temperature conditions in weakly doped semiconductors, when $kT/E_{00} \gg 1$, the thermionic emission mechanism without tunneling prevails. For heavily doped (degenerate) semiconductor at low temperatures $kT/E_{00} \ll 1$, the field emission (FE) is predominant. When $kT/E_{00} \approx 1$, the thermionic field emission (TFE) mechanism is operating.

In case of thermionic emission, the ratio for estimating the boundary resistivity r_b is obtained on the basis of standard equations of thermionic emission and is given by [21,25,27]

$$r_b = \frac{k}{eAT}\exp\left(\frac{E_b}{kT}\right), \tag{2}$$

where $A = \dfrac{em^*k^2}{2\pi^2\hbar^3}$ is the effective Richardson constant.

In the cases of tunneling of carriers, for the calculation of r_b one can use the approximate analytical expressions [27-29]:

$$r_b = \frac{k\sin(\pi c_1 kT)}{e\pi AT}\exp\left(\frac{E_b}{E_{00}}\right), \quad \text{when } kT/E_{00} \ll 1, \tag{3}$$

$$r_b = \frac{k^2\cosh(E_{00}/kT)\sqrt{\coth(E_{00}/kT)}}{eA\sqrt{\pi(E_b-\varphi_F)E_{00}}}\exp\left(\frac{E_b-\varphi_F}{E_{00}\coth(E_{00}/kT)}+\frac{\varphi_F}{kT}\right), \text{ when } kT/E_{00} \approx 1, \tag{4}$$

where $c_1 = \dfrac{1}{2E_{00}}\ln\left(\dfrac{4E_b}{-\varphi_F}\right)$, φ_F are the energies of semiconductor Fermi level (φ_F is counted from the bottom of conduction band and for the degenerate semiconductors is a negative value).

Thus, from the analytical expressions (2) – (4) it is clear that the value of TEM-metal boundary resistivity r_b depends on the temperature, the height of potential barrier E_b and the impurity concentration in TEM N_d. In the mode of thermionic emission the value of r_b is actually independent of the impurity concentration and is determined only by the height of potential barrier: $r_b \sim \exp\left(\dfrac{E_b}{kT}\right)$.

In tunneling mode, the exponential dependence of r_b on barrier height is supplemented by the dependence on impurity concentration. For the mechanism of FE $r_b \sim \exp\left(E_b/\sqrt{N_d}\right)$, and for TFE $r_b \sim \exp\left(E_b\left/\left(\sqrt{N_d}\coth\dfrac{E_{00}}{kT}\right)\right.\right)$ [29]. Under the condition of high impurity concentration N_d, when the mechanism of FE is operating, r_b assumes low values. With decreasing impurity concentration, the FE tunneling mechanism is substituted by TFE and goes over to thermionic emission TE, and the resistance r_b in this case increases.

It also follows from (2) − (4) that the values of r_b will be low under conditions of low potential barriers. In [30], it was studied which boundary values can be reached by resistance r_b. The expression for estimating the minimum boundary resistance $r_{b\,min}$ was obtained which is given by [30]

$$r_{b\min} = \frac{k}{eAT}\frac{1}{\ln\left[1+\exp\left(-\varphi_F/kT\right)\right]} \cdot r_{b\min} = \frac{k}{eAT}\frac{1}{\ln\left[1+\exp\left(-\varphi_F/kT\right)\right]}. \qquad (5)$$

For the nondegenerate semiconductors $\varphi_F \gg kT$, the relation (5) is transformed into classical formula for calculating the resistivity of anti-locking contact [25, 30]:

$$r_{b\min} = \frac{k}{eAT}\exp\left(\varphi_F/kT\right) = \frac{k}{eAT}\frac{N_c}{N_d} = \frac{(2\pi m^* kT)^{1/2}}{e^2 N_d}, \qquad (6)$$

where $N_c = 2\dfrac{(2\pi m^* kT)^{3/2}}{h^2}$ is the effective density of energy states in conduction band.

For the case of degenerate semiconductors with $\varphi_F < -kT$ [30] the expression for $r_{b\min}$ is given by

$$r_{b\min} = \frac{k}{eAT\left[1+2\alpha\left(-\varphi_F\right)\right]}\frac{kT}{\left(-\varphi_F\right)}, \qquad (7)$$

where α is a nonparabolicity parameter of semiconductor conduction band.

The value of the Fermi energy φ_F, required for estimating r_b by the formulae (3), (4) and $r_{b\min}$ by formula (5), is a solution of electroneutrality equation, which for impurity semiconductor with the impurity concentration N_d on the assumption that all impurity atoms are single ionized, is of the form [30,31]

$$N_c F_{1/2}\left(-\frac{\varphi_F}{kT}\right) = N_d, \qquad (8)$$

where $F_{1/2}\left(\eta\right) = \dfrac{2}{\sqrt{\pi}}\displaystyle\int_0^\infty \dfrac{\sqrt{x}}{1+\exp(x-\eta)}\mathrm{d}x$ is the Fermi integral.

Thus, in order to obtain a low TEM-metal boundary resistivity, the impurity concentration in the near-contact region should be high and the height of potential barrier - low. These are classical requirements for improving the ohmicity of semiconductor-metal contact. It should be borne in mind that the barrier height E_b depends on semiconductor energy gap φ_g (Fig. 2). For wide-gap semiconductors it is difficult to achieve good ohmic contacts. In the majority of metals, the value of work function φ_m is high, which also does not contribute to formation of low TEM-metal potential barriers, and, accordingly, good ohmic contacts. Therefore, to get a low TEM-metal boundary resistivity, one can recommend traditional technologies for improving the ohmicity of contacts [27]. One of the methods is to make heavily doped a narrow layer of thermoelectric material which is in contact to metal.

Consider the results of calculating TEM-metal boundary resistivity for classical thermoelements based on Bi_2Te_3 and analyze the effect of heavier doping of the near-contact layer on this resistivity value.

Results of calculating the resistivity of TEM-metal boundary

The electrical boundary resistivity was estimated for thermoelectric legs of traditional *n*-type materials $Bi_2Te_{2.7}Se_{0.3}$ and *p*-type materials $Bi_{0.5}Sb_{1.5}Te_3$ that are in contact to nickel anti-diffusion layers. The parameters of these TEM required for calculations are given in Table 1.

TEM parameters

Parameter	TEM		Reference
	$Bi_2Te_{2.7}Se_{0.3}$ *n*-type	$Bi_{0.5}\ Sb_{1.5}Te_3$ *p*-type	
Optimal impurity concentration in TEM $N_{d\ opt}$, m^{-3}	$3\cdot10^{25}$	$2\cdot10^{25}$	[32]
Carrier mass m^* (m_0 – electron mass)	$1.25m_0$	$0.6m_0$	[32]
Relative dielectric constant ε	98	62	[23]

To estimate the effect of heavier doping of near-contact TEM layer, calculations were performed for different values of impurity concentration in this layer, which was increased by the order of magnitude with respect to its optimal value.

To calculate the electrical resistance of TEM-metal boundary r_b, it is primarily necessary to determine the mechanism of carriers passing through the potential barrier. For this purpose, the Padovani-Stratton E_{00} was calculated (1), and the temperature dependence of effective mass m^* and dielectric constant was not taken into account. The temperature dependences of dimensionless criterion kT/E_{00} of the mechanism of passing the barrier for different values of impurity concentration N_d in the near-contact layer of n- and p-type TEM are shown in Fig.3*a*. It follows from the figure that in the temperature range of 200 – 350 K under condition of optimal impurity concentration $N_{d\ opt}$ for *n*-type thermoelectric leg $kT/E_{00} > 1$, and for *p*-type leg – $kT/E_{00} \sim 1$. If the near-contact concentration of impurities, hence of carriers, will be of the order of 10^{26}m^{-3}, then for *n*-type leg $kT/E_{00} \sim 1$, and for *p*-type leg $kT/E_{00} < 1$. Thus, in order to calculate the electrical boundary resistance of *n*-type leg with the optimal impurity concentration, it is expedient to use relation (2), valid for TIE mechanism of passing the barrier, and for the leg with impurity concentration in the near-contact layer of the order of 10^{26} m^{-3} – formula (4) for TFE mechanism. For *p*-type leg with optimal concentration use was made of formula (4), and for high concentrations – formula (3) for FE mechanism to overcome the barrier.

Also, for the calculations one should first of all determine the value of the Fermi energy φ_F in TEM and the height of potential barrier E_b. The temperature dependences of the dimensionless Fermi energy φ_F/kT for Bi_2Te_3-based TEM with different impurity concentrations calculated on the basis of Eq. (8) are shown in Fig. 3*b* and were used to calculate the boundary resistance r_b for these TEM contacts with nickel.

The height of potential barrier can be estimated by simple relations, namely for metal-*n*-type semiconductor boundary $E_b = \varphi_m - \chi_n$, for metal-*p*-type semiconductor boundary $E_b = \varphi_g - (\varphi_m - \chi_p)$ [27]. However, these relations are almost never satisfied [27]. This is due to such major reasons as the presence of a contact gap between metal and semiconductor, the existence of contact energy states, the lowering of the barrier height due to the forces of images, etc.

Therefore, the height of TEM-metal barrier should be determined experimentally. In [33], potential barriers between individual metals and semiconductors are presented. It is shown that the

height of barriers $E_b \leq 0.1\,\text{eV}$, including the boundary between two TEM Bi_2Te_3/Sb_2Te_3 (E_b=0.035 eV). In [22], the barriers between Bi_2Te_3 and Sb_2Te_3 with metal were taken to be E_b=0.1eV. In [34], for the contacts between Ni and solid solutions $(Bi,Sb)_2(Se,Te)_3$, the value of barrier height E_b=0.13eV was proposed, which we used to calculate the electrical boundary resistance between nickel and Bi_2Te_3 - based TEM.
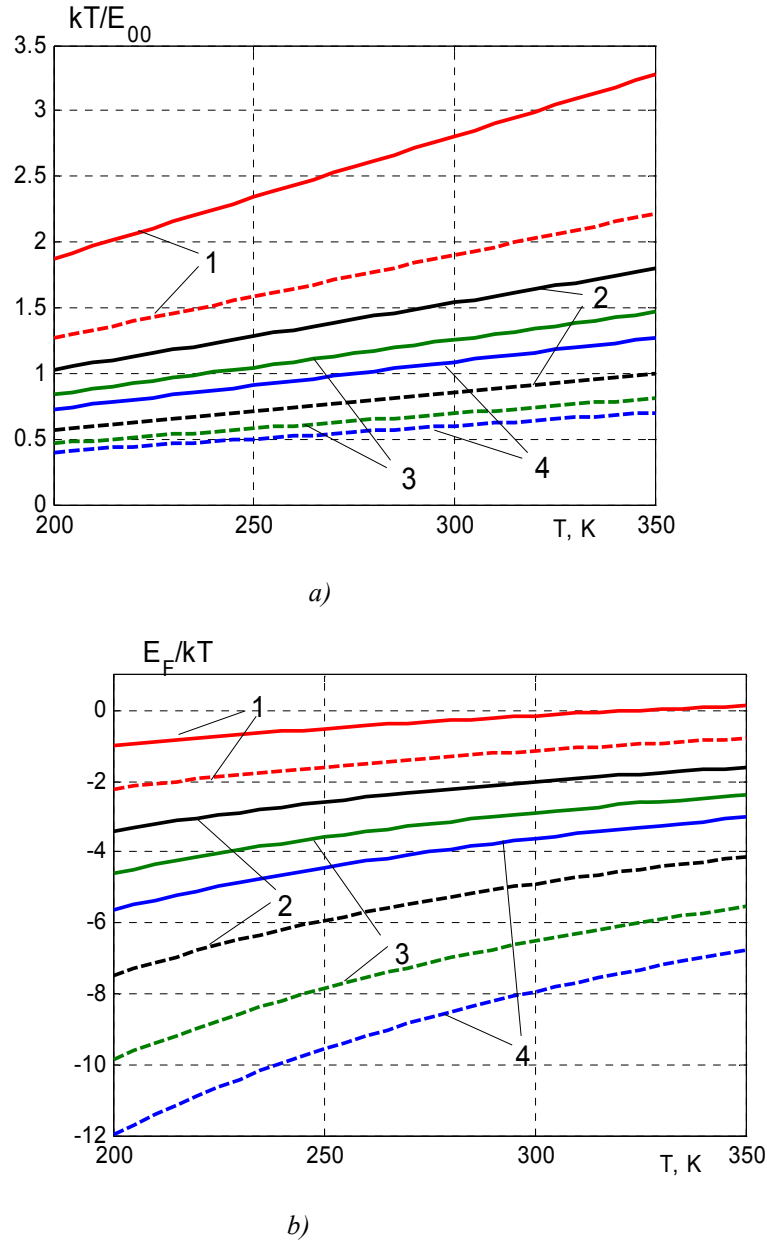

a)

b)

Fig.3. Temperature dependences of the dimensionless criterion kT/E_{00} of barrier passing mechanism (a) and the dimensionless Fermi energy φ_F/kT (b) for n-type $Bi_2Te_{2.7}Se_{0.3}$ (solid lines) and p-type $Bi_{0.5}Sb_{1.5}Te_3$ (dashed lines). Impurity concentration N_d in TEM contact layer: 1 – optimal concentration in TEM, 2 – N_d=10^{26} m^{-3}, 3 – N_d=$1.5 \cdot 10^{26}$ m^{-3}, 4 – N_d=$2 \cdot 10^{26}$ m^{-3}.

The temperature dependences of the electrical boundary resistance $r_b(T)$, calculated for different concentrations of doping impurities in the near-contact layer, are shown in Fig. 4. As the temperature decreases from 350K to 200 K, under optimal concentration of impurities in TEM, the value of r_b

increases from $0.5 \cdot 10^{-7}$ to $2.5 \cdot 10^{-7}$ Ohm·cm². With a rise in impurity concentration, the boundary resistivity drastically decreases and actually is temperature-independent.
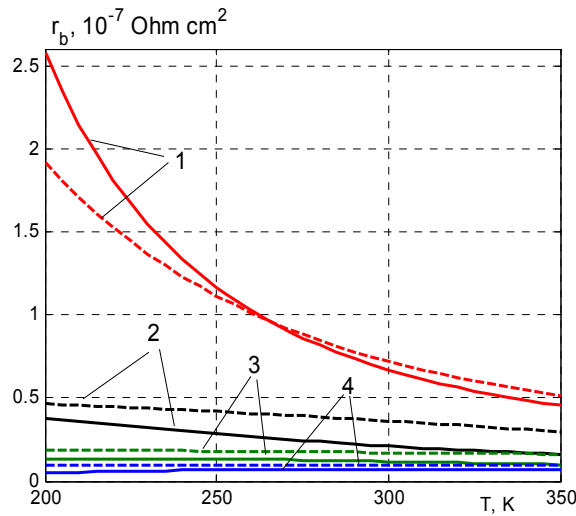

Fig.4. Temperature dependences of boundary resistivity r_b for contacts of nickel with
n-type $Bi_2Te_{2.7}Se_{0.3}$ (solid lines) and p-type $Bi_{0.5}Sb_{1.5}Te_3$ (dashed lines), calculated for
different concentrations of doping impurities N_d in the near-contact
TEM layer: 1 – optimal concentration in TEM, 2 – $N_d=10^{26}$ m⁻³,
3 – $N_d=1.5 \cdot 10^{26}$ m⁻³, 4 – $N_d=2 \cdot 10^{26}$ m⁻³.

Fig.5 shows the temperature dependences of minimum resistivity $r_{b\,min}(T)$ of TEM-*Ni* barrier, calculated by relation (5) for different values of N_d. $r_{b\,min}$ weakly depends on temperature, and the order of magnitude of this resistance is $10^{-9} – 10^{-10}$ Ohm·cm². $r_{b\,min}$ is a boundary value to which the value of TEM-*Ni* boundary resistance tends under condition of lowering the height of potential barrier.
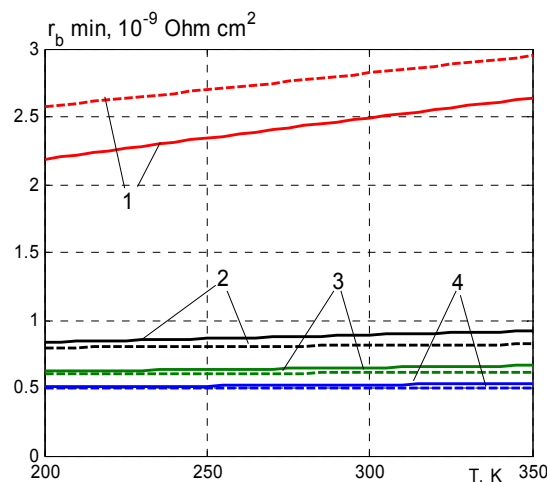
Fig.5. Temperature dependences of minimum boundary resistivity $r_{b\,min}$ for contacts
of nickel with n-type $Bi_2Te_{2.7}Se_{0.3}$ (solid lines) and p-type $Bi_{0.5}Sb_{1.5}Te_3$ (dashed lines),
calculated for different concentrations of doping impurities N_d in the near-contact TEM layer:
1 – optimal concentration in TEM, 2 – $N_d=10^{26}$ m⁻³, 3 – $N_d=1.5 \cdot 10^{26}$ m⁻³, 4 – $N_d=2 \cdot 10^{26}$ m⁻³.

Fig.6 shows the dependences of boundary resistivity on impurity concentration N_d under

conditions of heavier doping of near-contact layer. The same figure shows a similar dependence of minimum boundary resistance. If we increase the concentration of doping impurities in the near-contact TEM layer by one order with respect to its optimal value, the electrical boundary resistance is actually decreased by two orders. Under these conditions, its value r_b approaches minimum value of $r_{b\ min}$, and its order will make 10^{-9} Ohm·cm².
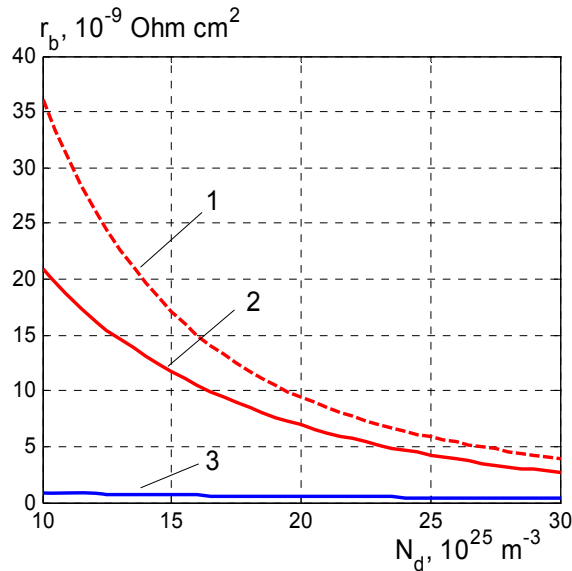

Fig.6. Dependences of boundary resistivity r_b on impurity concentration N_d in the nickel contact layer of p-type $Bi_{0.5}Sb_{1.5}Te_3$ (1) and n-type $Bi_2Te_{2.7}Se_{0.3}$ (2) under condition of T=300 K. 3 – dependences of minimum resistivity $r_{b\ min}(N_d)$ practically coincide for p- and n-type TEM.

Thus, the creation at the boundary between the Bi_2Te_3-based material and the nickel of a thin contact layer with a high concentration of charge carriers neutralizes the effect of the potential barrier and reduces the electrical boundary resistance and the contact resistance as a whole. This is confirmed, in particular, by the experimental results described in [34]. To obtain such heavily doped near-contact layers, special technologies are used, for example, ion implantation of impurities [34].

In [35], the results of theoretical and experimental studies of contact resistance in Bi_2Te_3 -based thermoelectric legs with anti-diffusion nickel layers were analyzed. It was shown that the value of contact resistance does not exceed $5 \cdot 10^{-6}$ Ohm·cm². Creating "ideal" contacts allows reducing this value to 10^{-9} Ohm·cm². Using the Comsol Multiphysics thermoelectric software package, we estimated the effect of contact resistance on the efficiency of a Bi_2Te_3-based thermoelectric converter with miniature legs 0.5 mm high. It was concluded that improving the contact technology which would reduce the contact resistance from $5 \cdot 10^{-6}$ Ohm·cm² to the minimum possible 10^{-9} Ohm·cm², helps to increase the converter efficiency by 20 %.

Conclusions

1. Methods for calculating the electrical resistance of TEM-metal boundary arising due to formation of potential barrier in the zone of contact between thermoelectric material and metal are proposed. The temperature dependences of the boundary resistance for thermoelectric legs made of Bi_2Te_3-based materials with the deposited anti-diffusion nickel layers are calculated.

2. It is established that boundary resistance in such structures under optimal impurity concentration in TEM reaches the value from $0.5 \cdot 10^{-7}$ to $2.5 \cdot 10^{-7}$ Ohm·cm² and is a function of temperature.

3. It is shown that the impact of potential barrier at the TEM-metal boundary can be effectively neutralized by creating a thin near-contact layer with a high concentration of carriers due to doping. This requires special technologies, such as ion implantation technique.

4. It is established that increasing the concentration of doping impurities in the nickel contact zone of TEM by one order of magnitude with respect to its optimal value results in decreasing the electrical boundary resistance actually by two orders of magnitude. Under these conditions, its value approaches the minimum possible value, and its order is 10^{-9} Ohm·cm^2, which helps to increase the efficiency of thermoelectric energy conversion by 20 %.

References

1. Aswal D.K., Basu R., Singh A. (2016). Key issues in development of thermoelectric power generators: high figure-of-merit materials and their highly conducting interfaces with metallic interconnects. *Energy Convers. Manag*, 114, 50-67.

2. Anatychuk L.I., Kuz R.V. (2012). The energy and economic parameters of Bi-Te based thermoelectric generator modules for waste heat recovery. *J.Thermoelectricity*, 4, 75-82.

3. Drabkin I.A., Osvensky V.B., Sorokin A.I., Panchenko V.P., Narozhnaia O.E. (2017). Kontaktnoie soprotivleniie v sostavnykh termoelektricheskikh vetviakh [Contact resistance in composite thermoelectric legs]. *Fizika i tekhnika poluprovodnikov – Semiconductors*, 51 (8), 1038-1040.

4. Anatychuk L.I. (2003). *Termoelektrichestvo. Tom 2. Termoelektricheskiie preobrazovateli energii [Thermoelectricity. Vol.2. Thermoelectric power converters]*. Kyiv, Chernivtsi: Institute of Thermoelectricity [in Russian].

5. Semenyuk V.A. (2006). Thermoelectric cooling of electro-optic components. *Thermoelectrics Handbook: Macro to Nano.* D.M. Rowe (Ed.). London, New York: CRC Taylor&Francis.

6. Semenyuk V. (2019). Effect of electrical contact resistance on the performance of cascade thermoelectric coolers. *J. Electron. Mater*, 48(4), 1870-1876.

7. H. Bottner, J. Nurnus, A. Schubert. (2006). Miniaturized thermoelectric converters, in: *Thermoelectrics Handbook, Macro to Nano.* D.M. Rowe (Ed.). London, New York: CRC Taylor&Francis.

8. Crane N.B., Mishra P., Murray J. L., Nolas G.S. (2009). Self-assembly for integration of microscale thermoelectric coolers. *J. of Electron. Mater*, 38(7), 1252-1256.

9. Huang I-Yu, Linb Jr-Ching, She Kun-Dian, et al. (2008). Development of low-cost micro-thermoelectric coolers utilizing MEMS technology. *Sensors and Actuators*, A 148, 176-185.

10. Navone C., Soulier M., Plissonnier M., Seiler A.L. (2010). Development of (Bi,Sb)$_2$(Te,Se)$_3$-based thermoelectric modules by a screen-printing process. *J. of Electron. Mater*, 39(9), 1755-1759.

11. Goncalves L.M., Couto C., Alpuim P., Correia J.H. (2008).Thermoelectric micro converters for cooling and energy-scavenging systems. *J. Micromech. Microeng*, 18, 064008-1 - 064008-5.

12. Y. Y. Zhou, J. L. Yu. (2012). Design optimization of thermoelectric cooling systems for applications in electronic devices. *Int. J. Refrig*, 35, 1139-1144.

13. Vikhor L.M., Anatychuk L.I., Gorskyi P.V. (2019). Electrical resistance of metal contact to Bi$_2$Te$_3$ based thermoelectric legs. *J. of Appl. Phys*, 126, 164503-1 – 164503-8.

14. Jing H., Li Y., Xu L., et al. (2015). Interfacial reaction and shear strength of SnAgCu/Ni/Bi$_2$Te$_3$-based TE materials during aging. *Mater. Eng. and Perform*, 24(12), 4844-4852.

15. Chen L., Mei D., Wang Y., Li Y. (2019). Ni barrier in Bi$_2$Te$_3$-based thermoelectric modules for reduced contact resistance and enhanced power generation properties. *J. Alloys and Comp*, 796, 314-320.

16. Chuang C.-H.mailto:please_login, Lin Y.-C., Lin C.-W. (2016). Intermetallic reactions during the solid-liquid interdiffusion bonding of $Bi_2Te_{2.55}Se_{0.45}$ thermoelectric material with Cu electrodes using a Sn interlayer. *Metals*, 6(4), 92-97.

17. Iyore O. D., Lee T. H., Gupta R. P., et al. (2009). Interface characterization of nickel contacts to bulk bismuth tellurium selenide. *Surf. Interface Anal*, 41, 440-444.

18. Gupta R.P., McCarty R., Sharp J. (2014). Practical contact resistance measurement method for bulk Bi_2Te_3 based thermoelectric devices. *J. of Electron. Mater*, 43(6), 1608-1612.

19. Joshi G., Mitchell D., Ruedin J., et al. (2019). Pulsed-light surface annealing for low contact resistance interfaces between metal electrodes and bismuth telluride thermoelectric materials. *J. Mater. Chem. C*, 7**,** 479-484.

20. Gupta R. P., Xiong K., White J. B., Cho K., Alshareef H.N., Gnade B.E.(2010). Low resistance ohmic contacts to Bi_2Te_3 using Ni and Co metallization. *J. of Electrochem. Soc*, 157(6), H666-H670.

21. Bartkowiak M., Mahan G.D. (2001). Heat and electricity transport through interfaces, in: *Recent Trends in Thermoelectric Materials, vol. II, Semiconductors and Semimetals*, vol. 70. New York: Academic Press.

22. Da Silva L. W., Kaviany M. (2004). Microthermoelectric cooler: interfacial effects on thermal and electrical transport. *Int. J. of Heat and Mass Transfer*, 47(10-11), 2417–2435.

23. Vikhor L.M., Gorskyi P.V. (2015). Heat and charge transport at thermoelectric material-metal boundary. *J. Thermoelectricity*, 6, 5-15.

24. Bartkowiak M., Mahan G.D. (1999). Boundary effects in thin-film thermoelctrics. *Proc. of Mat. Res. Soc. Symp*, 545, 265-272.

25. Rhoderick E.H. (1978). *Metal-semiconductor contacts*.Oxford: Clarendon Press.

26. Goldberg Yu.A. (1994). Omicheskii kontakt metall-poluprovodnik AIIIBV: metody sozdaniia i svoistva [Ohmic contact metal- AIIIBV semiconductor: methods of creation and properties]. *Fizika i tekhnika poluprovodnikov - Semiconductors*, 28(10), 1681-1698.

27. Sze S.M., Ng, Kwok K. (2007). *Physics of Semiconductor Devices*. (3rd Ed.). *Hoboken:* John Wiley & Sons, Inc.

28. Padovani F.A., Stratton R. (1966). Field and thermionic-field emission in Schottky barriers. *Sol. St. Electron*, 9, 695-707.

29. Yu. A. Y. C. (1970). Electron tunneling and contact resistance metal-silicon contact barriers. *Sol. St. Electron*.13, 239-247.

30. Kupka R.K., Anderson W.A. (1991). Minimal ohmic contact resistance limits to n-type semiconductors. *J. Appl. Phys*., 69 (6), 3623-3632.

31. Askerov B.M. (1970). *Kineticheskiie effekty v poluprovodnikakh [Kinetic effects in semiconductors]*. Leningrad: Nauka.

32. Okhotin A.S., Yefremov A.A., Okhotin V.S., Pushkarskiy A.S. (1971). *Termoelektricheskiie genetatory [Thermoelectric generators].A.R.Regel (Ed.)* Moscow: Atomizdat, 1971.

33. Mahan G.D., Woods L.M. (1998). Multilayer thermionic refrigeration. *Phys. Rev. Lett*, 80(18), 4016-4019.

34. Taylor P.J.*,* Maddux G.R., Meissner G.*,* Venkatasubramanian R., et al. (2013). Controlled improvement in specific contact resistivity for thermoelectric materials by ion implantation. *Appl. Phys. Lett,* 103, 043902-1 - 043902-4.

35. Vikhor L.M., Anatychuk L.I., Gorskyi P.V. (2019). Electrical resistance of metal contact to Bi_2Te_3 based thermoelectric legs. *J. Appl. Phys*, 126, 64503-1 – 164503-8.

Анатичук Л.І., *акад. НАН України*[1,2]
Вихор Л.М., *докт. фіз.-мат. наук*[1],
Мицканюк Н.В.[1,2]

Інститут термоелектрики НАН і МОН України,
вул. Науки, 1, Чернівці, 58029, Україна
e-mail: anatych@gmail.com

КОНТАКТНИЙ ОПІР ЗУМОВЛЕНИЙ ПОТЕНЦІАЛЬНИМ БАР'ЄРОМ НА ГРАНИЦІ ТЕРМОЕЛЕКТРИЧНОГО МАТЕРІАЛУ З МЕТАЛОМ

Розглянуто теоретичні аспекти оцінювання величини електричного опору, який зумовлений переходом носіїв заряду через потенціальний бар'єр на границі між термоелектричним матеріалом і металом. Розраховані температурні залежності питомого опору границі для термоелектричних віток з матеріалів на основі Bi_2Te_3 з нанесеними антидифузійними шарами нікелю. Встановлено, що величина опору границі в таких вітках змінюється з температурою від $0.5 \cdot 10^{-7}$ до $2.5 \cdot 10^{-7}$ Ом·см². Показано, що зменшити опір границі можна шляхом підвищення концентрації носіїв заряду в ультратонкому приконтактному з нікелем шарі термоелектричного матеріалу за рахунок легування. Встановлено, що підвищення концентрації легуючих домішок в приконтактній зоні на один порядок відносно її оптимального значення призводить до зменшення електричного опору границі на два порядки. За цих умов величина опору наближається до мінімально можливого значення, і становить 10^{-9} Ом·см². Бібл. 35, рис. 6, табл. 1.

Ключові слова: контакт термоелектричний матеріал - метал, потенціальний бар'єр,
електричний опір границі.

Анатичук Л.И., *акад. НАН Украины*[1,2]
Вихор Л.Н., *док. физ.-мат. наук*[1],
Мицканюк Н.В.[1,2]

Институт термоэлектричества НАН и МОН Украины,
ул. Науки, 1, Черновцы, 58029, Украина
e-mail: anatych@gmail.com

КОНТАКТНОЕ СОПРОТИВЛЕНИЕ, ОБУСЛОВЛЕННОЕ ПОТЕНЦИАЛЬНЫМ БАРЬЕРОМ НА ГРАНИЦЕ ТЕРМОЭЛЕКТРИЧЕСКИЙ МАТЕРИАЛ – МЕТАЛЛ

Рассмотрены теоретические аспекты оценки величины сопротивления, обусловленного переходом носителей заряда через потенциальный барьер на границе между

термоэлектрическим материалом и металлом. Рассчитаны температурные зависимости удельного сопротивления границы для термоэлектрических ветвей из материалов на основе Bi₂Te₃ с нанесенными антидиффузионных слоями никеля. Установлено, что величина сопротивления границы в таких ветвях изменяется с температурой от $0.5 \cdot 10^{-7}$ до $2.5 \cdot 10^{-7}$ Ом·см². Показано, что уменьшить сопротивление границы можно путем повышения концентрации носителей заряда в ультратонком приконтактном слое термоэлектрического материала за счет легирования последнего. Установлено, что повышение концентрации легирующих примесей в приконтактной зоне на один порядок относительно ее оптимального значения в материале в целом приводит к уменьшению электрического сопротивления границы на два порядка. Библ. 35, рис. 6, табл. 1.

Ключевые слова: контакт термоэлектрический материал – металл, потенциальный барьер, электрическое сопротивление границы.

References

36. Aswal D.K., Basu R., Singh A. (2016). Key issues in development of thermoelectric power generators: high figure-of-merit materials and their highly conducting interfaces with metallic interconnects. *Energy Convers. Manag*, 114, 50-67.

37. Anatychuk L.I., Kuz R.V. (2012). The energy and economic parameters of Bi-Te based thermoelectric generator modules for waste heat recovery. *J.Thermoelectricity*, 4, 75-82.

38. Drabkin I.A., Osvensky V.B., Sorokin A.I., Panchenko V.P., Narozhnaia O.E. (2017). Kontaktnoie soprotivleniie v sostavnykh termoelektricheskikh vetviakh [Contact resistance in composite thermoelectric legs]. *Fizika i tekhnika poluprovodnikov – Semiconductors*, 51 (8), 1038-1040.

39. Anatychuk L.I. (2003). *Termoelektrichestvo. Tom 2. Termoelektricheskiie preobrazovateli energii [Thermoelectricity. Vol.2. Thermoelectric power converters].* Kyiv, Chernivtsi: Institute of Thermoelectricity [in Russian].

40. Semenyuk V.A. (2006). Thermoelectric cooling of electro-optic components. *Thermoelectrics Handbook: Macro to Nano.* D.M. Rowe (Ed.). London, New York: CRC Taylor&Francis.

41. Semenyuk V. (2019). Effect of electrical contact resistance on the performance of cascade thermoelectric coolers. *J. Electron. Mater*, 48(4)**,** 1870-1876.

42. H. Bottner, J. Nurnus, A. Schubert. (2006). Miniaturized thermoelectric converters, in: *Thermoelectrics Handbook, Macro to Nano.* D.M. Rowe (Ed.). London, New York: CRC Taylor&Francis.

43. Crane N.B., Mishra P., Murray J. L., Nolas G.S. (2009). Self-assembly for integration of microscale thermoelectric coolers. *J. of Electron. Mater*, 38(7), 1252-1256.

44. Huang I-Yu, Linb Jr-Ching, She Kun-Dian, et al. (2008). Development of low-cost micro-thermoelectric coolers utilizing MEMS technology. *Sensors and Actuators*, A 148, 176-185.

45. Navone C., Soulier M., Plissonnier M., Seiler A.L. (2010). Development of (Bi,Sb)₂(Te,Se)₃-based thermoelectric modules by a screen-printing process. *J. of Electron. Mater*, 39(9), 1755-1759.

46. Goncalves L.M., Couto C., Alpuim P., Correia J.H. (2008).Thermoelectric micro converters for cooling and energy-scavenging systems. *J. Micromech. Microeng*, 18, 064008-1 - 064008-5.

47. Y. Y. Zhou, J. L. Yu. (2012). Design optimization of thermoelectric cooling systems for applications in electronic devices. *Int. J. Refrig*, 35, 1139-1144.

48. Vikhor L.M., Anatychuk L.I., Gorskyi P.V. (2019). Electrical resistance of metal contact to Bi₂Te₃ based thermoelectric legs. *J. of Appl. Phys*, 126, 164503-1 – 164503-8.

49. Jing H., Li Y., Xu L., et al. (2015). Interfacial reaction and shear strength of SnAgCu/Ni/Bi$_2$Te$_3$-based TE materials during aging. *Mater. Eng. and Perform*, 24(12), 4844-4852.

50. Chen L., Mei D., Wang Y., Li Y. (2019). Ni barrier in Bi$_2$Te$_3$-based thermoelectric modules for reduced contact resistance and enhanced power generation properties. *J. Alloys and Comp*, 796, 314-320.

51. Chuang C.-H.mailto:please_login, Lin Y.-C., Lin C.-W. (2016). Intermetallic reactions during the solid-liquid interdiffusion bonding of Bi$_2$Te$_{2.55}$Se$_{0.45}$ thermoelectric material with Cu electrodes using a Sn interlayer. *Metals*, 6(4), 92-97.

52. Iyore O. D., Lee T. H., Gupta R. P., et al. (2009). Interface characterization of nickel contacts to bulk bismuth tellurium selenide. *Surf. Interface Anal*, 41, 440-444.

53. Gupta R.P., McCarty R., Sharp J. (2014). Practical contact resistance measurement method for bulk Bi$_2$Te$_3$ based thermoelectric devices. *J. of Electron. Mater*, 43(6), 1608-1612.

54. Joshi G., Mitchell D., Ruedin J., et al. (2019). Pulsed-light surface annealing for low contact resistance interfaces between metal electrodes and bismuth telluride thermoelectric materials. *J. Mater. Chem. C*, 7**,** 479-484.

55. Gupta R. P., Xiong K., White J. B., Cho K., Alshareef H.N., Gnade B.E.(2010). Low resistance ohmic contacts to *Bi$_2$Te$_3$* using Ni and Co metallization. *J. of Electrochem. Soc*, 157(6), H666-H670.

56. Bartkowiak M., Mahan G.D. (2001). Heat and electricity transport through interfaces, in: *Recent Trends in Thermoelectric Materials, vol. II, Semiconductors and Semimetals*, vol. 70. New York: Academic Press.

57. Da Silva L. W., Kaviany M. (2004). Microthermoelectric cooler: interfacial effects on thermal and electrical transport. *Int. J. of Heat and Mass Transfer*, 47(10-11), 2417–2435.

58. Vikhor L.M., Gorskyi P.V. (2015). Heat and charge transport at thermoelectric material-metal boundary. *J. Thermoelectricity*, 6, 5-15.

59. Bartkowiak M., Mahan G.D. (1999). Boundary effects in thin-film thermoelctrics. *Proc. of Mat. Res. Soc. Symp*, 545, 265-272.

60. Rhoderick E.H. (1978). *Metal-semiconductor contacts*.Oxford: Clarendon Press.

61. Goldberg Yu.A. (1994). Omicheskii kontakt metall-poluprovodnik AIIIBV: metody sozdaniia i svoistva [Ohmic contact metal- AIIIBV semiconductor: methods of creation and properties]. *Fizika i tekhnika poluprovodnikov - Semiconductors*, 28(10), 1681-1698.

62. Sze S.M., Ng, Kwok K. (2007). *Physics of Semiconductor Devices.* (3rd Ed.). *Hoboken:* John Wiley & Sons, Inc.

63. Padovani F.A., Stratton R. (1966). Field and thermionic-field emission in Schottky barriers. *Sol. St. Electron*, 9, 695-707.

64. Yu. A. Y. C. (1970). Electron tunneling and contact resistance metal-silicon contact barriers. *Sol. St. Electron*.13, 239-247.

65. Kupka R.K., Anderson W.A. (1991). Minimal ohmic contact resistance limits to n-type semiconductors. *J. Appl. Phys*., 69 (6), 3623-3632.

66. Askerov B.M. (1970). *Kineticheskiie effekty v poluprovodnikakh [Kinetic effects in semiconductors]*. Leningrad: Nauka.

67. Okhotin A.S., Yefremov A.A., Okhotin V.S., Pushkarskiy A.S. (1971). *Termoelektricheskiie genetatory [Thermoelectric generators]*.A.R.Regel (Ed.) Moscow: Atomizdat, 1971.

68. Mahan G.D., Woods L.M. (1998). Multilayer thermionic refrigeration. *Phys. Rev. Lett*, 80(18), 4016-4019.

69. Taylor P.J., Maddux G.R., Meissner G., Venkatasubramanian R., et al. (2013). Controlled improvement in specific contact resistivity for thermoelectric materials by ion implantation. *Appl. Phys. Lett,* 103, 043902-1 - 043902-4.

70. Vikhor L.M., Anatychuk L.I., Gorskyi P.V. (2019). Electrical resistance of metal contact to Bi_2Te_3 based thermoelectric legs. *J. Appl. Phys*, 126, 64503-1 – 164503-8.

Submitted 19.09.2019

ARTICLE SUBMISSION GUIDELINES

For publication in a specialized journal, scientific works are accepted that have never been printed before. The article should be written on an actual topic, contain the results of an in-depth scientific study, the novelty and justification of scientific conclusions for the purpose of the article (the task in view).

The materials published in the journal are subject to internal and external review which is carried out by members of the editorial board and international editorial board of the journal or experts of the relevant field. Reviewing is done on the basis of confidentiality. In the event of a negative review or substantial remarks, the article may be rejected or returned to the author(s) for revision. In the case when the author(s) disagrees with the opinion of the reviewer, an additional independent review may be done by the editorial board. After the author makes changes in accordance with the comments of the reviewer, the article is signed to print.

The editorial board has the right to refuse to publish manuscripts containing previously published data, as well as materials that do not fit the profile of the journal or materials of research pursued in violation of ethical norms (for instance, conflicts between authors or between authors and organization, plagiarism, etc.). The editorial board of the journal reserves the right to edit and reduce the manuscripts without violating the author's content. Rejected manuscripts are not returned to the authors.

Submission of manuscript to the journal

The manuscript is submitted to the editorial office of the journal in paper form in duplicate and in electronic form on an electronic medium (disc, memory stick). The electronic version of the article shall fully correspond to the paper version. The manuscript must be signed by all co-authors or a responsible representative.

 In some cases it is allowed to send an article by e-mail instead of an electronic medium (disc, memory stick).

English-speaking authors submit their manuscripts in English. Russian-speaking and Ukrainian-speaking authors submit their manuscripts in English and in Russian or Ukrainian, respectively. Page format is A4. The number of pages shall not exceed 15 (together with References and extended abstracts). By agreement with the editorial board, the number of pages can be increased.

To the manuscript is added:

1. Official recommendation letter, signed by the head of the institution where the work was carried out.

2. License agreement on the transfer of copyright (the form of the agreement can be obtained from the editorial office of the journal or downloaded from the journal website – Dohovir.pdf). The license agreement comes into force after the acceptance of the article for publication. Signing of the license agreement by the author(s) means that they are acquainted and agree with the terms of the agreement.

3. Information about each of the authors – full name, position, place of work, academic title, academic degree, contact information (phone number, e-mail address), ORCID code (if available). Information about the authors is submitted as follows:

authors from Ukraine - in three languages, namely Ukrainian, Russian and English;
authors from the CIS countries - in two languages, namely Russian and English;
authors from foreign countries – in English.

---

4. Medium with the text of the article, figures, tables, information about the authors in electronic form.

5. Colored photo of the author(s). Black-and-white photos are not accepted by the editorial staff. With the number of authors more than two, their photos are not shown.

Requirements for article design

The article should be structured according to the following sections:

- *Introduction*. Contains the problem statement, relevance of the chosen topic, analysis of recent research and publications, purpose and objectives.
- *Presentation of the main research material* and the results obtained.
- *Conclusions* summing up the work and the prospects for further research in this direction.
- *References*.

The first page of the article contains information:

1) in the upper left corner – UDC identifier (for authors from Ukraine and the CIS countries);

2) surname(s) and initials, academic degree and scientific title of the author(s);

3) the name of the institution where the author(s) work, the postal address, telephone number, e-mail address of the author(s);

4) article title;

5) abstract to the article – not more than 1 800 characters. The abstract should reflect the consistent logic of describing the results and describe the main objectives of the study, summarize the most significant results;

6) key words – not more than 8 words.

The text of the article is printed in Times New Roman, font size 11 pt, line spacing 1.2 on A4 size paper, justified alignment. There should be no hyphenation in the article.

Page setup: "mirror margins" – top margin – 2.5 cm, bottom margin – 2.0 cm, inside – 2.0 cm, outside – 3.0 cm, from the edge to page header and page footer – 1.27 cm.

Graphic materials, pictures shall be submitted in color or, as an exception, black and white, in .opj or .cdr formats, .jpg or .tif formats being also permissible. According to author's choice, the tables and partially the text can be also in color.

Figures are printed on separate pages. The text in the figures must be in the font size 10 pt. On the charts, the units of measure are separated by commas. Figures are numbered in the order of their arrangement in the text, parts of the figures are numbered with letters – a, b, .. On the back of the figure, the title of the article, the author (authors) and the figure number are written in pencil. Scanned images and graphs are not allowed to be inserted.

Tables are provided on separate pages and must be executed using the MSWord table editor. Using pseudo-graph characters to design tables is inadmissible.

Formulae shall be typed in Equation or MatType formula editors. Articles with formulae written by hand are not accepted for printing. It is necessary to give definitions of quantities that are first used in the text, and then use the appropriate term.

Captions to figures and tables are printed in the manuscript after the references.

Reference list shall appear at the end of the article. References are numbered consecutively in the order in which they are quoted in the text of the article. References to unpublished and unfinished works are inadmissible.

Attention! In connection with the inclusion of the journal in the international bibliographic abstract database, the reference list should consist of two blocks: CITED LITERATURE and REFERENCES (this requirement also applies to English articles):

CITED LITERATURE – sources in the original language, executed in accordance with the

Ukrainian standard of bibliographic description DSTU 8302:2015. With the aid of VAK.in.ua (http://vak.in.ua) you can automatically, quickly and easily execute your "Cited literature" list in conformity with the requirements of State Certification Commission of Ukraine and prepare references to scientific sources in Ukraine in understandable and unified manner. This portal facilitates the processing of scientific sources when writing your publications, dissertations and other scientific papers.

REFERENCES – the same cited literature list transliterated in Roman alphabet (recommendations according to international bibliographic standard APA-2010, guidelines for drawing up a transliterated reference list "References" are on the site http//www.dse.org.ua, section for authors).

To speed up the publication of the article, please adhere to the following rules:

- in the upper left corner of the first page of the article – the UDC identifier;

- family name and initials of the author(s);

- academic degree, scientific title;

begin a new line, Times New Roman font, size 12 pt, line spacing 1.2, center alignment;

- name of organization, address (street, city, zip code, country), e-mail of the author(s);

begin a new line 1 cm below the name and initials of the author(s), Times New Roman font, size 11 pt, line spacing 1.2, center alignment;

- the title of the article is arranged 1 cm below the name of organization, in capital letters, semi-bold, font Times New Roman, size 12 pt, line spacing 1.2, center alignment. The title of the article shall be concrete and possibly concise;

- the abstract is arranged 1 cm below the title of the article, font Times New Roman, size 10 pt, in italics, line spacing 1.2, justified alignment in Ukrainian or Russian (for Ukrainian-speaking and Russian-speaking authors, respectively);

- key words are arranged below the abstract, font Times New Roman, size 10 pt, line spacing 1.2, justified alignment. The language of the key words corresponds to that of the abstract. Heading "Key words" - font Times New Roman, size 10 pt, semi-bold;

- the main text of the article is arranged 1 cm below the abstract, indent 1 cm, font Times New Roman, size 11 pt, line space spacing 1.2, justified alignment;

- formulae are typed in formula editor, fonts Symbol, Times New Roman. Font size is "normal" – 12 pt, "large index" – 7 pt, "small index" – 5 pt, "large symbol" – 18 pt, "small symbol" – 12 pt. The formula is arranged in the text, center aligned and shall not occupy more than 5/6 of the line width, formulae are numbered in parentheses on the right;

- dimensions of all quantities used in the article are represented in the International System of Units (SI) with the explication of the symbols employed;

- figures are arranged in the text. The figures and pictures shall be clear and contrast; the plot axes – parallel to sheet edges, thus eliminating possible displacement of angles in scaling; figures are submitted in color, black-and-white figures are not accepted by the editorial staff of the journal;

- tables are arranged in the text. The width of the table shall be 1 cm less than the line width. Above the table its ordinary number is indicated, right alignment. Continuous table numbering throughout the text. The title of the table is arranged below its number, center alignment;

• references should appear at the end of the article. References within the text should be enclosed in square brackets behind the text. References should be numbered in order of first appearance in the text. Examples of various reference types are given below.

Examples of LITERATURE CITED

Journal articles

Anatychuk L.I., Mykhailovsky V.Ya., Maksymuk M.V., Andrusiak I.S. Experimental research on thermoelectric automobile starting pre-heater operated with diesel fuel. *J.Thermoelectricity*. 2016. №4. P.84–94.

Books

Anatychuk L.I. *Thermoelements and thermoelectric devices. Handbook.* Kyiv, Naukova dumka, 1979. 768 p.

Patents

Patent of Ukraine № 85293. Anatychuk L.I., Luste O.J., Nitsovych O.V. Thermoelement.

Conference proceedings

Lysko V.V. *State of the art and expected progress in metrology of thermoelectric materials.* Proceedings of the XVII International Forum on Thermoelectricity (May 14-18, 2017, Belfast). Chernivtsi, 2017. 64 p.

Authors' abstracts

Kobylianskyi R.R. *Thermoelectric devices for treatment of skin diseases*: extended abstract of candidate's thesis. Chernivtsi, 2011. 20 p.

Examples of REFERENCES

Journal articles

Gorskiy P.V. (2015). Ob usloviakh vysokoi dobrotnosti i metodikakh poiska perspektivnykh sverhreshetochnykh termoelektricheskikh materialov [On the conditions of high figure of merit and methods of search for promising superlattice thermoelectric materials]. *Termoelektrichestvo - J.Thermoelectricity,* 3, 5 – 14 [in Russian].

Books

Anatychuk L.I. (2003). *Thermoelectricity. Vol.2. Thermoelectric power converters*. Kyiv, Chernivtsi: Institute of Thermoelectricity.

Patents

Patent of Ukraine № 85293. Anatychuk L. I., Luste O.Ya., Nitsovych O.V. Thermoelements [In Ukrainian].

Conference proceedings

Rifert V.G. Intensification of heat exchange at condensation and evaporation of liquid in 5 flowing-down films. In: *Proc. of the 9th International Conference Heat Transfer.* May 20-25, 1990, Israel.

Authors'abstracts

Mashukov A.O. *Efficiency hospital state of rehabilitation of patients with color carcer.* PhD (Med.) Odesa, 2011 [In Ukrainian].